BINNENZIJDE OMSLAG

Connectivity and Neurotransmission

in Experimental Epileptogenesis

Connectivity and Neurotransmission in Experimental Epileptogenesis

Connectiviteit en neurotransmissie tijdens experimentele epileptogenese
(met een samenvatting in het Nederlands)

The studies in this thesis were performed at
the Rudolf Magnus Institute for Neuroscience and
the experimental *in vivo* NMR group of the department
of radiology of the UMC Utrecht, The Netherlands as
well as at the Magnetic Resonance Research Center
at the Yale School of Medicine in New Haven, USA

Dit proefschrift werd (mede) mogelijk gemaakt met
financiële steun van het Nederlands Epilepsie Fonds
(NEF), The Focal Epilepsies of Childhood Fund,
Beurzen van de National Institute of Health (NIH),
Vrije Universiteit Medisch Centrum, UCB pharma BV,
GE Healthcare, Cyberonics, Europe en B. Braun Medical BV.

Book design: Robert van Sluis, www.eyefordetail.nl

Proefschrift

ter verkrijging van de graad van doctor aan
de Universiteit Utrecht op gezag van de
rector magnificus, prof.dr. G.J. van der Zwaan,
ingevolge het besluit van het college voor
promoties in het openbaar te verdedigen op
donderdag 21 april 2011 des middags te 12:45 uur

door
Pieter van Eijsden

geboren op 24 februari 1976
te Amersfoort

Promotor

Prof. Dr. O. van Nieuwenhuizen
Department of Pediatric Neurology,
University Medical Center Utrecht,
The Netherlands

Co-promotores

Dr. K.P.J. Braun
Department of Pediatric Neurology,
University Medical Center Utrecht,
The Netherlands

Dr. R.A. de Graaf
Department of Diagnostic Radiology,
Yale School of Medicine,
New Haven, CT, USA

The two – the hero and his ultimate god, the seeker and the found – are thus understood as the outside and the inside of a single self-mirrored mystery, which is identical with the mystery of the manifest world. The great deed of the supreme hero is to come to the knowledge of this unity in multiplicity and then to make it known.

The hero with a thousand faces – *Joseph Campbell*

Contents

1

A short history of epilepsy

Recounting the history of epilepsy is recounting the history of medicine. Epilepsy with its considerable prevalence, especially in primitive and violent societies, and its awe-inspiring symptomatology has always spoken to the imagination and has motivated mankind to evolve medicine. Prehistoric trephinations,[1] shock therapy with the electrical "cramp fish" in medieval Iran[2] and present day sophisticated presurgical workup with robot-guided stereotactic intracranial EEG[3], show that epilepsy has always been a driving force and testing ground for medical progress.

Ancient beliefs

The region around the rivers Tigris and Euphrates has been called the Cradle of Civilization, because the world's first known literary texts stem from this region (Sumer, 2600 B.C.). The world's oldest medical handbook also comes from this region (Akkad, ~2000 B.C.) and describes an epileptic seizure as follows: "his neck turns left, his hands and feet are tense and his eyes are wide open, and from his mouth froth is flowing without his having any consciousness."[4] Epilepsy is referred to as *antasubbû*, the hand of sin, and considered a consequence of angering the god of the moon. Hypotheses on the connection between epilepsy, the supernatural and the lunar cycle are apparently as old as civilization itself. Another medical textbook, *Sakikku* or "all diseases" from the region (Babylon ~1050 B.C.), recognizes epilepsy in all its familiar detail.[5] There are descriptions of febrile seizures, infantile spasms, simple and complex partial seizures, status epilepticus, gelastic seizures and the postictal state.[6]

The passive tense of the Greek verb επιλαμβάνειν is the origin of the word epilepsy, which therefore means "to be seized or possessed". Although the Greek founder of atomic theory, Democritus of Abdera (~500 B.C.), already postulated epilepsy to be a consequence of an organic brain disorder in his book on epilepsy (Περί επιληψίας), it would take more than two millennia before western medicine was fully committed to

this idea.[7] The superstitious amongst the ancient Greeks considered epilepsy to be a μιασμα ("bad air") that was cast on the soul as a punishment by the lunar deity Artemis. Paradoxically Artemis' twin brother Apollo was believed to use epilepsy in a beneficial sense, instilling genius and heroism in its sufferers and earning it the name ιερη νόσος, "the sacred disease". The demi-god Hercules, the Persian king Cambyses II, and the Roman emperor Caesar were (wrongly) pointed out as examples of these sacred heroes.

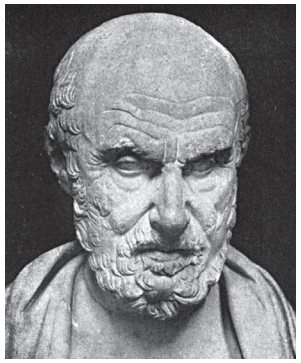

Fig 1.1 | Statue of Hippocrates, 2nd to 3rd century B.C. (Collection of British Museum)

More enlightened ideas from the same period can be found in the famous Hippocratic texts. In the volume *On the Sacred Disease* it says: "This disease is no more divine than any other; it has the same nature as other diseases, and the causes that give rise to individual diseases…. My own view is that those who first attributed a sacred character to this malady were like the magicians, purifiers, charlatans and quacks of our own day, men who claim great piety and superior knowledge. Being at a loss, and having no treatment which would help, they concealed and sheltered themselves behind superstition, and called this illness sacred, in order that their utter ignorance might not be manifest".[8] Considering the lack of scientific knowledge and widespread superstitious convictions of its time, the insight of Hippocrates into this disease (and the practitioners of medicine) can hardly be overstated. Hippocrates described epilepsy to be sometimes caused by head injury, noticing that it provoked seizures in the contralateral side of the body. He wrote about hereditary factors, which he formulated in surprisingly familiar terms as εκ γενεης (ek genès).[8] He described different seizure and aura types, while coining the term "great disease", adopted in French as *grand mal*. He described the prognosis of epilepsy in children as grim and for adults as generally treatable "unless by long lapse of time it be so ingrained as to be more powerful than the remedies that are applied".[8] His understanding of the suffering of patients is evident from the following passage: "[The people who] are habituated to their disease have a presentiment when an attack is imminent, and run away from men, home, if their house be near, if not, to the most deserted spot, where the fewest people will see the fall, and immediately hide their heads. This is the result of shame at their malady, and not, as the many hold, of fear of the divine".[8]

Although his observations were strikingly accurate, the pathophysiological factors Hippocrates proposed were typical for the timeframe he lived in. He blamed climatic factors and disturbances in one of his famous four humors as causative agents. Therapies were therefore aimed at equilibrating the humors by phlebotomy, vomiting agents, enemas or diuretics and by general strengthening of the body. Two interesting ideas stand out. In his Epidemics, Hippocrates recommends complete abstinence from food and drink, which conceivably could contribute to a reduction in seizures through the ketogenic mechanism we employ today.[8] He also recommended that young women suffering from epilepsy become pregnant, which is compatible with the observation that many women experience a reduction in seizure frequency during pregnancy. Through the post-Hippocratic Greek and Roman era these therapies persisted as well as many absurd and torturous therapies. In this sense therapies described by two prolific encyclopedists of the "enlightened" Roman Empire are worth a special mentioning. Aurelius Cornelius Celsus (25 B.C.–50 A.D.) prescribed sexual intercourse and the drinking of still warm blood of slain gladiators for young epileptic boys, while Pliny the Elder (23–79 A.D.) advised patients to drink spring water from the skull of a murdered man.[9,10]

Hippocrates' views were seminal through the influence he exerted on the work of Aristotle (384 B.C. – 322 B.C.), who unfortunately did not share the denunciation of supernatural ideas about epilepsy. Because the teachings of Aristotle were considered indisputable by the Catholic Church, religious and magical beliefs regarding epilepsy persisted and hardly any medical progress was made for more than a thousand years. This is illustrated by the Malleus Maleficarum, the papal handbook for witch hunting published in 1494, which described epilepsy as an identifying characteristic of a witch, punishable by burning at the stake. Over time an estimated 200.000 epileptic women would suffer this horrible fate.[11]

Prophets, visionaries, healers and the course of history

The holy scriptures of all three monotheistic religions contain elements that allude to epileptic phenomena in both the authors and their characters. One enticing, yet speculative theory is that several parts of the Pentateuch and the book of Ezekiel were written by someone suffering from the Geschwind syndrome.[12;13] This interictal behavioral pattern is sometimes seen in patients suffering from left temporal lobe epilepsy and is characterized by hallucinations, hyperreligiosity and hypergraphia.[14] The writings of these patients are described as obsessed with details, aggressive and pedantic.[15] The aforementioned writings meet these criteria and are excessively long compared to other texts from the bible. In addition, Ezekiel (~600 B.C.) himself described having suffered from multiple episodes of fainting spells (Ezekiel 1:28; 3:23; 43:3; and 44:4) and mutism (Ezekiel 3:22-26; 24:25-27; and 33:21) that fit the diagnosis of left temporal lobe epilepsy.

According to the muslim faith, the archangel Gabriel revealed the will of Allah to Muhammad through visions, which were accompanied by a loss of consciousness and motor control. These physical signs were seen by Muhammads contemporaries as evidence for the divine origin of these revelations. A differential diagnosis of the known symptoms is extensively discussed by Freemon who concludes that psychomotor seizures or temporal lobe epilepsy would be the most tenable diagnosis.[16] Fyodor Dostoevsky, an epileptic himself, wrote that his attacks had "a supreme exaltation of emotional subjectivity in which time stands still… Probably it was of such an instant, that the epileptic Mahomet was speaking when he said that he had visited all the dwelling places of Allah within a shorter time than it took for his pitcher full of water to empty itself."[17]

Christianity's position as one of the major world religions is heavily dependent on the missionary work of Paul of Tarsus. Initially a rabid persecutor of the young religion, he was converted when traveling to Damascus, when suffering an attack that consisted of being blinded by a sudden flash of light, dropping to the ground and having an intense religious experience. Paul mentions in his second letter to the Corinthians that his wealth of visions represents a metaphoric "thorn in the flesh", which periodically physically racks him. Obviously not enough information is present to come to a definite diagnosis, but the idea of an epileptic syndrome similar to Geschwind is tempting.[18]

Fig 1.2. | Raphael (1483 - 1520) integrated the transfiguration of Christ at mount Tabor and the healing of an epileptic boy into one great masterpiece. "The story of the boy with the unclean spirit" (Matthew 17:14-21; Mark 9:14-29, Luke 9:37-43) describes a boy who has lost motor control, foams at the mouth, gnashes his teeth and has a history of casting himself in fire or water. Jesus orders a demon to leave the boy, upon which the boy screams and is left "as one dead", before he regains consciousness.

Renaissance

The renaissance (14th – 17th century) was characterized by a new attitude towards art, science and organization of society. The old Roman catholic dogma's were slowly, and against much opposition, put to the test of reason. The debate concerning epilepsy can be centered around three major issues.

The first issue was the widely held belief that epilepsy patients were "possessed" or were witches and warlocks. An important contribution is made by Andreas Caesalpinus (1519–1603 A.D.). In his *daemonum investigatio peripatetica*, he tries to differentiate true epileptic seizures from daemonic possession.[19] His purpose was to identify the best candidates for exorcism, but it also represented an important step in discerning epilepsy from many other misunderstood diseases. Jean Taxil went one step further in his *Traicté de l'épilepsie* (1602) in which he stated that any case of demonic possession published in literature could be traced to epileptic symptoms.[20] To support his point, he published a (flawed) long list of famous historical people that had displayed symptoms of epilepsy. Superstitious beliefs about epilepsy remained common until well into the 19th century and can manifest itself in the present day when confronted with patients and families from other cultures.

The next heavily debated issue was the question from which organ epilepsy or seizures originated. The aforementioned Jean Taxil actually performed autopsies on several children who died of epilepsy from which he concluded that epilepsy must be due to an irritation of the brain caused by poisonous substances.[20] In his treatise on epilepsy, Charles Le Pois (1563–1636 A.D.) gives a surprisingly correct definition of epilepsy when stating: "[epilepsy] starts in the head, manifests itself and is first felt in a specific part of the body before the fit becomes generalized and the senses lost.[21] However, other influential ideas were that the uterus (eclampsia) or the liver (icteric seizures) were responsible.

These explanations were related to the next topic of debate; the pathophysiology of epilepsy. Most explanations invoked a disturbance in the balance of the four humors, especially the phlegm, that affected the aforementioned internal organs. Thomas Willis (1621–1675) on the other hand, assumed the existence of "spasmodic explosive copula". For Willis "heterogeneous and explosive particles, being diffused from the blood into the brain, or its medullarie appendix, are afterwards derived to the nervous stock, and there grow together with the spirits".[22] The ensuing explosion of animal spirits causes all the mental symptoms of the epileptic attack, and a series of similar explosions occur along the rest of the nervous system to bring about the convulsions of the body.

It is obvious that the debate was characterized by arguments from sometimes elaborate hypotheses, but show few attempts to test these hypotheses by scientific means. Scientific arguments from careful observation or autopsies were not considered to be of greater importance than a cleverly formulated hypothetical.

The advent of science

Some early attempts at true scientific explorations into epilepsy must be mentioned. Both Joannes Rhodius (1587–1659) and Felix Plater (1536–1617) describe finding a brain tumor in the autopsy of patients suffering from seizures.[23,24] The first true experiment was performed and described by Charles Drélincourt (1633–1694) who provoked epileptic convulsions in a dog by driving a needle into the fourth ventricle.[25] Gaspar Ferdinand Fontana (1730–1803) showed that convulsions could be produced by pressure on the brain.[26] However, mainstream medicine remained a mixture of educated guesses, plagiarism of past pseudoscience and superstition until the 19th century, when neurology was elevated as a new science, separate from psychiatry. The first hospital for the crippled and epileptics was founded in France. This example was quickly followed in other European countries and enabled the creation of what we would now call databases of knowledge about the clinical and post mortem findings in epilepsy patients.

This new organization of epilepsy care resulted in the *Observations sur la nature et le traitement de l'epilepsie* by Antoine Baron de Portal (1742-1832) in which he presented his clinical experience supported by a large amount of clinical data and postmortem reports.[27] In the same year, 1827, Louis François Bravais (1801–1843), published his thesis R*echerches sur les symptômes et le traitement de l'épilepsie hémiplégique*, in which he describes what was later called the Jacksonian march, which he coupled to damage in the contralateral hemisphere.[28] The book *Des accès incomplets d'épilepsie* by the French neurologist Théodore Herpin (1799–1865) is based on 300 cases of epilepsy and emphasizes the early recognition and treatment of epilepsy.[29] Herpin's study therefore focused on the symptoms preceding the onset of major seizures, the initial symptoms with which major attacks began, and the minor attacks occurring in the intervals between complete attacks.

In Britain, in the mean time, Edward Goodman Clarke, summarized the existing knowledge on epilepsy in *The Modern Practice of Physic*.[30] He listed an interesting and recognizable array of etiologies: hereditary cases, tumors compressing the brain, malformations of the skull, brain injury, abscesses, worms, hemorrhage, syphilis, over-distension of the blood-vessels of the brain, a diseased state of the liver, but also terror, anger, pungent odors and violent joy. His contemporary James Cowles Prichard (1786–1848) was the first to establish the term partial epilepsy and to describe the emotional states that accompanied these partial seizures.[31] Richard Bright (1789–1858) attempted to combine anatomical data with clinical cases similarly to the practice of the French. Bright was able to show changes in the cortical grey matter, from which he also concluded that this was the main functional part of the cerebral hemispheres.[32] Robert Bentley Todd (1809–1860) made the observation that epileptic attacks were followed by a paralysis of the affected side, a phenomenon he called "epileptic hemiplegia" but which we now know as "Todds paralysis".[33]

Fig. 1.3 | Autographed picture of John Hughlings Jackson (Archive of the Royal London Hospital Trust)

John Hughlings Jackson (1835–1911) inaugurated the modern period in the scientific research of epilepsy. Working at the British National Hospital for the Relief and Cure of the Paralysed and Epileptic, he was able to deal with a large number of epileptic cases. This is illustrated by a series of lectures by his assistant William Richard Gowers (1845–1915) to the Royal College of Physicians in 1879 in which he presented the clinical features of a series of 1500 cases whom he observed and treated personally. In a subsequent book an additional 1500 cases were described.[34] Another reason for the success of Hughlings Jackson was his elaborate network. He was in contact with many of the aforementioned pioneers in Britain and France as well as with forerunners from more basic scientific fields. Jackson studied epilepsy on a pathological and anatomical basis and came to the conclusion that the grey matter in the brain was responsible for seizure disorders. In his seminal work *Study of Convulsions* he contributed to the understanding of epilepsy like possibly only Hippocrates before him. He distinguished four factors responsible for convulsions. The first is a localized lesion in the cortex that is involved in the localized spasms; the second is a functional change at the cellular level in the grey matter. The pathological process that brought about the functional change (embolus, tumor, syphilis, or other cause) is the third factor, and the fourth is the various provocative circumstances that trigger the seizure.[35] In 1873, Jackson gave the following definition for epilepsy: "Epilepsy is the name for occasional, sudden, excessive, rapid and local discharges of grey matter".[35] An added benefit to this definition was that many different clinical entities were now recognized as "epilepsy", while other were excluded (various psychiatric disorders, tics or Tourette syndrome). He also introduced the concept of localized versus generalized seizures and introduced a further localizing dimension to the understanding of epilepsy, by for instance noticing aphemia (aphasia) in patients with left sided lesions or by indicating the characteristic march of symptoms in the extremities that he interpreted as indicative of adjacency in representation in the motor cortex. This epileptic phenomenon is still referred to as the "Jacksonian march". John Hughlings Jackson is mainly recognized as the first to come up with a practical classification system for epilepsy. He is also recognized for the fact that he was the first to recognize limbic seizures, which he called "intellectual auras" or "dreamy states," and which he coupled to lesions in mesial temporal structures.[36,37] These lesions, now known as hippocampal sclerosis, were further characterized by the neuropathologists

Sommer and Bratz in 1880.[38,39] The CA1 region of the hippocampus that shows most neuronal loss is still sometimes referred to as Sommer's section.

In the early 20th century another important step was the implementation of the electroencephalography for the study of epilepsy by Hans Berger.[40] It became recognized that epileptic seizures were accompanied by changes in the electrical activity of the brain which could be classified. In 1937 Gibbs published the first classification of seizures based on their EEG characteristics.[41] In 1969 the first ILAE classification based on semiological and electrophysiological characteristics was published, which has been revised ever since, the latest proposal dating from 2010.[42]

Treatment

During Hughlings Jackson's life not much could be done for epilepsy patients. One of the few known treatments was fasting, which only worked in small subgroup of patients. In 1922 this observation led to the development of the ketogenic diet, still in use today.[43] Hughlings Jackson (†1911) also did not live to see the day that the first anti-epileptic drug was developed. In 1912, two groups of chemists created phenobarbital.[44] Other important drug discoveries were that of phenytoin in 1939 and carbamazepine in 1953.[44] At least 30 different drugs are now registered for epilepsy.

Bailey and Gibbs were the first to perform anterior temporal lobectomy on the basis of EEG evidence,[45] but it was the "en bloc" resection of Falconer,[46] which included the mesial temporal lobe structures, that made it possible to perform systematic pathologic analysis of resected tissue. Not only was hippocampal sclerosis identified as being present in a high percentage of patients with medically refractory temporal lobe epilepsy, it also became apparent that surgical outcome in patients in whom this pathologic abnormality was demonstrated was exceptionally good, supporting the argument that this structural lesion was the cause, and not the effect, of recurrent epileptic seizures. Falconer also recognized the association between hippocampal sclerosis and both febrile convulsions and a family history of epilepsy, which suggested the existence of a specific syndrome.[47,48]

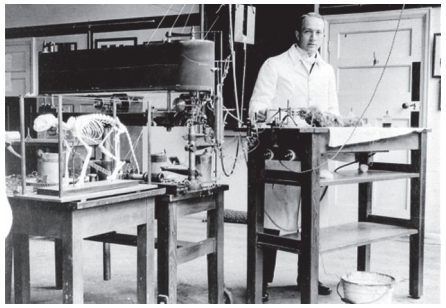

Fig. 1.4 | A young Wilder Penfield in Charles Sherrington's laboratory for mammalian Physiology in 1916

Wilder Penfield (1891-1976) is the one to credit for the rise of epilepsy surgery. His training by famous physiologists (Sir Charles Sherrington and Sir William Osler at Oxford) on the one hand, and by the pioneering neurosurgeon Harvey Cushing on the other hand was a potent one, leading to the development of new and safe surgical procedures with impressive results. Penfield and Jasper published a landmark book *Epilepsy and the Functional Anatomy of the Human Brain* in 1954.

Interestingly, after this initial excitement, surgical treatment for epilepsy went out of favor for several decades until it was brought into mainstream neurosurgery once again due to surgical developments (operation microscope) and diagnostic developments (neuroimaging). Its value was unequivocally shown in a randomized controlled trial published by Wiebe *et al.* in 2001 that compared temporal lobe resection with a conservative treatment.[49] Many different surgical options are available these days for an array of epileptic syndromes.

Despite these modern developments in the understanding and treatment of epilepsy, until 1990 several states in the U.S. had archaic laws that prohibited epilepsy patients to marry and allowed for their forced sterilization. With the Disability Act these laws disappeared. However, there are still many nations and cultures where little progress has been made compared to the ancient ideas of Akkad and Sumer.

2

Introduction, aims and outline of the thesis

Temporal lobe epilepsy

Definitions

Definitions of temporal lobe epilepsy (TLE) and temporal lobe seizures have varied through the years and confusion persists concerning their use. The terms temporal lobe seizure, psychomotor seizure, and limbic seizure are often used interchangeably to denote seizures with signs and symptoms that derive from activation of mesial temporal limbic structures. In the currently used international league against epilepsy (ILAE) classification of epilepsies and epileptic syndromes dating from 1989, TLE is defined by characteristic anterior temporal interictal EEG spikes, temporal lobe hypometabolism on PET and associated clinical features, such as increased incidence of febrile convulsions and family history of epilepsy.[50] The current classification was made before the introduction of modern neuroimaging and research techniques and therefore does not account for various etiologic factors or structural lesions on MRI, such as hippocampal sclerosis (HS), the most common pathologic substrate of TLE.[51] In some cases, patients with a diagnosis of TLE can actually have extratemporal epileptogenic regions that quickly propagate to temporal structures.

The proposal for a new classification places less emphasis on localization and more on underlying pathology. The idea of "constellations" is introduced for entities that are not electroclinical syndromes, but represent diagnostically meaningful forms of epilepsy that may guide treatment, particularly surgery.[42] TLE with HS is one of these constellations, because disabling seizures and their consequences can be eliminated by anteromesial temporal lobectomy in 60% to 80% of patients and early surgical intervention provides the opportunity for complete psychosocial rehabilitation.[49,52] *The research in this thesis pertains to this new entity of TLE with HS.*

Epidemiology

In developed countries, the age-adjusted incidence of at least one unprovoked seizure ranges from 26 to 70 per 100,000 person-years.[53-57] The incidence of recurrent unprovoked seizures ranges from 24 to 53 per 100,000 person-years.[54-58] The life time risk of having a seizure is estimated at 5.4%.[57] The incidence in studies of predominantly

Western, industrialized countries is remarkably consistent across geographic areas. Seizure-specific incidences from Minnesota,[58] the Faeroer Islands,[57] and Sweden[53] show that slightly more than 50% of incidence cases were classified as partial seizures, making it the most frequent seizure class. A worldwide census of 107 epilepsy surgery centers confirmed that in surgical centers, TLE is by far the most common type of epilepsy. Of 8,234 operations performed between 1985 and 1990, 66% involved the temporal lobe.[59] Unfortunately, series from specialty units are biased toward patients who are surgical candidates, have more severe epilepsy and are more intensely investigated. Consequently, the true frequency of TLE in the population is unknown.

Initially temporal lobe seizures can often be treated by anti epileptic drugs (AEDs). However, over time these medications fail to control disabling seizures and result in intolerable side effects in approximately 30-40% of people with TLE.[60] The subgroup of patients suffering from TLE that show HS on MRI or in resection material is an important one, to the degree that is has now been proposed to be a separate entity ("constellation"). Because of its recent (re-)definition, no reliable epidemiological data is available. In surgical series as many as 70% of patients with medically refractory TLE have HS.[51] Two studies provide numbers from non-surgical series evaluated with high-resolution MRI. In both centers, approximately 25% of patients suffered from TLE ánd had sufficient atrophy of the hippocampus to be visible on MRI.[61,62] The true percentage is probably higher because not all patients with HS have sufficient atrophy or sclerosis to be discriminated on MRI. *In these series, TLE with HS was both the most common ánd the most medically intractable form of epilepsy encountered, emphasizing the problematic nature of this disease.* Surgery has been proven to be an excellent treatment alternative, leading to seizure freedom in 60%-80% of all cases and more than 90% of cases with a structural temporal lobe lesion (*i.e.* HS).[63] Despite present knowledge of TLE, its notorious medical intractability, the importance of early treatment and the excellent outcome of surgery, it still takes an average of fifteen years before surgical treatment is performed.[64]

Another important epidemiological factor is the relationship between TLE and prolonged (>15 min) febrile seizures. In 2-5% of children, fever will provoke a generalized seizure in the absence of intracranial infection.[65] Retrospective studies have shown that between 30 and 60% of patients with TLE have histories of prolonged or complex febrile seizures and that children with prolonged febrile seizures have an eightfold increased risk of developing epilepsy.[66-68]

Seizure characteristics

The clinical debut of TLE occurs during puberty or early adolescence. Ictal clinical characteristics can be divided into subjective and objective components. The subjective component in mesial temporal lobe seizures is the aura. Auras are very common, occurring in more than 90% of TLE patients.[69,70] They can occur as the first manifestation of a complex partial seizure or in isolation as simple partial seizures.[71,72] By far the most common type of aura is a rising epigastric sensation, with fear as a distant second.[69] Other frequently described auras, such as déjà vu, jamais vu, micropsia, macropsia, olfactory hallucinations, and feelings of depersonalization, do occur, but are uncommon.[69] The objective manifestations of mesial temporal lobe seizures usually occur when consciousness is impaired, so the patient is seldom aware of them. The seizures often begin with motor arrest, staring, and pupillary dilation. The seizure may not progress beyond this point, but usually automatisms occur, such as lip smacking, chewing, licking, and tooth-grinding, are highly characteristic, but fumbling, picking, and gesticulating movements are also common for mesial temporal lobe seizures.

Some objective seizure characteristics may have lateralizing or localizing value. Unilateral tonic or dystonic posturing and (post-)ictal paresis are reliably displayed contralateral to the side of seizure onset.[73] Ictal vomiting has been related to right temporal lobe onset.[1] Both ictal aphasia and ictal speech arrest have been equated with seizure onset in the language-dominant temporal lobe,[74,75] whereas verbalization of coherent speech is associated with seizure onset in the temporal lobe that is not speech dominant.[76] More recent reports that specifically evaluated postictal language function following temporal lobe seizures confirm that postictal aphasia reliably lateralized seizure origin to the language-dominant side.[75] Patients occasionally wipe their nose at the end of a seizure and when they do, they almost always use the hand ipsilateral to ictal onset.[77] Head and eye deviation have long been recognized as clinical seizure manifestations, which have a localizing value. However, a case report from our own center illustrated that the localizing value should be carefully weighed against other clinical evidence, because unexpected phenomena may play a role in TLE[78] (see pp. 30-31).

Diagnosis and treatment

In TLE patients, results of neurologic examination are usually normal, with the exception of a mild to moderate memory deficit. The characteristic interictal EEG abnormality consists of anterior temporal sharp waves, spikes, and slow waves. The discharges demonstrate a characteristic field with a maximum in basal derivations, such as sphenoidal, true temporal, or earlobe electrodes. Specific ictal patterns can help differentiate mesial from lateral temporal lobe epilepsies.[92] Auras are usually not associated with any EEG changes, although frequent interictal spikes may be seen to disappear during the

simple partial seizure. High-resolution MRI can demonstrate hippocampal atrophy in a high percentage of patients with medically refractory TLE.[93-95] FLAIR or T_2-weighted images often show increased signal in the area of HS to confirmation a diagnosis of TLE.[95] FDG-PET is the most sensitive interictal imaging technique for identifying the focal functional deficit associated with hippocampal sclerosis.[96] Interictal SPECT is capable of showing unilateral temporal hypoperfusion in TLE, but with a much lower yield than PET. Ictal SPECT, however, demonstrates a characteristic pattern of hyperperfusion of the involved temporal lobe when the tracer is injected during a seizure, and of lateral hypoperfusion with persistent mesial hyperperfusion when it is injected shortly after a seizure, during the early postictal phase.[97,98] MEG can localize interictal and ictal epileptiform discharges to mesial temporal structures in patients with TLE.[99]

Oftentimes seizures respond well to anti epileptic drugs (AEDs) initially and patients do well for several years.[64] However, over time these medications fail to control disabling seizures in almost half of patients or result in intolerable side effects. Based on the known pathophysiology, there is evidence that cell death and neuronal reorganization continue with recurrent seizures.[100] *The latent period between occurrence of a precipitating event (febrile seizures or status epilepticus in early childhood) and onset of recurrent temporal lobe seizures (in puberty or adolescence), and the period between initiation of medical therapy and development of medical intractability, both suggest an ongoing process of epileptogenesis, which is the subject of this thesis.*[69]

Hippocampal pathology in TLE

Hippocampal anatomy

The human hippocampus is located in the medial wall of the temporal horn of the lateral ventricle and consists of two distinct regions: the hippocampal cortex (cornu ammonis) and the dentate gyrus (DG). The hippocampal cortex is divided in four separate regions, aptly called CA1 to 4 (fig 2.1.A 1-4), based on differences in cell size and cell density. CA1 is characterized by small pyramidal neurons, CA2 by tightly packed large pyramidal cells, CA3 by broad loosely packed pyramidal cells and CA4 by dispersed large ovoid neurons. The DG is a narrow band of tightly packed granule cells (GCL) that forms the interior aspect of these cortical layers (fig 2.1.A 5). The hippocampus has two main connections with the rest of the brain. The subiculum (fig 2.1.A 7) relays almost all afferent information (from cingulum, amygdala, primary olfactory area and several other neocortical areas) through the adjacent entorhinal cortex, while the fimbriae fornix (FF) (fig 2.1.A 9) provides the main efferent pathways to the septum, hypothalamus, thalamus and corpora mamillaria. It also relays some afferent information from the contralateral hippocampus and entorhinal cortex through the commissura fornicis.

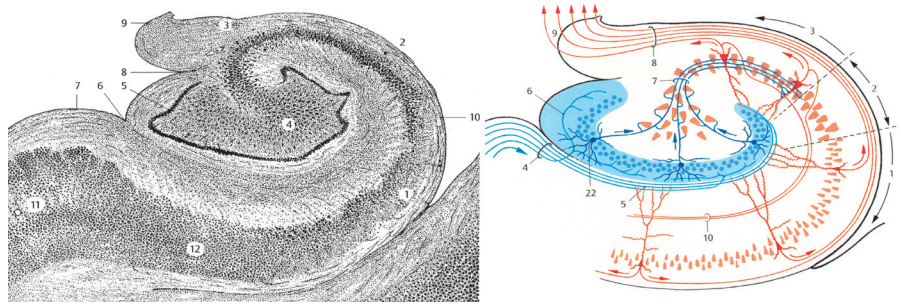

Fig. 2.1 A | Hippocampal anatomy as drawn by Ramón y Cajal, reduced to a schematic diagram of hippocampal connections

B | Key anatomical components are explained in the text below. Blue fibers indicate afferent pathways, while the red fibers indicate efferent pathways. (*Atlas van de anatomie, Deel 3, Zenuwstelsel en zintuigen*, SESAM 1975)

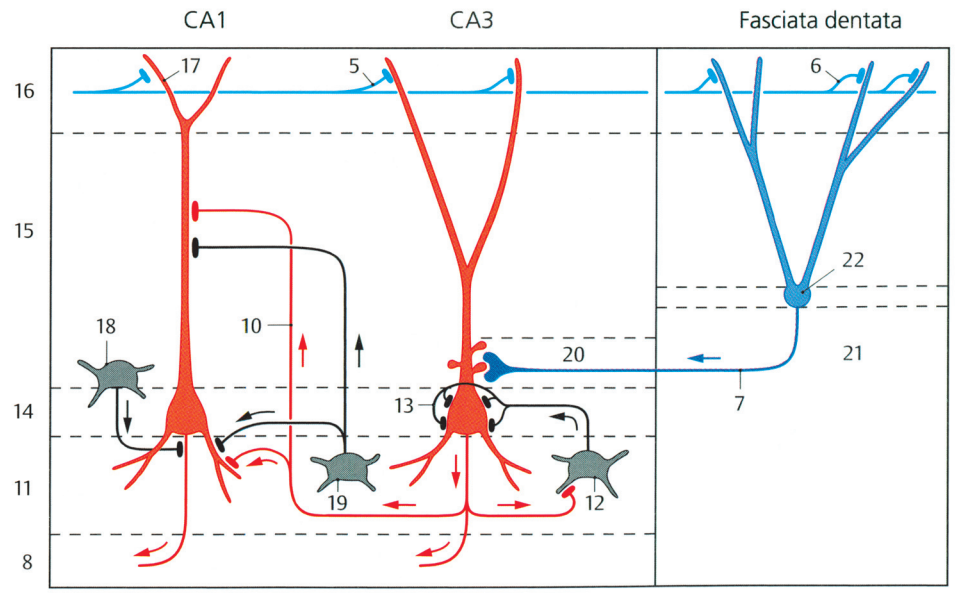

Fig. 2.2 | Schematic diagram of the hippocampal layers and connections.

However, the general direction of signal transduction is from entorhinal cortex to subiculum through the hippocampal circuitry to the alveus and the fornix (fig 2.1.B).

The cortex of the hippocampus consists of five layers of which the middle one, the *stratum pyramidale* (fig 2.2 14), contains the somata of the pyramidal cells. Their dendrites lie in the *stratum radiatum* (fig 2.2 15), which receive their input from the innermost layer, the stratum *lacunosum-moleculare* (fig 2.2 16), which is in turn connected to the subiculum and entorhinal cortex. Axons from the pyramidal cells connect to inhibitory basket cells (fig 2.2 12) in the *stratum oriens* (fig 2.2 11). These basket cells project back by very quick direct axo-somatic synapses (fig 2.2 13) on the pyramidal cells to form a negative feedback loop. Other axons from the pyramidal cells project to the *alveus* (fig 2.2 8) and eventually the FF.

The axons from the subiculum project to the hippocampal cortex, but also for a large part directly to the granule cells (fig 2.2 22) in the GCL of the DG. The molecular layer or supragranular layer, above the GCL contains the apical dendrites of the granule cells and some dispersed interneurons. The polymorphic layer or *hilus* (fig 2.2 21) contains the axons of the granule cells, usually referred to as mossy fibers (fig 2.2 7), and some inhibitory interneurons. These mossy fibers connect to the CA3 region. From the CA3 pyramidal cells recurrent branches, the collaterals of Schaffer, synapse on the dendrites of the CA1 pyramidal cells. In animals, the brain location and orientation of the hippocampus is different, but the organization and circuitry is largely identical, although the term CA4 has been dropped for small animals.

In short, the hippocampus contains a well characterized network of neurons that displays several negative feedback loops and that processes information that mainly runs from entorhinal cortex to fornix. Crucial elements are the GABAergic basket cells, necessary for the negative feedback loops, and the mossy fibers that integrate the neuronal network of the DG with that of the CA regions.

Hippocampal sclerosis

Neuroanatomically, HS is characterized by neuronal loss, most notably in the hilus, CA1 and CA3 region, gliosis and synaptic reorganization by mossy fiber sprouting. Extensive knowledge exists on the neuropathology of HS in humans, because sclerotic hippocampi become available after surgical treatment for TLE. In addition, much is known of the clinical, imaging and electrophysiological properties of the sclerotic hippocampus, because the surgical treatment necessitates extensive presurgical testing, sometimes involving invasive electrophysiological recordings.

HS is the most frequently observed pathological substrate in TLE. Several studies have shown that any significant medical event, not necessarily associated with seizures, that could possibly injure the brain in young children, was strongly linked to HS in surgical cases.[100-103] After suffering from TLE for a very long time (>15 years), progressive hippocampal neuron loss is found, but scattered through áll subfields of the hippocampus.[104] This means that seizures do induce hippocampal neuronal death, but differently from neuronal death in HS. These observations support the notion that childhood seizures are not a necessary cause for HS and that (the pathophysiology causing) HS predates the onset of epilepsy.[102,105]

An important caveat in studies of HS in human medically refractory TLE is that they reveal only the end result of the epileptogenic process. The pathologic changes observed in these patients could be either the cause or the consequence of recurrent epileptic seizures and in case of the latter, they could result in further epileptogenicity or reflect natural homeostatic mechanisms acting to suppress seizure occurrence. In addition, research is complicated by the superimposed effects of AEDs, which have invariably been used. To follow the development of HS in the period before spontaneous recurrent seizures (SRS) occurs, the lesions seen in TLE with HS in human brain have been modeled in the animal laboratory using a variety of techniques that cause hippocampal cell loss and neuronal reorganization. *For these reasons, this thesis will focus on the pre-epileptic hippocampal pathology in relationship to the future development of SRS. This type of research into mechanisms of epileptogenesis, before seizures occur, can only be done in animal models.*

Animal models of TLE

There are several ways to induce epileptic seizures, status epilepticus (SE) or SRS in animals and there are many animals to choose from. We will focus here on the models that mimic the pathophysiological features of TLE as closely as possible. These main features are: the localization of seizure foci in the hippocampus,[106] the frequent finding of an "initial precipitating injury", often SE at young age, that precedes the appearance of TLE,[102] a seizure-free time interval following the precipitating injury known as the "latent period"; and a high incidence of HS.[105]

Models that employ febrile seizures as a precipitating event deserve a special mentioning, because they so closely mimic the best known risk factor for development of TLE. In this model hyperthermia is induced in rats aged 10-17 days or mice aged 8-10 days. This induces febrile seizures to the degree of full blown SE depending on the severity and duration of the hyperthermia. Despite developments with regard to this model, investigators have difficulty to induce SRS in rats and have never succeeded in inducing SRS in mice, which is congruent with the observation that febrile seizures in humans are neither a sufficient nor necessary prerequisite for the development of TLE.

Many models induce SE as a precipitating event in rats and mice by chemical convulsants. Kainate, a specific agonist for a glutamate receptor, the kainate receptor, is one of the most popular ones. It induces SE by mimicking the effect of glutamate.[107-109] Olney *et al.* showed its effect to be particularly prominent in the hippocampus, because

Continued on p. 32

Version versus non-version

In 1880, Hughlings Jackson wrote that initial turning of the head and eyes to one side indicated a "discharging lesion" in the contralateral hemisphere.[36] Fifty years later, Foerster and Penfield called this phenomenon "adversive movements," similarly implying a contralateral epileptic focus.[79] The introduction of video-EEG showed that this hypothesis had been too simple, and controversies arose about the lateralization significance of head and eye movements during seizures. Head turning is reported in 65–96% of focal seizures.[80-82] Whereas some studies found no lateralization value at all, others showed that this clinical sign could predict seizure-onset lateralization when differentiating "version" from "non-version."[73,80-83] Version is defined as clonic or tonic head and eye deviation, unquestionably forced and involuntary, resulting in sustained and unnatural posturing of head and eyes.[80,81,83] The seizure focus is located in the contralateral hemisphere in 89% of these cases.[82] "Late ipsiversion" clinically resembles version but occurs at the end of generalized tonic–clonic seizures with ipsilateral EEG activity while contralateral activity ceases. All other forms of head turning are referred to as "non-versive" and make up 55–65% of ictal head deviations. In temporal lobe seizures, non-versive head deviation is associated with ipsilateral seizure onset focus in 94% of observed head deviations if no generalization follows within thirty seconds.[73] Hence, the distinction between version and non-version allows a high predictive value for the side of the epileptic focus in TLE.

Despite uncertainty surrounding the localizing value of many seizure phenomena such as head deviation, and the availability of many modern techniques of source localization, clinical observation attempting to understand semiology remains paramount in the treatment of epilepsy patients. This is particularly true for long-term video-EEG monitoring with intracranial electrodes used in candidates for epilepsy surgery. Because such invasive EEG covers only part of the cortex, it should be ascertained that recorded ictal discharges fit the semiology as captured simultaneously on video.

Case Description†

A 30-year-old right-handed female, suffering from medically intractable epilepsy since the age of 15, was admitted to the Dutch Collaborative Epilepsy Surgery Program. Seizures consisted of staring, impaired consciousness, orofacial automatisms, turning of head and eyes to the right and motor restlessness with profound postictal agitation and amnesia. She never has any recollection of sensations or warning signs prior to seizure onset. Seizures occurred approximately once per month, predominantly during the night. Standard and long-term EEG and interictal MEG showed frequent spikes in the posterior part of the left temporal lobe and left temporal seizure onset. The 1.5-Tesla MRI and FDG PET were normal. The Wada test showed dominance of the left hemisphere for language and asymmetric memory performance.

For exact localization of the epileptogenic source and functional eloquent cortex, 112 subdural electrodes were implanted over the left frontal, parietal and temporal lobe, including antero-, sub-and mesiotemporal areas (fig 2.3), and the video-ECoG was recorded during 5 days. Interictal ECoG showed almost continuous spiking with a pacemaker-like appearance (1–2 Hz) on the mid to posterior superior temporal gyrus, suggesting pathology with disturbance of cortical architecture.[84] After withdrawal of medication, two spontaneous seizures during wakefulness were captured, as well as a cluster of seven shorter seizures during sleep and twelve seizures following electrical stimulation. Electrographically the seizure started with gamma activity over the left medial? to posterior superior temporal gyrus, followed by spread to more inferior and posterior temporal electrodes and subtemporal and frontal electrodes (fig 2.3).

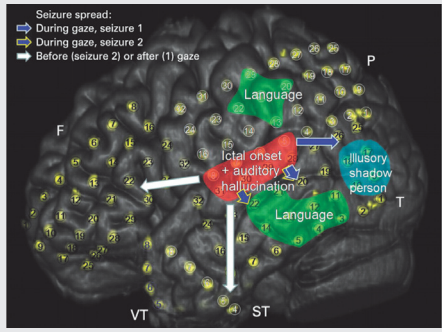

Fig 2.3 | Position of the subdural electrodes. Red area: ictal onset zone and auditory hallucinations upon electrocortical stimulation. Blue area: electrocortical stimulation of these electrodes elicited an illusory shadow person experience. Green area: electrocortical stimulation of these electrodes inferred with language tasks. F, frontal lobe grid electrodes; P, parietal lobe grid electrodes; ST, subtemporal electrodes; T, temporal lobe grid electrodes; VT, anterior temporal pole electrodes.

The first sign was a sudden, slow deviation of eyes and head towards the right. This occurred a few seconds after the first electrographical change, during spread to lower temporal electrode contacts. This was accompanied by automatisms of predominantly the left hand and face and unresponsiveness. The seizure was further characterized by orofacial automatisms, aggressive exclamations and postictal restlessness and unwillingness to cooperate. The second spontaneous seizure during wakefulness had a more insidious onset with unresponsiveness and automatisms, followed by a head and eyes movement to the right. The electrographical onset was similar to the first seizure, but the seizure spread to the frontal and subtemporal electrode contacts first and later, during gaze deviation, to the inferior and posterior temporal electrode contacts. As the gaze deviation was slow, it was interpreted as non-versive. Temporal lobe seizures with non-versive head and eye movements are strongly associated with an ipsilateral focus, so the direction of gaze was the opposite of that expected.

Later during the recording, the same head and eye movements were consistently reproduced by electrical stimulation of the contralateral temporo-parieto-occipital junction (fig 2.3). During stimulation, the patient described an irresistible urge to look to the right, because she thought a person was standing next to her. She felt this presence as a threat. It was unclear whether the feeling was based upon a visual or auditory input, or both. Further, stimulation of the medial to posterior superior temporal gyrus elicited auditory hallucinations without gaze deviation (fig 2.3).‡

The seizure-onset focus was localized in the posterior part of the superior temporal gyrus. Although this is classically the Wernicke area, electrocortical stimulation with language testing suggested that the functional language area in the patient had moved away from this seizure-onset zone (fig 2.3). A topical corticectomy with intraoperative ECoG was performed. Histological examination of the removed tissue showed disturbed cortical organization. The patient had two postoperative seizures but has now been seizure-free for over a year.

Discussion

We describe a patient with reproducible, seizure induced head deviations of unexpected origin, to illustrate that this clinical phenomenon can have various causes with diverse implications for the localization of seizure onset. Our patient exhibited non-versive movements of the head and eyes to the contralateral side at seizure onset and after stimulation. These non-versive movements might result from contralateral spatial neglect as seen after stroke involving the parietal lobe.[82] This idea is supported by ictal SPECT showing relative hypoperfusion in the parietal lobe ipsilateral to the direction of gaze.[85] However, it has never been confirmed by electrocortical stimulation, probably because there is no specific site for this negative phenomenon. Electrical stimulation of the occipital lobe has elicited head and eye movements by inducing saccadic eye movements or voluntary gazing to an aura of lights appear ing in the contralateral visual hemifield.

A reproducible gaze deviation after stimulation of the posterior temporal region, as observed in this patient, has not been described before. After stimulation of the temporo-parieto-occipital junction, our patient described a person standing beside her, but she could not specify whether this sensation was visual or auditory in nature. This phenomenon, called an "illusory shadow person," has been described after electrical stimulation of the temporo-parieto-occipital junction.[86] This area has been shown to be involved in other illusory perceptions like autoscopy and out-of-body experience.[87,88] We propose that auditory hallucinations and/or the feeling that a person was standing next to her were the reasons for the contralateral non-versive head and eye deviation at seizure onset, with inability to recall due to postictal amnesia.

Epileptic activity in intracranial EEG and associated semiology should be matched to ensure that all potential epileptogenic zones have been electrographically covered. Differentiating the nature (version or non-version) of gaze deviation can aid correct matching. In case of discrepancies, alternative hypotheses should be tested to improve understanding. The combination of the susceptibility of the posterior temporal region for auditory hallucinations,[89] "illusory shadow person" experience and left temporal, secondarily generalized seizures for postictal amnesia might explain paradoxical non-versive gaze deviations in temporal-lobe seizures.[90,91]

† We thank the patient for allowing us to publish this case history.

‡ A video of the seizures and evoked phenomena is published online at http://jnnp.bmj.com/content/vol80/issue6

Illusory shadow person causing paradoxical gaze deviations during temporal lobe seizures. JNNP 2009

Zijlmans M, van Eijsden P, Ferrier CH, Kho KH, van Rijen PC, Leijten FS.

Continued from p. 29

of the relative abundance of kainate receptors there.[110] The systemic administration of kainate induces a pattern of cortical and subcortical damage involving the piriform and entorhinal cortices, the hippocampus, the lateral septum, and several thalamic and amygdala.[111] In the hippocampus, degenerating neurons are found in the DG, hilus, CA1, and CA3, while the Timm staining shows an initial sprouting of mossy fibers that increases during the latent phase, reaching its maximum at the onset of spontaneous seizures.[112] Despite striking similarities with human TLE and HS, both in animal behavior and in neuropathology, the drawback of this model is that the flooding of the glutamate receptor system in the entire brain with a glutamate analogue may also interfere with the results of future experiments on the glutamatergic system and induce more than just hippocampal pathology. *Because this thesis focuses for a considerable part on the glutamatergic system, we preferred a model in which SE is induced by a more distant mechanism*.

Pilocarpine offers this opportunity, because it acts as a parasympathicomimetic by stimulating the muscarinic acetylcholine receptors. *In vitro* experiments have shown that the epileptogenic effect of cholinergic agents depends on the facilitation of burst discharges in hippocampal pyramidal neurons.[113,114] This mechanism explains the massive activation of hippocampal neurons during pilocarpine-induced SE. The ensuing damage is not attributed to a direct toxic effect of pilocarpine, but to a seizure-related excitotoxic effect involving glutamatergic excitotoxicity by massive Ca^{2+} influx. Furthermore, the inability of anticholinergic agents, such as atropine, to stop ongoing pilocarpine-induced SE suggests the recruitment of other excitatory mechanisms, so that SE becomes self-sustaining. The neuropathological consequences of pilocarpine induced SE are very similar to those seen after kainate injection, meaning severe neuronal damage especially in the DG, CA1 and CA3 region of the hippocampus, and hippocampal mossy fiber sprouting.[115,116]

The first evidence that the cholinergic agent pilocarpine induces SRS after a silent period was provided by Turski *et al.*[117] After injection the animal goes through several behavioral stages that have a clear EEG correlate[118-121] (Fig 2.4). Initially the animal is hypoactive (stage 1). Subsequently there is the appearance of facial automatisms, including chewing and eye blinking (stage 2), followed by head bobbing and forelimb clonus (stage 3). After this the animal rears on its hind limbs (stage 4). In the next stage, the animals cannot maintain postural control (stage 5). SE with tonic clonic convulsions represents the final stage, usually occurring 40 to 80 minutes after the injection, depending on the injected dose.[119,122] Pilocarpine-induced SE is generally fatal within 24 hours, but this can be prevented by repeated injection of diazepam or barbiturates.

Several variations of this model now exist that reduce the dose of pilocarpine needed for SE. Pretreatment by lithium approximately 20 hours before induction of SE allows for a tenfold decrease in the pilocarpine dose for the same effect.[124] The under-

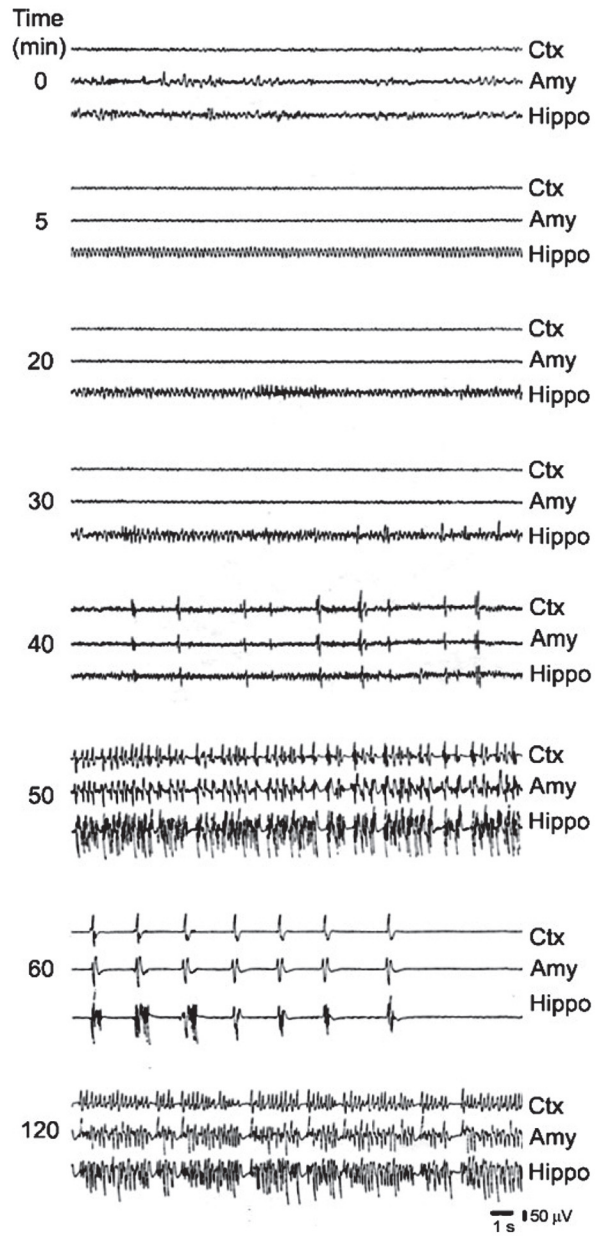

Fig. 2.4 | EEG recordings after injection of pilocarpine (400 mg/kg, i.p). Note that 5 min after injection, a theta rhythm is evident in the hippocampus. Fifteen minutes later spikes appear in the hippocampus. In the 30 min traces, high voltage spikes are detected first in the hippocampus while at 40 min, high voltage spikes are recorded from all the fields. After 50 min from the injection, electrographic seizures are seen and followed by postictal depression (60 min sample).[123]

lying mechanism for this phenomenon is unknown. Animals treated with lithium and pilocarpine show a higher success rate of inducing SE (100% vs 60%) and decreased variability in time to SE onset.[125] The systemic cholinergic effects can be diminished by adding α-methyl-scopolamine 30 min before injection of pilocarpine. This cholinergic antagonist does not cross the blood brain barrier so it cannot interfere with the central actions of pilocarpine.[115] Without this pretreatment, animals exhibit classic signs of cholinergic stimulation, including salivation, tremor and diarrhea after pilocarpine injection.[115] There is no evidence that these low doses (1 mg/kg) of alpha-methylscopolamine alter central effects of pilocarpine.[121,122] Behaviorally, metabolically, electrographically and neuropathologically these animals are indistinguishable from animals treated with only high doses of pilocarpine.

After surviving SE, animals develop normally until the SRS that characterize the chronic period appear and recur with a variable frequency of 2 to 15 per month.[117,122] In the adult pilocarpine model, the duration of the latent period lasts from 1 up to 6 weeks with a mean time interval of 14.8 days,[126] but this interval is heavily dependent on the duration of SE and whether it was treated with diazepam or other drugs.[123] It is important to stress that most studies rely upon video monitoring to establish seizure frequency. Therefore, stage 3 to 6 seizures are preferentially detected, while the less severe seizure stages (1 and 2) are frequently overlooked. This point is particularly relevant because many TLE patients hardly ever suffer from generalized seizures.[118-121] This fact, combined with the high mortality rate of approximately 30% during SE, makes this a very severe SE and TLE model.

Evidence obtained from different studies shows that behavioral and EEG changes following systemic administration of pilocarpine to rats are age-dependent.[126,127] In general, in younger rats a lower percentage of animals reaches SE, the latent phase is longer and the percentage of animals that develops SRS is lower as is their frequency.[121,126,128] Priel *et al.* found that 7–17 day old Wistar rats do not develop SRS even when all of them received a high dose of pilocarpine (380 mg/kg).131 Among rats exhibiting lithium-pilocarpine induced SE at P21, roughly the age of a human toddler, three groups of rats could be distinguished 2–3 months later.[129] The first group (~24%) developed SRS after a mean period of 74 days with behavioral manifestations very similar to those seen in adult rats. Rats in the second group (~43%) did not develop SRS but seizures could be triggered by handling, loud noises or stress. The third group (33%) developed neither SRS nor stress-induced seizures. Depending on the exact protocol used to induce and arrest SE, the percentages of animals included in these groups may vary. With our protocol, SRS are present in 44% after 19 weeks, while in another 37% seizures can be triggered, making this a fairly robust model of epileptogenesis.[130] *While it is difficult to reproduce all the features of the adult pilocarpine model when SE is induced at 21 days of age, and working with young animals is more expensive and time consuming than with adult rats, there is no doubt that the longer latency to SRS and the younger age at induction offer a better homology with the human disease.[123] The severity of the behavioral, histological and electrophysiological changes is also less severe and more congruent with human TLE than those observed in the adult model. For this reason the research in this thesis has been largely performed in the juvenile lithium pilocarpine model.*

Pilocarpine-treated animals generally show normal behavior and EEG activity during the latent period following SE. Although SE induces a weight drop, animals gain the weight quickly again and are otherwise indistinguishable from their litter mates. It has, however, been shown that during the latent period several pathophysiological phenomena possibly related to epileptogenesis occur, that will be discussed later.[104] As mentioned before, research into mechanisms of epileptogenesis during the time period that SRS occur, prevents the differentiation between the epileptogenic process itself and the pathology induced by seizures. When performing non-survival experiments in the silent phase, a major drawback is that the observed changes can only be directly related to the preceding SE, inherent to the model and shared by all animals. Post-SE pathological alterations cannot be automatically attributed to the process of epileptogenesis, since only a (large) proportion of animals will develop spontaneous or handling-induced seizures, and the epileptic fate of the animals remains unknown at the time of study. Therefore the epileptogenicity of these observations remains a matter of debate, despite the fact that a substantial number of animals develop SRS. *However, for the research in this thesis, we have decided that the benefits of evaluating the silent phase outweigh the drawbacks. Our observations will be viewed in the light of being a post SE phenomenon, but in case of persistent or progressive changes, the possibility of a role in epileptogenesis will be discussed.*

Connectivity and neurotransmission

From experiments using tissue from humans with HS and from the experimental models of TLE just described, several molecular and cellular changes have emerged that play an important role in the propensity of the human hippocampus to generate seizures. Propagation of aberrant activity however requires signal transduction from one neuron to the next and from epileptogenic cell clusters to other areas in the vicinity or, in case of generalization, to distant brain structures. *While possible mechanisms of epileptogenesis are many, from the molecular to the macroscopic level, the studies described in thesis will explore epileptogenicity in hippocampal neurotransmitter systems and their connectivity to the rest of the brain.*

Connectivity

Aberrant axonal and synaptic reorganization, in association with neuronal loss, is a characteristic feature of human HS.[131,132] The best studied type of aberrant axon sprouting is the synaptic reorganization of the mossy fiber system, which is characterized by the formation of novel, aberrant and recurrent synaptic contacts of mossy fibers onto the dendrites of hippocampal DG neurons.[133,134,135] The traditional concept is that death of hippocampal pyramidal neurons causes loss of targets for the mossy fibers.[136] This idea is in line with neuropathologic studies demonstrating that the amount of hippocampal pyramidal cell loss in the CA3 region correlates with the extent of mossy fiber sprouting.[137] The formation of recurrent collaterals of granule cell axons onto other granule cells has been proposed as a major epileptogenic mechanism that may compromise the inhibitory function of the DG, promoting spontaneous seizures.[131,132]

On a larger connectivity scale, evidence is accumulating that widespread changes occur in the white matter of epilepsy patients. Most of these studies were performed with MRI. Volumetric studies focus on determining the relative size of several brain structures and comparing these between groups. The simplest way of doing this is by outlining these structures based on neuro-anatomical knowledge and differences in signal intensity. More sophisticated tools are available now for automatic extraction of volumetric data. These techniques are particularly useful for determining white matter volume, as white and grey matter have very different signal intensities when employing the right MR protocol.

The initial evidence for involvement of distant white matter tracts in focal epilepsy came from Hermann *et al.*, who showed significantly reduced overall cerebral white matter volumes, compared to controls.[138] The relationship with epilepsy can be inferred from the fact that in both left and right sided TLE, the white matter decreases are most prominent in the ipsilateral temporal lobe.[139] The relationship with seizures became more apparent in a follow up study that showed a correlation between the duration of TLE and the decrease in corpus callosum volume.[140] These differences have also been shown for many individual fiber tracts in both adults and children.[141-146]

Another MR technique commonly used is diffusion tensor imaging (DTI), which compares the amount of water diffusion in a voxel along various axes. In pure water the diffusion is equal along all axes and is called isotropic, while in a white matter tract the diffusion is high along the tract (axial diffusivity, represented by the diffusion tensor eigen value or λ_1) and low perpendicular to the tract (radial diffusivity, reflected by λ_{2+3}). The mean diffusivity (MD) is the total amount of diffusion in a voxel, while the fractional anisotropy (FA) is a measure of the relative amount of anisotropy in a voxel (0 is perfect isotropy, 1 is perfect anisotropy). This technique will be explained in further detail in the next section (for a review see Le Bihan).[147] The earliest study is

by Arfanakis *et al.* who reported significantly increased radial diffusivity and reduced FA in the external capsule and the posterior and anterior corpus callosum.[148] Rugg Gunn demonstrated that FA decrease and MD increase have a lateralizing value in TLE patients.[149] Several studies have since been performed in humans and animals, confirming that epilepsy is associated with widespread white matter changes, characterized by a progressive lateralized reduction in volume and anisotropy, and a lateralized increase in radial and mean diffusivity.[143,150-155] It has also been shown that these changes do not recover after resection of the mesial temporal structures in TLE.[150] Another interesting point is that the white matter changes in patients with TLE with HS are similar to those in patients without HS, with the exception of the tracts directly related to the mesial temporal structures, particularly the fimbriae fornix (FF) and cingulum, which was confirmed in a histopathological study of surgical specimens.[151] The most intuitive explanation for histological findings seen in the FF of TLE patients is that they reflect downstream degeneration of the output fibers from the mesial temporal region. On the other hand, severance of the FF with its efferent projection from the hippocampus produces epileptiform discharges in the hippocampus.[156] This underlines the fact that it remains unclear whether the white matter changes are a cause or consequence of epilepsy. *For these reasons, one of the aims of this thesis is to explore the relationship between epileptogenesis and white matter pathology.*

The important question which underlying pathology causes these MR changes has received only limited attention. DTI results are usually explained by a theoretical model that proposes the FA and λ_1 reduction to be caused by axonal damage, while the λ_{2+3} and/or MD increase is supposed to indicate myelin damage, but this remains largely speculative and has thus far hardly been systematically studied in epilepsy.[151] *For these reasons we will attempt to correlate white matter pathology as identified by DTI, with histopathology in an animal model of TLE.*

Neurotransmission

In the hippocampus virtually all neurons are either glutamatergic or GABAergic. Glutamate is an amino acid that serves a multitude of roles in the mammalian brain. It is an excitatory neurotransmitter and also the immediate precursor of the inhibitory neurotransmitter GABA, and it is a building block of proteins and an energy substrate. It is crucial that extracellular levels of glutamate are kept low to allow for glutamatergic signaling and to prevent glutamatergic neurotoxocity.[157] This neurotoxicity is believed to play a role in a number of conditions, including epilepsy. Ongoing synchronized activity causes a persistent increase in extracellular glutamate and subsequent calcium influx and cell death. In the GABAergic cell, glutamate is converted to the amino acid GABA, the predominant inhibitory neurotransmitter in the adult brain which plays a

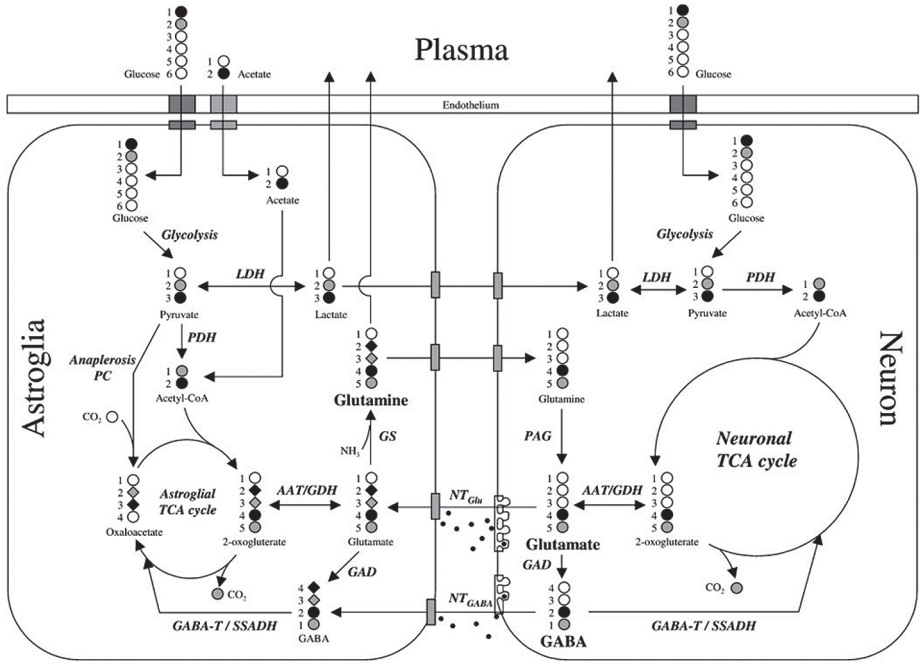

Fig 2.5 | Model of cerebral metabolism in neuronal and astroglial compartments and metabolite ^{13}C labeling patterns following the intravenous infusion of [1-^{13}C]-glucose (black circle), [2-^{13}C]-glucose (gray circle) or [2-^{13}C]-acetate (black circle). Only ^{13}C labeling during the first (half) turn of the neuronal and astroglial TCA cycles is considered. Glucose enters both neuronal and astroglial compartments and labels pyruvate and subsequently lactate through the glycolytic pathway. Astroglial lactate may be shuttled to the neuronal compartment to function as substrate in the neuronal TCA cycle. Labeling via the astroglial pyruvate carboxylase pathway (anaplerosis) is denoted by diamonds, whilst labeling via both neuronal and astroglial pyruvate dehydrogenase is denoted by circles.While anaplerosis will ultimately label the neuronal metabolite pools through the glutamate–glutamine neurotransmitter cycle, only labeling of astroglial pools is shown. Gray circles and diamonds indicate labeling from [2-^{13}C]-glucose, black diamonds show labeling from [1-^{13}C]-glucose and black circles mark labeling from either [1-^{13}C]-glucose or [2-^{13}C]-acetate. Solid boxes represent specific membrane transporter proteins like GLUT-1 for glucose transport across the blood-brain barrier. AAT, aspartate aminotransferase; GABA-T, GABA transaminase; GDH, glutamate dehydrogenase; LDH, lactate dehydrogenase; SSADH, succinate semialdehyde dehydrogenase (courtesy of De Graaf *et al* 2003).[166]

critical role in the regulation of the excitability of neuronal networks.[158] The multiple roles of glutamate and GABA require a complex homeostatic system involving several cell specific elements including membrane transporters and enzymes in both neurons and astrocytes. The predominantly glial uptake of glutamate[157,159] and the fact that neurons lack the enzyme pyruvate carboxylase (PC), necessary for de novo synthesis of glutamate and GABA from glucose,[160] creates a complex cycle between neurons and glia to replenish neuronal neurotransmitters stores.[64,161,162] In this cycle, glutamate is released and taken up into surrounding astrocytes, transformed into glutamine by the astrocyte-specific enzyme glutamine synthetase (GS),[163] and released into the extracellular space from which it is taken up into neurons and transformed back to glutamate by phosphate-activated glutaminase (PAG).[160] In the GABAergic synapse, GABA is taken up into astrocytes and catabolized to the tricarboxylic acid (TCA) cycle intermediate succinate, which is used for synthesis of glutamine. Glutamate formed by PAG activity in the GABAergic neurons is quickly converted by glutamate decarboxylase (GAD) to GABA. This metabolic system is summarized in figure 2.5, which includes the labeling pattern for the ^{13}C MRS experiments discussed in a later section.

An important question related to glutamate and GABA homeostasis is the stoichiometry of the glutamate/GABA-glutamine cycle. It is crucial that for the cycle to work, neurons must receive at least the same number of building blocks as they lose in a given time period, meaning that the transfer of glutamine from astrocytes must at least equal that of the lost neurotransmitters glutamate or GABA. In addition, there appears to be a linear correlation between increments of cerebral energy metabolism and total neurotransmitter cycling.[164] This relation was subsequently refined by separating the contributions of excitatory glutamatergic and inhibitory GABAergic neurotransmission.[165] This means that above a certain "maintenance level" of approximately 20%, each additional quantum of energy produced in the brain is used for the neurotransmitter cycle. This central role of the glutamate/glutamine-GABA cycle implies that any significant brain pathology will be caused by, or have consequences for, neurotransmitter metabolism, and that any serious disruption of the complex interaction between neurons and glia will lead to a pathological condition. *This thesis will therefore focus for a substantial part on the role of the glutamate-glutamine-GABA cycle in epileptogenesis.*

Neurotransmitter changes in HS

Considerable effort has been expended on characterizing inhibitory and excitatory neurotransmission in the epileptic human hippocampus. During and Spencer showed by *in vivo* micro-dialysis during surgery, that glutamate release occurs not only during seizures, but also preceding seizure onset.[167] Furthermore, the glutamate release was much greater ipsilateral to the seizure onset in patients with HS compared to contralateral. For GABA, they showed a prominent release during seizures in the non-sclerotic hippocampus compared to the sclerotic one.[167] This suggests that in HS, glutamate plays a role in the initiation of seizures, while the GABAergic system ipsilateral to the seizure onset zone is insufficient to counteract this. Their study also showed that the high levels of glutamate occurring during seizures could reach neurotoxic levels, suggesting they play a role in the progressive neuronal loss associated with HS. Apart from changes in

glutamate and GABA homeostasis, a study by Cavus *et al.* using zero flow measures of baseline amino acids during temporal lobe surgery, showed that HS is associated with high lactate levels and a general reduction in the glutamate-glutamine cycle.[168] Biopsy studies of sclerotic hippocampal tissue from human subjects suffering from epilepsy have also revealed a decreased level of glutamate-glutamine cycling.[169]

In the pilocarpine model, SE is mediated by a glutamate release that leads to excitotoxicity and neuronal death.[170] This has several consequences on a metabolic level. It has for instance been shown that remodeling of the glutamate receptor system at the protein level occurs as early as 5 hours after SE and proceeds during the course of the disease.[120] Many different changes in the glutamate receptor and transporters have been described in the chronic phase.[171,172] Concerning the glutamate-glutamine cycle, a study in the chronic adult lithium-pilocarpine model of TLE by *ex vivo* ^{13}C MRS indicated that astrocytic metabolism is not compromised in these animals, but that glutamate turnover was reduced suggesting a preferential metabolic malfunction in the neuronal compartment.[173] This is in contrast with many observations in animal models that show metabolic disturbances of both neurons and astrocytes. Proof for glial involvement comes from studies showing decreases in GS, a glial enzyme, in both human hippocampal sclerosis and the juvenile lithium pilocarpine model.[103,174,175]

However, while much is known about the metabolism of the epileptogenic hippocampus in human or experimental TLE, the preceding latent phase has received more limited attention. This silent phase is marked by an important imbalance between inhibition and excitation,[119] but more elaborate research on the metabolic background behind this imbalance is lacking. Several glutamate transporters that are reduced in human chronic TLE show no reduction in the latent phase of the lithium pilocarpine model. The only component of the neurotransmitter cycle that was shown to be reduced in the latent phase is GS.

Some metabolic changes, such as loss of GABAergic inhibition and reduction in GS activity precede the onset of SRS. *However, relatively little is known of metabolic hippocampal changes after SE and before the onset of SRS. Therefore, one of the aims of this thesis is to determine concentrations and metabolic rates of several important metabolites in the hippocampus in the weeks after SE.*

Nuclear magnetic resonance

Principles of NMR

NMR is such a versatile technique that it can be used to contribute to all of the diverse aims formulated in this introduction. NMR was first developed in 1946 by research groups at Stanford and M.I.T. The radar technology developed during World War II made many of the electronic aspects of the NMR spectrometer possible and after the war, scientists began to apply the technology to chemistry and physics problems. In 1952 the Nobel prize was awarded to Felix Bloch and Edward Mills Purcell for their discoveries in this field. Over the next 50 years NMR developed into the premier technique available to determine detailed chemical structure. During the 1970's, the technique was adapted by to enable imaging of the human body for which Paul Lauterbur and Peter Mansfield earned the Nobel Prize in 2003.

Water is a molecule composed of hydrogen and oxygen atoms. The nuclei of the hydrogen atoms act as microscopic compass needles when exposed to a strong magnetic field. They align with the magnetic field, but also rotate with a known frequency which is dependent on the strength of the magnetic field. By varying the magnetic field with a known gradient along two axes, the frequency of the hydrogen atoms can be manipulated to reflect their location. The sample can also be perturbed selectively by RF pulses that are for instance chosen in such a way that only atoms in a slice of the sample resonate with the pulse. After the pulse, a resonance wave is emitted when the nuclei return to their previous state. The small changes in the oscillations of the nuclei are detected and through both the gradient and the slice selection, it is possible to build up a 3D image that reflects aspects of the chemical structure of the tissue, including differences in the water content and in movements of the water molecules. The developments in NMR have been explosive and new techniques are developed on almost a weekly basis, because cleverly combining the properties the gradients with RF pulse design, allows for an unimaginable array of possibilities. *This thesis will focus on diffusion based imaging techniques and several in vivo MRS techniques that range from straightforward ^{1}H MRS to new developments in GABA-edited and dynamic ^{1}H-[^{13}C]-MRS.*

Diffusion based imaging techniques

When encoding the spatial position of an atom by combining gradients and slice selection pulses, acquiring the signal from this atom must be performed rapidly, because otherwise diffusion may have moved the nucleus to a different location causing dephasing and signal loss and thereby obscuring the outcome of the experiment. However, as often in NMR, this phenomenon can be exploited to our advantage. Most diffusion based techniques encode the atoms in a voxel and then dephase them with one gradient only to rephrase them with the exact inverse gradient. Only atoms that have remained

in the same position will return to the initial state. Atoms that have diffused are permanently dephased and lost for detection. By varying the strength of the gradients and their timing, a curve can be reconstructed that describes how sensitive a certain tissue is for this phenomenon. The coefficient of this curve is called the apparent diffusion coefficient (ADC) and is taken as a quantified measure of the amount of diffusion in a voxel.

This experiment can subsequently be made sensitive to the direction of diffusion by applying the gradients in a series of separate directions. In a liquid environment the diffusion will be the same in all directions, but in a laminar structure as the corpus callosum (CC), diffusion along the tracts will be higher than perpendicular to tracts. As described in a previous section, the degree of anisotropy is generally expressed as the FA in a value between 0 and 1. Mathematically, the diffusion in a voxel is recalculated into a tensor, a 3D vector, that can be described as a combination of three principal vectors, called Eigen vectors, designated λ_1, λ_2 and λ_3. λ_1 is the main axial vector and is also referred to as the axial diffusivity. λ_2 and λ_3 are usually averaged to represent the radial diffusivity. The average of the three is called the mean diffusivity (MD), a measure of total diffusion in a voxel and equivalent to the rotationally invariant trace ADC. An advanced technique like "fiber tracking" infers the directionality of white matter tracts from the axial versus radial diffusivities and uses this to align anisotropic voxels with a post processing algorithm to reconstruct entire tracts.

Spectroscopic techniques

As mentioned previously, NMR has been developed as a technique that enabled the analysis of molecular structure. Without much adaptation, this technique can also be used to determine the presence and concentration of chemical compounds in the human body. Each atom with a nucleus with an odd mass or odd atomic number can be magnetized and therefore be detected by NMR. Because the resonance frequencies of these nuclei are significantly different, usually different RF coils are used for different nuclei. The signal intensity is proportional to the number of nuclei, meaning their concentration, while the exact resonance frequency is not only determined by the species of the nucleus, but also by the molecular structure surrounding the nucleus. This allows for both the determination of molecular structure and the quantification of its concentration. These experiments are usually combined with some type of localization technique to exclude unwanted signals (*i.e.* fatty tissue surrounding the skull) or to allow for selective sampling of a structure of interest (*i.e.* the hippocampus). Quantification of the concentration of the metabolites can be performed in two ways. The first is determination of the area under the peak in relationship to the known concentration of a stable metabolite (water, creatine) or in relationship to the concentration of a compound in a

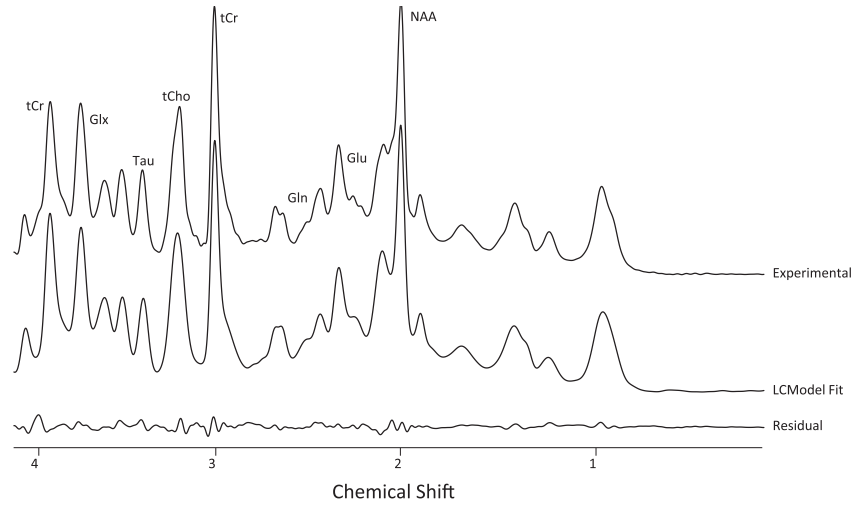

Fig 2.6 | ^{1}H MR Spectrum of rat brain (top trace), analyzed with LCModel producing the spectral fit in the bottom trace. This modeled spectrum resembles the original experimental spectrum very closely. Various important metabolites are indicated.

reference tube. The other method, more commonly used, is LCModel.[176] This is a mathematical model that attempts to recreate the entire spectrum from a library of chemical compounds with known resonance frequencies. *Most MRS quantification analyses in this thesis will be performed with this technique.* Most experiments are performed with a hydrogen coil, because hydrogen is the most abundant atom in organic material. However, in these experiments, the water signal overwhelms the signal of any other metabolite. To suppress this signal an inversion or dephasing pulse is used at the water frequency. Many interesting cerebral metabolites can then be probed, a few of which will be discussed here.

N-Acetyl aspratate (NAA) is the second most concentrated molecule in the brain after glutamate and gives off the largest signal in ^{1}H MRS of the brain. It is synthesized in neurons from aspartate and acetyl-coenzyme A. The proposed functions of NAA are many; the molecule is a neuronal osmolyte involved in fluid balance in the brain, a source of acetate for lipid and myelin synthesis, a precursor for the synthesis of the important neuronal dipeptide N-Acetylaspartylglutamate, and/or a contributor to energy production from glutamate in neuronal mitochondria. In the brain, NAA is thought to be present predominantly in neuronal cell bodies, by which it can act as a neuronal marker.

A group of molecules that all contain a choline group are jointly referred to as choline. Choline and its metabolites are needed for three main physiological purposes: structural integrity and signaling roles of cell membranes, cholinergic neurotransmission, and as a major source of methyl groups for methylation of DNA to adapt gene expression patterns. However, the bulk of the MR visible choline containing compounds is involved in membrane homeostasis. Decreases are therefore often explained as lysis of membranes, while increases are indicative of gliotic or neoplastic processes.

Several neurotransmitters are visible in the ^{1}H MR spectrum, such as glutamate and glutamine. GABA is heavily overlapped by other metabolites and therefore not reliably quantifiable. However, a technique called GABA- editing was developed to circumvent this problem. In short the technique consists of a simple ^{1}H MRS sequence but with an inversion pulse added at the frequency of one of the GABA resonances. This inversion pulse is carried forward to the other two GABA resonances. The experiment is performed both with, and without the inversion pulse. After subtraction of the two spectra, clean GABA peaks are left for quantification. *Because the most important excitatory (glutamate) and inhibitory neurotransmitters (GABA) and their metabolic intermediate glutamine can be measured non- invasively and in vivo with ^{1}H and GABA-edited MRS, the studies described in this thesis aim to quantify changes in concentrations of these metabolites following status epilepticus and during the process of epileptogenesis.*

Unfortunately, another abundant proton in biological tissues, ^{12}Carbon, is MR invisible. In general, however, every drawback in MR provides the opportunity for an interesting experiment. In this case infusion of substances containing the MR visible isotope ^{13}C enables the analysis of the replacement rate or incorporation rate of this isotope in the biochemistry of the living subject, thus selectively probing metabolic steps. Detection of the ^{13}C isotope can be done directly with a dedicated ^{13}C coil or indirectly by detection of the influence the ^{13}C isotope exerts on nearby protons with a regular ^{1}H coil. This technique has some advantages over its competitor because it has a higher sensitivity and provides the regular ^{1}H MRS data in the same experiment. The drawback is that in the so called proton observed carbon edited sequence (^{1}H-[^{13}C]), the resonances overlap heavily. This is especially problematic for low concentration metabolites such as GABA and has prevented detection of GABA under normal physiological circumstances. *One of the aims of this thesis will therefore be to optimize currently available techniques to attempt the detection of GABA turnover under normal physiological conditions. If this aim is met, full neurochemical profiling of the hippocampus during epileptogenesis is the next aim.*

Aims and outline of the thesis

TLE with HS is characterized by seizures originating in the temporal lobe in conjunct with sclerotic changes of the mesial temporal structures. This type of seizure disorder is both the most common ánd the most medically intractable form of epilepsy. Pathophysiologically a precipitating event in early childhood, *i.e.* prolonged febrile seizures or status epilepticus, is followed by a latent period, after which SRS commence. Initially these seizures can be treated by AEDs, but over time medical intractability develops, suggesting a progressive process: epileptogenesis, which starts with the initial precipitating event.

Studies of human TLE and/or HS suffer from the inherent problem that the observed pathology could be the cause, but also the consequence of seizures. This thesis aims to probe the process of epileptogenesis and the changes that occur before the onset of SRS. This type of research can only be done in animal models. We chose the juvenile lithium pilocarpine model of TLE because it models many of the age-dependent, histopathological, behavioral and electrophysiological features of human TLE in a considerable percentage of animals (~80%) without directly interfering with the glutamatergic system. Investigating the silent phase in this model in terminal experiments, carries the inherent risk that strict relationships between observations and SRS cannot be made definitively. For this reasons, our observations will be viewed in the light of being a post-SE phenomenon, but in case of persistent or progressive changes, the possibility of a role in epileptogenesis will be discussed.

While possible mechanisms of epileptogenesis are many from the molecular to the macroscopic level, this thesis will explore epileptogenicity from the perspective of hippocampal neurotransmitter systems and hippocampal connections to the rest of the brain. In these connections, the white matter tracts, several changes have been shown with MRI. These changes are more severe on the side of the seizure onset zone and increase with the duration of TLE, indicating a direct relationship with the seizure disorder. Because severance of the main efferent white matter tract of the hippocampus can actually cause seizures, it also remains uncertain whether these changes are a cause or consequence of these seizures. In addition, the histopathological correlate of these findings remains unclear. *The first aim of this thesis therefore is, to explore the evolution of these white matter changes and their histopathological correlate during epileptogenesis* ***(Chapter 3)***.

Many studies have indicated that TLE with HS is characterized by neuronal loss, gliosis, and by an imbalance between inhibitory and excitatory neurotransmission. During human temporal lobe seizures, glutamate increases before seizures start and reaches neurotoxic levels during seizures. On the other hand GABA levels in the epilepto-

genic temporal lobe increase, but remain lower than in the contralateral lobe, indicating an insufficiency of this inhibitory system. The interaction between the sclerotic structural changes in the hippocampus,their metabolic consequences, and the imbalance in neurotransmitter concentrations remains elusive, as is their role in epileptogenesis. *The second aim of this thesis is to study acute structural brain changes during status epilepticus with MR* ***(Chapter 4)****, and to characterize long-term hippocampal structural pathology in relation to neurotransmitter levels following SE, during epileptogenesis, in the latent phase of the juvenile pilocarpine model of TLE* ***(Chapter 5)***.

The stoichiometric relationship between energy metabolism and neurotransmitter cycling implies that any significant brain pathology will be caused by, or have consequences for, neurotransmitter metabolism and that any serious disruption of the complex interaction between neurons and glia will lead to a pathological condition. Although current methods allow for the MR characterization of glutamatergic neuronal glial interactions, GABA turnover remained below detection threshold under normal physiological conditions in MRS studies. *Therefore, the third aim of this thesis is to optimize currently available techniques to detect and quantify GABA turnover in vivo with MRS under normal physiological conditions* ***(Chapter 6)***.

When this aim is met, full neurochemical profiling of the hippocampus, for both excitatory and inhibitory neurotransmission is possible. Currently, no studies have been performed that give a comprehensive description of Glutamate-Glutamine-GABA cycling in a live organism in epilepsy or epileptogenesis. Although these studies are technically challenging, we aim to perfect current methods to enable such a study. *The fourth aim of this thesis is to provide a comprehensive description of both excitatory and inhibitory neurotransmission in the course of the process of epileptogenesis that follows status epilepticus with dynamic MRS* ***(Chapter 7)***.

3

In vivo ^{1}H magnetic resonance spectroscopy, T_2-weighted and diffusion-weighted MRI during lithium-pilocarpine induced status epilepticus in the rat

Pieter van Eijsden[1,2]
Robbert G.E. Notenboom[3]
Ona Wu[4]
Pierre N.E. de Graan[3]
Onno van Nieuwenhuizen[1]
Klaas Nicolay[5]
Kees P.J. Braun[1]

1. Departments of Pediatric Neurology, Rudolf Magnus Institute of Neuroscience, University Medical Center Utrecht, The Netherlands
2. Department of Neuroscience & Pharmacology, University Medical Center Utrecht, The Netherlands
3. Biomedical MR Imaging and Spectroscopy Group, Image Sciences Institute, University Medical Center Utrecht, The Netherlands
4. Department of Biomedical Engineering, Eindhoven University of Technology, Eindhoven, The Netherlands

Brain Research, Volume 1030, Issue 1, 24 December 2004, pages 11-18

TLE is associated with febrile convulsions and childhood SE. Since the initial precipitating injury, triggering epileptogenesis, occurs during this SE, we aimed to examine the metabolic and morphological cerebral changes during the acute phase of experimental SE noninvasively. In the rat lithium–pilocarpine model of SE, we performed quantified T_2- and isotropic DW MRI at 3 and 5 h of SE and acquired single-voxel ^{1}H MR spectra at 2, 4 and 6 h of SE. T_2 was globally decreased, most pronounced in the amygdala (Am) and piriformic cortex (Pi), in which also a significant decrease in ADC was found. In contrast, ADC values increased transiently in the hippocampus and thalamus. MR spectra showed a decrease in NAA and choline and an increase of lactate in a hippocampal voxel.

The T_2 decrease, attributed to raised deoxyhemoglobin, and the presence of lactate both indicate a mismatch between oxygen demand and delivery. The ADC decrease, indicative of excitotoxicity, confirms that the amygdala and piriformic cortex are particularly vulnerable to lithium–pilocarpine-induced seizures. The transient ADC increase in the thalamus may reflect the breakdown of the blood–brain barrier, which is shown to occur in this region at these time points. Neuronal damage and failure of energy-dependent formation of NAA are likely causes of an observed decrease in NAA, while the decrease in choline is possibly due to depletion of the cholinergic system. This study illustrates that relative hypoxia, excitotoxicity and concomitant neuronal damage associated with SE can be probed noninvasively with MR. These pathological phenomena are the first to contribute to the pathophysiology of spontaneous recurrent seizures in a later stage in this animal model.

Introduction

In about 80% of the patients suffering from partial complex epilepsy, the primary focus lies in the temporal lobe.[177] Adequate seizure control can be achieved in 50% of these patients with anti-epileptic medication. Another 35% can be helped with surgical intervention, which leaves 15% with drug-resistant and sometimes severely disabling TLE.[178] Unfortunately, the etiology of TLE remains largely unknown.

A relationship has been established between the development of TLE and seizures or status epilepticus (SE) during early childhood.[179] Furthermore, there is convincing evidence that SE and prolonged seizures are associated with lasting brain damage,[67] cognitive impairment[66] and increased risk of seizure recurrence. Characterizing the very early metabolic and morphologic changes induced by SE in the healthy brain is therefore a necessary step in the elucidation of epileptogenesis in TLE.

Epilepsy-induced pathology has been extensively characterized *ex vivo* in the lithium–pilocarpine model of TLE. In this rat model, acute SE is induced by systemic administration of the cholinergic muscarinic agonist pilocarpine after pretreatment with lithium.[121,180] After a latent phase, spontaneous seizures occur, originating in the amygdalo–hippocampal complex. The histopathology, electro-encephalographic features and clinical symptoms of this model strongly resemble human TLE.[117] The histopathological correlate is HS, a gliotic lesion in the temporal lobe in humans frequently associated with TLE. Furthermore, the highly stereotyped and predictable progression of SE and the subsequent development of intractable chronic epilepsy make the model robust and ideally suited to study the pathophysiology of human TLE.

MRI and MRS enable the characterization of cerebral morphology and metabolism noninvasively and *in vivo*. Therefore, clinical diagnostic tools based on MR may be developed for analysis of the progression of SE and subsequent cerebral damage on an individual basis. However, the *in vivo* MR research on this subject has yielded contradictory results. In the present study, single-voxel ^{1}H MRS high-resolution quantified T_2- and isotropic DW MRI were combined for the first time during acute lithium–pilocarpine-induced SE in the rat to examine the metabolic and morphological changes that occur in the very early stages following the induction of SE.

Methods

Animal model

Ten male Wistar rats (400 g; UWU-CPD; Harlan, Utrecht, The Netherlands) were injected intraperitoneally with 3 mEq/kg lithium chloride 18 to 20 h prior to induction of SE. Thirty minutes before the subcutaneous administration of 40 mg/kg pilocarpine hydrochloride (Sigma-Aldrich Chemie, Zwijndrecht, The Netherlands), 1 mg/kg of scopolamine methyl nitrate (Sigma-Aldrich Chemie) was injected intraperitoneally to antagonize the peripheral cholinergic effects of pilocarpine.[122] Because immobilization and accurate anesthesia are a prerequisite for MR experiments and the seizing animals are hard to handle and to intubate during SE, we chose to induce anesthesia prior to administration of pilocarpine immediately after injection of scopolamine. Anesthesia was induced with a mixture of fluanisone (5.5 mg/kg) and fentanylcitrate (0.17 mg/kg). Subsequently, animals were intubated and mechanically ventilated with 1.2% halothane in O_2/N_2O (30%:70%) at 70 ventilations a minute with 33% inspiration. One hour after pilocarpine injection, halothane was discontinued for 10 min to observe clinical signs of seizure activity, indicating successful induction of SE. Ventilation with halothane was then restarted, and animals were positioned in the magnet. During MR experiments, body temperature was continuously measured and kept at 37 °C using a heating pad. Expiratory CO_2 was monitored (Datascope, Paramus, NJ) to control the depth of anesthesia. After the experiments, which lasted 7 h, halothane was discontinued again to assess whether epileptic activity was still present. Immediately after seizure observation, rats were sacrificed by transcardial perfusion with 4% formaldehyde under pentobarbital (nembutal, Sanofi Santé, France) (300 mg/kg) anesthesia. Eleven weight-matched control animals underwent exactly the same experimental protocol but were not injected with pilocarpine hydrochloride.

Two pilot experiments were performed to show the reproducibility and reliability of the animal model. In the first, seizures were induced with the above-described protocol in 10 non-anesthetized rats, with the objective to determine whether the animals consistently showed the sequential pattern of behavioral seizure characteristics reported before by various authors.[121,126] This pattern of behavior includes the following stages: mouth and facial movements, head nodding, forelimb clonus, rearing, rearing and falling and, finally, loss of postural control. The second pilot experiment aimed to determine whether anesthesia during MR experiments had any effect on the occurrence of seizure activity. For this purpose, EEG measurements were performed in two separate animals while applying the above-described anesthesia protocol. Epidural electrodes were placed over the parietal lobes and referenced versus a grounding electrode attached to the tail. EEGs were digitally recorded with a sample rate of 1000 Hz. A baseline EEG under anesthesia was acquired for 1 h, after which scopolamine and pilocarpine were injected. EEG monitoring was then continued for 6 h and visually inspected for signs of epileptic activity. All experimental procedures were approved by the Committee on Animal Experiments of the medical faculty of the University Medical Center Utrecht.

MR protocol

The MR experiments were performed using a Varian INOVA console (Varian Associates, Palo Alto, CA) interfaced to a 4.7-T magnet (Oxford instruments, Oxford, UK) equipped with a high-performance gradient insert (rise time=220 mT/m in 300 μs.). A Helmholtz volume coil and a circular 2-cm diameter inductively coupled surface coil were used for pulse transmission and signal detection, respectively. Sagittal scout images were generated to determine the position of the slice stack used in the DW and T_2 experiments. MRI was performed at 3 and 5 h after confirmation of SE, while MRS was done at 2, 4 and, in seven animals, also at 6 h SE. In control animals, MR images and spectra were acquired only once.

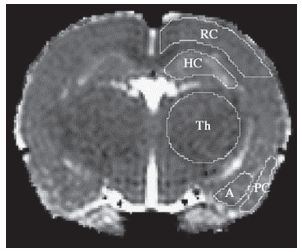

Fig. 3.1 | T_2 map during SE. Average T_2 values were calculated for the regions of interest (ROIs) indicated. RC: retrosplenial cortex, HC: hippocampus, Th: thalamus, A: amygdala, PC: piriformic cortex. ROIs were chosen on the basis of the Paxinos brain atlas.[20]

Quantitative T_2 imaging was performed using a multi-spin-echo multislice sequence acquiring 14 coronal slices of 1 mm thickness with a repetition time (TR) of 3 s and echo times (TE) of 17.5, 35, 52.5, 70, 87.5, 105, 122.5 and 140 ms (128×128 data matrix, zero-filled to 256×256, field of view 3.2×3.2 cm, two acquisitions). A parametric T_2 map was generated on a pixel-by-pixel basis with a linear regression fit of the log of the signal intensity (Fig. 3.1).

A multislice spin-echo sequence was weighted for diffusion in three orthogonal directions (X, Y and Z) (TR=2 s, TE=45 ms, b values=30, 538 and 1670 s/mm^2, diffusion time=21.6 ms, 128×128 data matrix, zero-filled to 256×256, field of view 3.2×3.2 cm, two acquisitions) with a TR of 2 s and a TE of 45 ms. apparent diffusion coefficient (ADC) maps were calculated separately for the three directions with a linear regression fit of the log of the signal intensity (Fig. 3.2, overleaf). The resulting images were averaged for calculation of the trace ADC [(X+Y+Z)/3].

For single-voxel ^{1}H MRS, a PRESS localization technique[181] was used to define a 100-mm^3 (X=10 mm, Y=2.5 mm, Z=4 mm) voxel containing the hippocampal area (CHESS water suppression, TR=2 s, 256 averages). A TE of 144 ms was used because the phase modulation at this TE causes inversion of the lactate doublet (Fig. 3.3, overleaf).

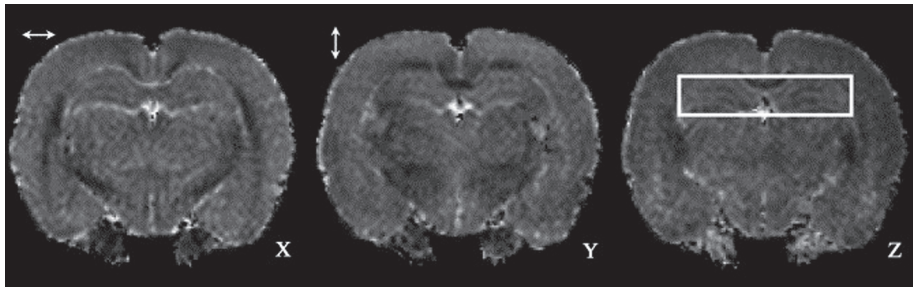

Fig. 3.2 | ADC maps during SE, with diffusion gradients applied in X, Y and Z direction separately. Anisotropy is clearly visible in the corpus callosum, which is hyperintense, when the gradient is applied in the X direction and hypointense when applied in the Y or Z direction. ADC values were determined in the areas defined in Fig. 3.1 for all directions separately to calculate the trace ADC. In the right-sided image, the voxel of interest used for ^{1}H spectroscopy is shown.

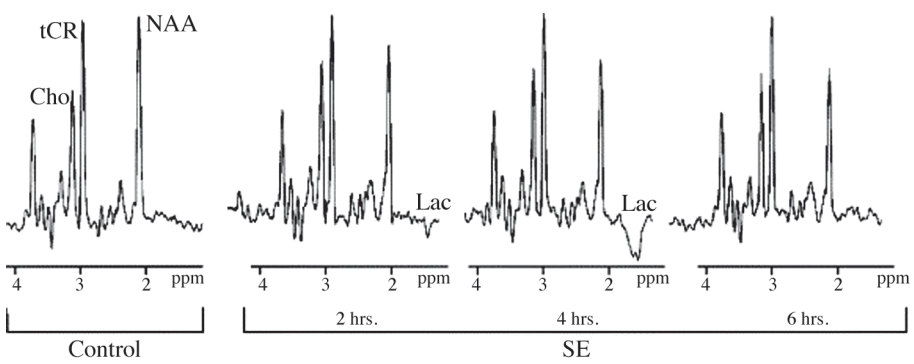

Fig. 3.3 | Typical ^{1}H MR spectra obtained from the hippocampal voxel of interest shown in Fig. 3.2. The metabolites analyzed are N-acetylaspartate (NAA), total creatine (tCr),choline (Cho) and lactate (Lac). A control spectrum is shown on the left-hand side. The three spectra on the right-hand side were obtained after 2, 4 and 6 h of SE, respectively, in the same animal. It can be seen that an inverted lactate peak was present after 2 and 4 h SE, but it had disappeared after 6 h. The NAA and choline-resonances progressively decreased.

MR data analysis

The T_2 and ADC maps were spatially coregistered with an automated image registration software package, AIR 5.2.3 (UCLA, CA)[182] and evaluated with the image-analysis software package Alice v 4.4.3 (Parexel Int., Waltham, MA). Regions of Interest (ROI) were manually drawn in the retrosplenial cortex (C), piriformic cortex (Pi), hippocampus(HC), thalamus (Th) and amygdala (Am) in both the right and left hemispheres as illustrated in Fig. 3.2. ROIs were chosen on the basis of the Paxinos brain atlas.[183] The mean T_2 and ADC were calculated for the selected structures.

Spectra were manually phased (zero and first order). The NAA resonance peak was assigned a chemical shift of 2.02 ppm. The relative peak areas of the metabolite resonances were determined using iterative fitting of the time domain signals with the variable projection method VARPRO.[184] Metabolite concentrations were expressed as ratios. NAA/choline-containing compounds (Cho), NAA/total creatine (tCr) and Cho/tCr ratios were calculated. Lactate was scored as a dichotomous variable and considered present if an inverted doublet exceeded the baseline noise at 1.33 ppm.

Statistics

Tissue water T_2 and ADC values of the right and left hemispheres were first compared for each ROI in each animal separately. A two-tailed Student's t test revealed no significant differences between hemispheres. Data from both sides were therefore averaged for further analysis. T_2, ADC and spectroscopic data of SE rats were compared with those of control animals for every time point, and statistical significance was calculated with two-tailed Student's t tests with Bonferroni correction. Data are expressed as mean±the standard error of the mean (S.E.M.). In all statistical analyses, $p<0.05$ was considered significant, while $p<0.01$ was considered highly significant.

Results

Animal model

In the first pilot experiment, 10 adult non-anesthetized lithium–pilocarpine injected animals showed behavior closely resembling the behavior described in literature.[119,121,122,180] Mouth and facial movements started within minutes of injection, progressing to intermittent periods of head nodding and clonus of the forelimbs after approximately 30 min. These partial seizures become more general after about 40 min, reflected in rearing and falling and eventually loss of postural control. This behavioral pattern was very robust, showing little variation amongst injected animals. All animals eventually showed seizures, which, if left untreated, resulted in death.

In the second pilot experiment, EEGs of both animals injected with lithium and pilocarpine under halothane anesthesia show a clear progression from normal baseline to epileptic activity. These epileptiformic EEG manifestations were clearly present approximately 40 min after pilocarpine injection and lasted until termination of the experiment 6 hours later. Fig. 3.4 (overleaf) shows a typical example of an EEG trace of an anesthetized epileptic animal before and 2 hours after injection of pilocarpine. Analogous to EEG recordings of awake pilocarpine-injected rats during SE, in the anesthetized animal, pilocarpine injection led to bursts of spiking and spike-wave activity, as well as episodes with EEG synchronization (Fig. 3.4B and C).[117,126,128] EEG abnormalities started approximately 45 min after injection and were observed during the entire

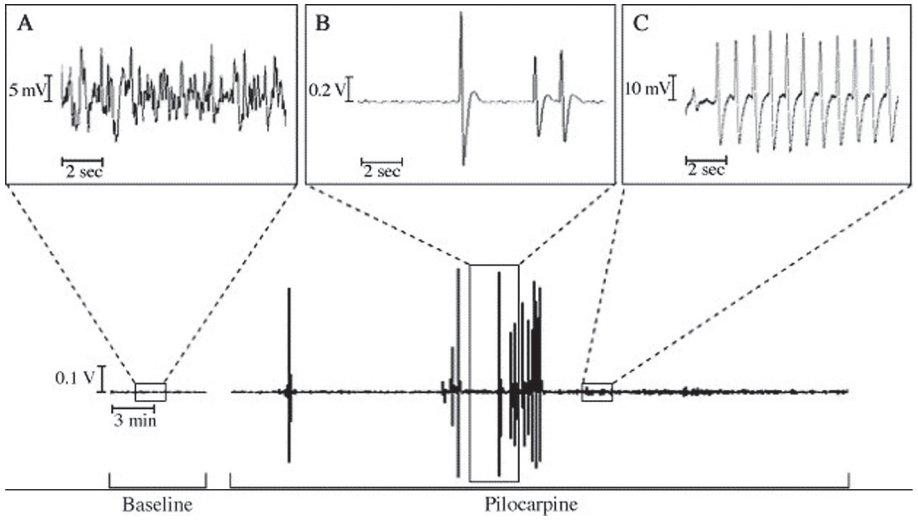

Fig. 3.4 | Typical EEG recording of anesthetized pilocarpine-injected rat. Panel (A) illustrates the irregular low-amplitude baseline EEG prior to injection of pilocarpine. Panels (B) and (C) are examples of epileptic EEG changes during SE, characterized by irregular high-amplitude spike-wave complexes and synchronization of the background pattern (B) and series of rhythmic spike-wave complexes (C).

duration of the experiment. However, no behavioral manifestations of seizures were observed during anesthesia.

In the animals on which MR was performed, body weight of control (397 g.±6.0) and experimental (406 g.±7.5) animals did not differ significantly. When halothane was discontinued, before and after the MR protocol, all pilocarpine-injected animals showed behavioral manifestations of seizures, as was expected from the pilot experiments. During the MR experiments, all control and experimental animals were stable, showing normal CO_2 curves and having normal body temperature. No motion artifacts due to seizures were observed.

MR imaging

T_2 maps

A typical example of a parametric T_2 image during SE is shown in Fig. 3.1. Tissue water T_2 values are given in Table 3.1. T_2 significantly decreased by 10–15% compared to control animals in all ROIs 5 hours after onset of SE. The hippocampus, amygdala and piriformic cortex also showed a significant decrease after 3 h, the latter two being most severely affected.

	Control (n=11)	3 Hours (n=10)	5 Hours (n=10)
Amygdala	60.2 ± 0.7	56.6 ± 0.5**	55.4 ± 0.6**
Retrosplenial Cortex	50.8 ± 0.7	48.2 ± 1.9	46.2 ± 2.0*
Hippocampus	55.5 ± 0.9	51.2 ± 1.7*	49.6 ± 2.0*
Piriformic Cortex	62.4 ± 0.9	58.3 ± 0.5**	56.7 ± 0.6**
Thalamus	49.7 ± 0.4	48.3 ± 0.9	46.7 ± 1.1*

Table 3.1 | Mean T_2 values (ms)±S.E.M. for control animals and animals after 3 and 5 h SE
* p<0.05 vs. controls (two-tailed Student's t test with Bonferroni correction).
** p<0.01 vs. controls (two-tailed Student's t test with Bonferroni correction).

	Control (n=11)	3 Hours (n=10)	5 Hours (n=10)
Amygdala	73.5 ± 0.6	70.6 ± 0.6*	68.4 ± 0.8**
Retrosplenial Cortex	67.1 ± 0.3	68.1 ± 0.6	67.7 ± 0.5
Hippocampus	71.9 ± 0.5	76.0 ± 1.0*	72.7 ± 0.8
Piriformic Cortex	71.5 ± 0.4	67.9 ± 0.7**	67.9 ± 0.8**
Thalamus	68.3 ± 0.6	74.1 ± 1.5**	67.5 ± 0.9

Table 3.2 | Mean ADC values (10–5 mm^2/s)±S.E.M. for controls and animals after 3 and 5 h SE
* p<0.05 vs. controls (two-tailed Student's t test with Bonferroni correction).
** p<0.01 vs. controls (two-tailed Student's t test with Bonferroni correction).

ADC maps

Examples of ADC maps during SE, weighted for diffusion in X, Y and Z, respectively, are shown in Fig. 3.2. Tissue water trace ADC values are given in Table 3.2. Trace ADC decreased significantly at 3 and 5 hours in the amygdala and piriformic cortex, and it transiently increased in the hippocampus and thalamus at 3 hours after induction of SE. No significant ADC changes were observed in the retrosplenial cortex.

MR Spectroscopy

Fig. 3.3 illustrates typical ^1H MR spectra of a control and an SE animal. Peak ratios were calculated and are listed in Table 3.3 (overleaf). Two hours after confirmation of SE, a significant decrease in NAA/tCr and NAA/Cho ratios was observed, as compared to controls, without a change in the tCr/Cho ratio. With continuing SE at 4 and 6 hours after confirmation of SE, a persistent and progressive decrease in NAA/tCr was observed, while NAA/Cho ratios normalized. Furthermore, the tCr/Cho ratio at 4 and 6 h showed a significant increase. Lactate was not detected in any of the control animals. At 2 h of

	Control (n=11)	2 Hours	4 Hours	6 Hours (n=7)
NAA/Cho	1.44 ± 0.049	1.29 ± 0.030**	1.38 ± 0.076	1.53 ± 0.065
NAA/tCr	0.95 ± 0.016	0.88 ± 0.013**	0.85 ± 0.041**	0.83 ± 0.023**
tCr/Cho	1.53 ± 0.050	1.46 ± 0.026	1.63 ± 0.031*	1.83 ± 0.051**

Table 3.3 | ^{1}H MRS ratios in hippocampal VOI for control animals and animals after 2, 4 and 6 h SE
* p<0.05 vs. controls (two-tailed Student's t test with Bonferroni correction).
** p<0.01 vs. controls (two-tailed Student's t test with Bonferroni correction).

SE, a lactate resonance at 1.33 ppm was detected in 8 out of 10 experimental animals. Lactate was still visible in seven out of nine and two out of seven pilocarpine-injected rats at 4 and 6 hours of SE, respectively. The change in number of animals analyzed is due to the fact that only reliable spectra with small line width and sufficient signal to noise were analyzed.

Discussion

In this study, we combined ^{1}H MRS and MRI to monitor cerebral (patho)–physiological changes during the very early stages of SE in the rat. Tissue T_2 was shown to be globally decreased. The ADC was decreased in the amygdala and piriformic cortex, and it transiently increased in the hippocampus and thalamus. Lactate was increased, and NAA/tCr as well as NAA/Cho ratios were decreased in the first hour of SE. After several hours, tCr/Cho increased, indicating a decrease not previously described in Cho.

T_2 alterations

The literature regarding T_2 changes during experimental SE shows contradictory results. The global progressive decrease in tissue T_2 we observed is in contrast with the results of Wall *et al.*[185] In their study on non-lithium-pretreated pilocarpine-induced epileptic status in rats, increased T_2 values were found in the piriformic cortex,amygdala and thalamus at 3 and 6 hours of SE, which generalized to all areas analyzed after 12 h. In the same model, Fabene *et al.* have reported an increase of T_2 at 12 hours after SE, which was, however, localized in the hippocampus, amygdala, thalamus and cingulate cortex.[186] In the lithium–pilocarpine model on the other hand, Roch *et al.* were unable to detect any significant changes in T_2 values after 6 hours of SE.[187]

Our results correspond well with the T_2 decrease described by Bhagat *et al.* after 3 to 12 hours of soman-induced SE in the rat.[188] This model is similar to the lithium–pilocarpine model in the sense that it also causes SE by raising acetylcholine levels.

These authors speculated that the decrease in T_2 might indicate a decline in extracellular water. An alternative explanation we suggest is that an increased concentration of paramagnetic deoxyhemoglobin causes a decrease in T_2. This so-called negative BOLD effect has been shown to occur in MR studies of hypoxic hypoxia in the rat.[189] Deoxyhemoglobin increases in situations in which the metabolic requirement for oxygen is not met by the delivery of oxygen. During lithium–pilocarpine induced SE ^{14}C-2-deoxyglucose, studies have shown that glucose utilization increases 3–7-fold in virtually all brain regions, leading to increased oxygen extraction.[190] In addition to this, Pereira *et al.* have shown that this hypermetabolism is not matched by comparable local cerebral blood flow (CBF) increases.[191] Hypermetabolism that is not compensated for by local CBF increases leads to a mismatch between oxygen delivery and demand, which is reflected in deoxygenation of hemoglobin. This is further supported by the higher prevalence of lactate accumulation in the ^{1}H MR spectra, also reflecting anaerobic glycolysis, as will be discussed below. BOLD fMRI measurements possibly in conjunct with CBF measurements could, in the future, show whether this explanation can be further confirmed.

ADC changes

The trace ADC measurements showed a significant selective decrease in the amygdala and piriformic cortex. In general, decreases in ADC during SE have been shown before in experimental[192,193] and clinical studies.[194,195] These changes are usually attributed to cell swelling and changes in cytoskeletal motility, limiting the freedom of motion of water molecules. The excitatory dysregulation during SE, caused by activation of the glutamatergic NMDA receptors, leads to massive calcium influx, resulting in neuronal damage or death. The glutamate stored intracellularly is released from damaged cells and causes additional excessive excitation. Cell swelling accompanies these neurotoxic events. The structures that show greatest activation during seizures also exhibit most severe neuronal damage,[190] which was reflected in excitotoxic cell swelling.[196] Under these extreme conditions, changes in cytoskeletal motility have been hypothesized to occur as an additional source of ADC decrease.[193]

The specific ADC changes in the amygdala and piriformic cortex in pilocarpine-induced SE we demonstrated have previously been described by Wall *et al.*[185] The reason that these areas are particularly sensitive to the cholinergic agent pilocarpine is due to the relative abundance of cholinergic fibers from the olfactory bulb. In addition to this, these areas have electrophysiological properties that allow for rapid depolarization.[197] This specific vulnerability is affirmed by the fact that the amygdala and piriformic cortex also showed the most pronounced decrease in T_2. This most likely reflects a more severe mismatch between oxygen demand and delivery due to excessive activation in these regions.

The acute temporary and selective increase of tissue ADC values in the hippocampus and thalamus were also present in a study on non-lithium-pretreated pilocarpine-induced SE but did not prove to be statistically significant.[185] Increases in ADC are generally attributed to vasogenic edema (in contrast to cytotoxic edema), which can occur for instance in blood–brain barrier (BBB) breakdown. Leroy *et al.* have recently shown a transient BBB breach in the thalamus after 2 h of SE, using gadolinium-enhanced MRI and have confirmed this histologically.[198] The thalamus is known for playing a key role in the propagation of limbic seizures in this model through its many connections to the limbic system and its excitatory input to these structures. This is illustrated by the fact that thalamic stimulation leads to excitatory responses in the entorhinal cortex and hippocampus.[199,200] The transient increase in ADC, possibly reflecting a BBB breach, may be the first noninvasively detectable sign of the permanent epileptogenic damage to the thalamus. Whether a similar mechanism is involved in the hippocampus is unclear. High time resolution ADC measurements combined with gadolinium-enhanced MRI and histology may help us solve this question.

Spectroscopic changes

While lactate was not detected in any of the control animals, 2 h after confirmation of SE, a lactate resonance at 1.33 ppm was detected in 8 out of 10 experimental animals. The number of animals showing lactate decreased to two out of seven after 6 hours. Lactate has repeatedly been shown to increase in experimental[201-203] as well as clinical MRS studies.[204,205] The fact that lactate is detected above noise level in the experimental animals in contrast to control animals can be attributed to an increase in anaerobic glycolysis, which is likely to occur under the hypermetabolic conditions caused by SE. It shows that O_2 demand cannot be met by its delivery, which has also been suggested above as a cause for the changes in T_2 imaging. The decrease in the number of animals that display a lactate resonance after 6 h of SE is consistent with a study by Fernandes *et al.* showing that, after an acute initial increase in arterial lactate, a plateau phase or decrease in lactate was observed at 105 min after lithium–pilocarpine-induced SE.[190]

After 2 hours of SE, ^{1}H MRS showed a decrease of NAA/tCr and NAA/Cho. At later time points, NAA/tCr continued to decrease, while NAA/Cho and tCr/Cho increased. In the ^{1}H spectrum, tCr is generally insensitive to tissue pathology in the early (<24 hours) stages. A decrease in NAA/tCr would therefore imply a progressive NAA decrease throughout the experiment. Under the assumption that tCr remains stable, Cho is not affected in the very early stages of SE but decreases at later time points. There is some evidence that, under (ischemic) hypoxic conditions, tCr can decrease.[206] It is not unlikely that this plays a role in our model, but this would only make the claim of decreasing concentrations of NAA and Cho stronger.

The progressive decrease of NAA is most likely attributed to neuronal death or dysfunction.[207] It has been shown in experimental animals that the processes leading to neuronal death start within as little as 30 min after (induction of) SE.[208-210] In addition to this, the energy-dependent formation of NAA in the neuronal mitochondria might be affected by the compromised energy metabolism during SE. This is a hypothesis put forward by Hugg *et al.*, which is based on the fact that NAA shows recovery after temporal lobe surgery[194] and on the close relationship between rate of NAA and ATP synthesis.[211]

One putative mechanism for the late decrease in Cho during SE is an impairment of oxygen-dependent formation of phosphorylcholine, a major constituent of the Cho resonance measured in ^{1}H MRS.[212] Relative changes in the MR visible choline-containing compounds could also be explained by the injection of a cholinergic agent, analogous to the observed Cho decrease after administration of another cholinergic agent, xanomeline.[213] *Ex vivo* studies in the lithium–pilocarpine model during SE show a transient increase in choline and acetylcholine in the rat brain, which reached plateau levels 150 min after pilocarpine administration and decreased afterwards due to depletion of the cholinergic system by excessive stimulation.[214,215] Although choline and acetylcholine constitute only a minor part of the MR visible Cho peak, a sizable change in their concentrations may be reflected in a decrease in the Cho peak.[216]

Conclusion

We show that changes in tissue architecture, energy metabolism and neuronal viability can be probed *in vivo* with T_2W MRI, DW MRI and MRS in acute experimental SE with high temporal and spatial resolution. Application of these MR techniques provides indications for early-onset hypermetabolism with relative hypoxia and lactate accumulation, BBB disruption, neuronal dysfunction and choline depletion.

Further sophistication and application of these techniques will increase our understanding of the pathophysiology of seizure initiation and epileptogenesis. The techniques we used are already available for routine clinical use. MR may therefore enable us to noninvasively monitor and assess (imminent) cerebral damage in patients with SE, creating possibilities for early diagnosis and treatment, thereby possibly preventing late complications such as TLE.

Acknowledgements

This research was supported by the Dutch Epilepsy Fund (NEF 0415). We gratefully acknowledge E. Blezer and W. Veldhuis for their valuable support.

4

In vivo diffusion tensor imaging and *ex vivo* histological characterization of white matter pathology in a post status epilepticus model of temporal lobe epilepsy

Pieter van Eijsden[1,2]
Wim M. Otte[3]
W. Saskia van der Hel[4]
Onno van Nieuwenhuizen[1]
Rick M. Dijkhuizen[3]
Robin A. de Graaf[5]
Kees P.J. Braun[1]

1. Departments of Pediatric Neurology, Rudolf Magnus Institute of Neuroscience, University Medical Center Utrecht, The Netherlands
2. Department of Neurosurgery, Free University Medical Center, Amsterdam, The Netherlands
3. Biomedical MR Imaging and Spectroscopy Group, Image Sciences Institute, University Medical Center Utrecht, The Netherlands
4. Department of Anatomy, Division of surgical specialties, University Medical Center Utrecht, The Netherlands
5. Magnetic Resonance Research Center, Department of Diagnostic Radiology, Yale School of Medicine, New Haven, CT, USA

Epilepsia, 2011, 52(3)

Although epilepsy is historically considered a disease of grey matter, recent diffusion tensor imaging (DTI) studies have shown white matter abnormalities in epilepsy patients. The histopathological correlate of these findings, and whether they are a cause or consequence of epilepsy, remains unclear. To characterize these changes and their underlying histopathology, DTI was performed in juvenile rats, four and eight weeks after pilocarpine induced status epilepticus (SE). In the medial CC, mean and axial diffusivity (MD and λ_1) as well as a myelin staining were significantly reduced at four weeks. Only the λ_1 decrease persisted at eight weeks. In the fornix fimbriae (FF), λ_1 and myelin staining were decreased at both time points while fractional anisotropy (FA) and MD were only significantly reduced at eight weeks We conclude that SE induces both transient and chronic white matter changes in the medial CC and FF that are to some degree related to myelin pathology.

Introduction

Although epilepsy is historically considered to be a grey matter disease, recent DTI studies have demonstrated that white matter structures, even distant from the primary epileptogenic zone, are affected in patients with focal epilepsies. A bilateral widespread reduction in FA and increase in MD and radial diffusivity (λ_{2+3}) have been described in adults with temporal lobe epilepsy (TLE).[150] However, the histopathological correlate of these findings, and whether they are a cause or consequence of epilepsy, remains unclear.

For this reason, longitudinal characterization of DTI changes during epileptogenesis is needed, as is a description of the underlying histopathology. The juvenile lithium-pilocarpine rat model of TLE is ideally suited for this purpose. In this experimental model, SE in 21-day old rats causes spontaneous or stimulus/handling-induced seizures in 67-80% of animals after a period of 10-16 weeks.[217] The latent phase allows for characterization of white matter changes occurring after SE, but before onset of spontaneous seizures. The aim of this study was to longitudinally characterize white matter changes after pilocarpine-induced SE in rats by combining *in vivo* high-field DTI with post mortem histological staining.

Methods

Animal model

SE was induced as described elsewhere.[117] Shortly, 20-day old male Wistar rats (n=43; 38.3 ± 4.5 g, mean ± SD) were injected with 3 mEq/kg lithium-chloride 20 hours before injection of 40 mg/kg pilocarpine-hydrochloride. After one hour of SE, Racine stage six animals were sedated with 4 mg/kg diazepam.[118] As expected from this model, animals did not show signs or symptoms of seizures during the 4 to 8 weeks time-interval between SE and further experiments. Eight littermates underwent the same experimental procedure except for the replacement of pilocarpine with saline. All experimental procedures were approved by the local Institutional Ethical Committees.

Magnetic resonance imaging

At 4 and 8 weeks after induction of SE, five post-SE and five control animals were intubated and ventilated with 0.5% halothane in N_2O and O_2 (30/70%). Animals were immobilized and placed in the RF probe for MR experiments, after which the rats were euthanized under anesthesia. Experiments were conducted on a dedicated animal MR system, consisting of a 9.4 T magnet (Magnex Scientific, Oxford, UK) equipped with a 9-cm diameter gradient coil insert (490 mT/m, 175 μs; Resonance Research Inc., MA, USA), interfaced to an AVANCE console (Bruker, Billerica, MA, USA). A 14 mm diameter surface coil was used for radiofrequency signal transmission and detection. For DTI, twenty-one slices of 0.5 mm were acquired with segmented spin-echo echo-planar MRI sequence (8 segments, resolution 0.2x0.2 mm, TR/TE = 3500/21 ms). Diffusion-weighting was applied in six directions with a b-value of 1200 s/mm^2. Quantitative T_1 (TR/TI 7000/10 - 6400 ms) and T_2 images (TR/TE 2500/10, 15, 25, 40, 60, 85ms) with a resolution of 0.1x0.1 mm were acquired. Images with optimal resolution (TE=25 ms) for discerning anatomical structures were used for drawing ROIs (fig 4.1).

MR data analysis and statistics

DTI data were used to calculate maps of eigen-values of the diffusion tensor (λ_1, λ_2 and λ_3), MD, and FA, as described elsewhere.[147] Images were aligned using the Elastix toolkit by nonlinear registration preceded by affine-only registration. DTI parameters were analyzed by a regions-of-interest (ROI) analysis. The FF, medial and lateral CC were bilaterally outlined on T_2-weighted images (fig 1). Differences between ROIs were analyzed using ANOVA with LSD post-hoc testing. Values are expressed as mean ± SD. $p < 0.05$ was considered statistically significant.

Histology

Luxol Fast Blue (LFB) myelin staining was performed on coronal paraffin brain sections (7 μm, including hippocampus). Briefly, rehydrated sections were placed in LFB solution overnight at 60°C. Sections were counterstained with cresyl violet (Nissl) for 1 minute, dehydrated, cleared and mounted.[218] Bielschowsky silver staining was used on alternating sections to evaluate axonal integrity.[219] The status of the FF, medial and lateral CC were evaluated by a blinded observer and graded as normal or abnormal. In addition, after converting the images to grey (white = 256, black = 0), staining intensity in the FF, lateral and medial CC was quantified relative to a cortical voxel using the software package ImageJ.[220]

Results

Animal model

Out of 43 animals injected with pilocarpine, 33 (77%) progressed to full SE, of which seven (16%) died within 24 hours. We studied five animals at four and eight weeks after SE with MRI, twelve additional animals were used for histology (six per group). No mortality or abnormal behaviour was observed in the age-matched control animals (n=8).

DTI

Figure 4.1 (overleaf) summarizes the results of ROI analysis. In the medial CC of post-SE animals, MD significantly decreased at four weeks, followed by recovery at eight weeks. FA tended to decrease without reaching statistical significance. At both time-points, λ_1 was significantly decreased. The lateral CC showed similar changes as the medial CC for all parameters, but without reaching statistical significance. In the FF, λ_1 was decreased at both time points, while FA and MD were significantly reduced only at eight weeks. λ_{2+3} and T_2 values were not significantly altered, but T_1 was reduced in the medial CC at four weeks.

Histology

LFB staining was less intense in 4-week post-SE animals and loss of characteristic banding in particularly the medial CC was obvious (fig 4.2, overleaf). All but one of the post-SE sections were scored abnormal by the blinded observer. At 8 weeks, staining patterns between post-SE and control animals revealed no clear differences. Bielschowsky silver-stained slices showed no differences between control and post-SE rats at both 4 and 8 weeks (not shown). Quantification of the relative staining intensity revealed a reduction in all white matter ROIs at four weeks, which only persisted in the FF at the eight week time point (fig 4.2).

Discussion

This study describes *in vivo* DTI and post mortem histology of white matter changes after experimental SE. Our data show that MD, λ_1 and LFB staining are significantly reduced in the medial CC four weeks after SE, followed by recovery after eight weeks, with the exception of λ_1. Similar changes were found in the lateral CC, although statistical significance was not reached with the relatively limited number of animals. In the FF, λ_1 and myelin staining were decreased at both time points, while FA and MD were significantly reduced at eight weeks. We found no significant changes in RD or axonal staining.

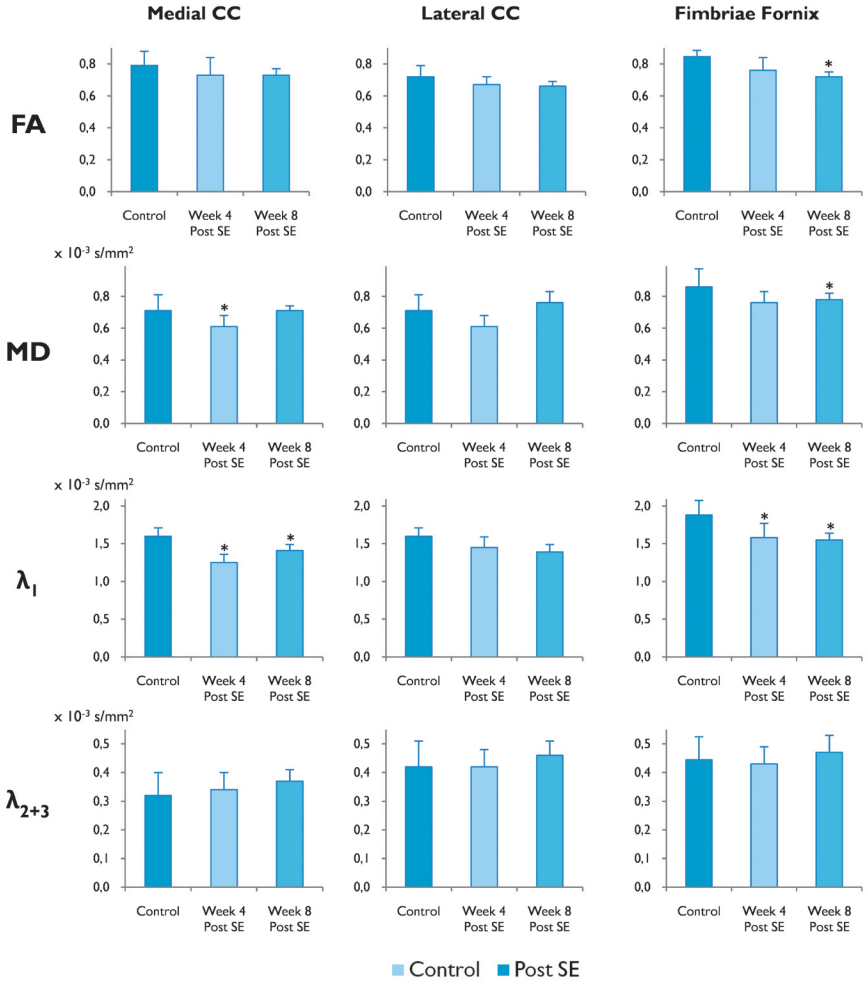

Fig. 4.1 | The panel on the right shows T_2W, MD and FA maps. In the FA maps, the pixel color represents the overall fiber orientation in that pixel. Red indicates a left-right orientation, green indicates a top-bottom orientation and blue indicates an orientation in the plane of the image. The panel above displays bar graphs comparing control animals with post-SE animals at four and eight weeks for the medial, lateral CC and FF. * = $p < 0.05$

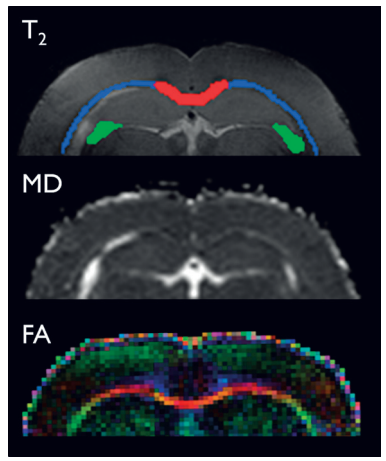

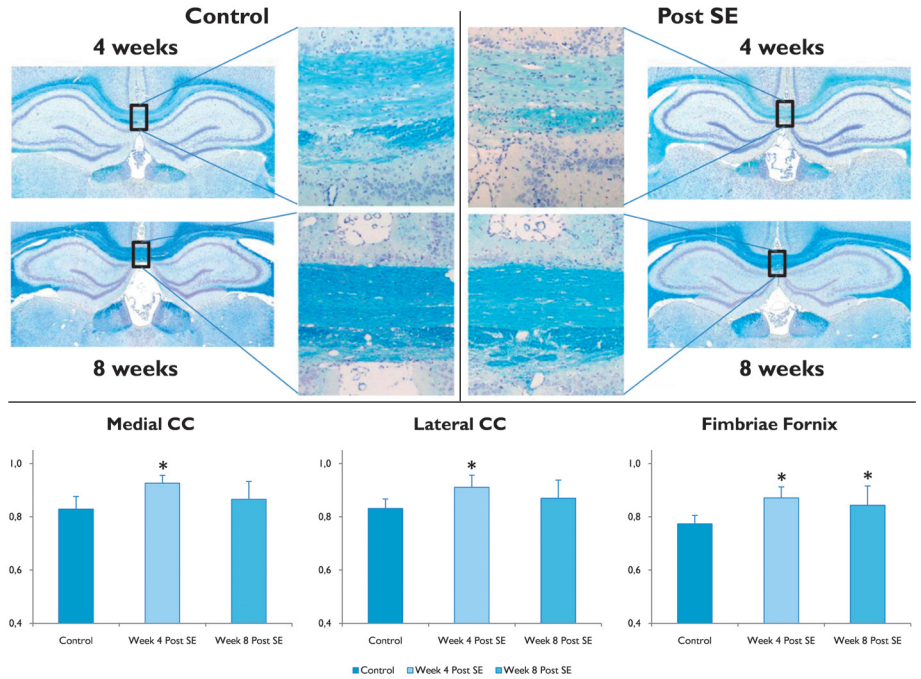

Fig. 4.2 | Luxol fast blue staining on coronal rat brain sections (7 µm) of post-SE and control animals four and eight weeks after injection of pilocarpine or saline. Medial CC areas are outlined and magnified. Loss of "banding" and general staining intensity is obvious in the medial CC of the post-SE animal at four weeks. In the bottom panel, results from the signal intensity quantification in the medial, lateral CC and FF relative to cortex are summarized in bar graphs. The y-axis is in arbitrary units. Higher values correspond with less intense coloring.

Several clinical and experimental studies have described white matter DTI changes in epilepsy which generally consist of widespread FA reduction in combination with MD or λ_{2+3} increase.[150,152] These results are usually explained by a theoretical model that proposes the FA and λ_1 reduction to be caused by axonal damage, while the RD and/or MD increase indicates myelin damage. A recent study compared pre-surgical DTI in TLE patients with post-surgical electron microscopy of their FF.[151] The only significant (positive) correlation was found between FA and the cumulative axonal membrane circumference, an estimate of total axonal perimeter in an area. Weaker correlations were found between FA and several other axonal or myelin-related parameters as well as with extra-axonal fractions. The same is true for λ_{2+3}. DTI abnormalities are in general probably the sum of several parameters that cannot be easily separated into strictly axonal or myelin contributions. For this reason it remains unclear what the pathophysiological substrate is of the observed DTI changes in chronic epilepsy. In our study, the LFB

staining unequivocally points towards myelin involvement, while the Bielschowsky staining revealed no clear axonal abnormalities.

The aforementioned DTI changes in chronic epilepsy can be related to either the cause or the consequence of recurrent seizures. Our study shows that isolated SE, without spontaneous recurrent seizures, is sufficient to cause long-lasting widespread white matter changes. However, the changes we find differ from those observed after the onset of spontaneous seizures. While we find MD and λ_1 reductions and only modest (FF) or non-significant (CC) FA reductions, chronic epilepsy is characterized by MD increase in combination with a prominent FA reduction.

It is possible that these results reflect an early stage of the same pathological process responsible for the DTI changes in chronic epilepsy. However, the (trend to) normalization of several parameters, especially the LFB stain, suggests that the SE-induced white matter pathology is at least partially reversible. It could be that SE causes excitotoxic white matter damage as has been shown for grey matter, but this is not reflected in a T_2 increase at either time point.[221] Alternatively, SE may interfere with the normal process of myelin deposition, which happens to peak around the day SE is induced.[222]

In the FF, the major efferent pathway of the hippocampus, the FA and λ_1 decrease appears more prominent and more progressive than in the other white matter ROIs. Possibly, the more reversible changes in the CC merely reflect SE-induced myelin pathology, while the progressive FF changes are not only caused by the preceding SE, but also parallel the ensuing hippocampal damage that is associated with epileptogenesis in this model.

In summary, SE in juvenile rats causes significant white matter pathology in the medial CC and FF that persists for several weeks and is followed by partial recovery. This process is characterized by MD, FA, and λ_1 reductions in DTI, and by reduced myelin staining in histological sections.

Acknowledgements

This research was supported by the Dutch Epilepsy Fund (NEF 0415). We thank Bei Wang for expert animal preparation, Peter Brown for construction and maintenance of the ^{1}H-[^{13}C] RF coil and Terence Nixon and Scott McIntyre for system maintenance.

5

In vivo MR spectroscopy and histochemistry of status epilepticus induced hippocampal pathology in a juvenile model of temporal lobe epilepsy

W. Saskia van der Hel[1]
Pieter van Eijsden[2,3]
Ineke W.M. Bos[1]
Robin A. de Graaf[4]
Kevin L. Behar[5]
Onno van Nieuwenhuizen[2]
Pierre N.E. de Graan[6]
Kees P.J. Braun[2]

1. Department of Anatomy, Division of surgical specialties, University Medical Center Utrecht, The Netherlands
2. Departments of Pediatric Neurology, Rudolf Magnus Institute of Neuroscience, University Medical Center Utrecht, The Netherlands
3. Department of Neurosurgery, Free University Medical Center, Amsterdam, The Netherlands
4. Magnetic Resonance Research Center, Department of Diagnostic Radiology, Yale School of Medicine, New Haven, CT, USA
5. Magnetic Resonance Research Center, Department of Psychiatry, Yale School of Medicine, New Haven, CT, USA
6. Dept Neuroscience & Pharmacology, Rudolf Magnus Magnus Institute of Neuroscience, University Medical Center Utrecht

The first two authors contributed equally to this paper

Childhood status epilepticus (SE) initiates an epileptogenic process that leads to spontaneous seizures and hippocampal pathology, characterized by neuronal loss, gliosis and an imbalance between excitatory and inhibitory neurotransmission. It remains unclear whether these changes are a cause or consequence of chronic epilepsy. In this study, *in vivo* magnetic resonance spectroscopy (MRS) was used in a post-SE juvenile rat model of TLE to establish the temporal evolution of hippocampal injury and neurotransmitter imbalance. SE was induced in P21 rats by injection of lithium and pilocarpine. Four and eight weeks after SE, *in vivo* ^{1}H and GABA-edited MRS of the hippocampus was performed and results were compared with *ex vivo* immunohistochemistry, that was done in a separate group of animals to interpretate and validate MRS findings. MRS showed a 12% decrease in N-acetyl-aspartate and 15% increase in choline concentrations, indicating neuronal death and gliosis respectively. These results were confirmed by fluorojade and vimentin staining.

Furthermore, a severe and progressive decrease in GABA (-41%), and glutamate (-17%) was found. The specific severity of GABAergic cell death was confirmed by parvalbumin-immunoreactivity (-68%). Unexpectedly, we found changes in glutamine, the metabolic precursor of both GABA and glutamate. Glutamine increased at four weeks (+36%), but returned to control levels at eight weeks. This decrease is consistent with the simultaneous decrease in GS immunoreactivity (-32%). In conclusion, *in vivo* MRS results reflect gliosis and (predominantly GABA-ergic) neuronal loss. In addition, an initial increase and subsequent normalization of glutamine is detected, accompanied by a decrease in GS-immunoreactivity. This may reflect GS-downregulation in order to normalize glutamine levels. All these changes occur before spontaneous seizures occur, but by creating a pre-epileptic state, may play a role in epileptogenesis. MRS can be applied in a clinical setting and may be used as a non-invasive tool to monitor the development of TLE.

Introduction

The pathophysiology of temporal lobe epilepsy (TLE) is still not well understood. Contributing factors appear to be a genetic predisposition and a "second hit" during infancy, e.g. febrile seizures or SE. The "second hit" presumably initiates a cascade of pathophysiological events that, after a latent seizure-free period, leads to spontaneous recurrent seizures (SRS).[66,179]

The hippocampus plays a crucial role in the pathology of TLE. Structurally, the epileptic hippocampus often shows hippocampal sclerosis (HS), characterized by neuronal loss and gliosis.[223] Functionally, a hippocampal imbalance between the excitatory and inhibitory neurotransmitters glutamate and GABA has been implicated to contribute to TLE.[224,225] These structural and functional changes were studied *ex vivo* in surgical or post-mortem specimens of the temporal lobe of TLE patients. Apart from the methodological problem in translating post-mortem result to *in vivo* function, the specimens analyzed represent an end-stage of disease in which the contribution of the initial epileptogenic injury is obscured by the pathological consequences of suffering from seizures for years.

For this reason we aim to investigate the early, but persistent consequences of SE to the developing brain. We chose the juvenile lithium-pilocarpine model, which has recently been adapted from the adult lithium-pilocarpine model. In this model, SE is induced in 21 day old rats by pilocarpine potentiated by lithium. Animals that recover from SE develop normally compared to litter mates but start to experience SRS with a mesiotemporal electrophysiological origin and semiology, after a latent phase of 10-16 weeks.[129,187,226] The developmental stage these animals are in, and the clinical and pathological similarities to human HS-associated TLE, make this model ideally suited for the purpose of this study.

MRS allows for both the non-invasive detection of structural changes, *i.e.* gliosis and neuronal damage, and for the quantification of functional changes, *i.e.* the concentrations of the neurotransmitters GABA and glutamate. Therefore, MR is an ideal tool to study post-SE pathology *in vivo*. An added benefit is that these techniques can

easily be adapted for application in a clinical setting. To validate MR findings, dedicated *ex vivo* immunohistochemistry was performed at the same time points after SE in a separate group of animals. In summary, this study aims to characterize the development of early but persistent changes in hippocampal structure and neurotransmission that are induced by juvenile SE and may precede a chronic seizure disorder.

Materials and methods

MR experiments were performed at the Magnetic Resonance Research Center of Yale Medical School, New Haven, USA. Immunohistochemistry was done at the Rudolf Magnus Institute of Neuroscience in Utrecht, The Netherlands. All experimental procedures were approved by the "institutional animal care & use committee" (IACUC) of the Yale School of Medicine (protocol no. #2003-10711) and the "animal experimental committee" (DEC) of Utrecht University (protocol no. 01.057).

Animal model

20-day old male Wistar rats (n=85; 42.6±2.0 g, [mean ± SEM]) were injected intraperitoneally (i.p.) with 3 mEq/kg lithium chloride (Merck, Darmstadt, Germany), 20 hours before induction of SE. Thirty minutes before the subcutaneous administration of 40 mg/kg pilocarpine hydrochloride (Sigma, St. Louis, MO), 1 mg/kg of scopolamine methyl nitrate (Sigma) was injected i.p. to antagonize the peripheral cholinergic effects of pilocarpine.[117] Age-matched control animals (n=28, 44.3±2.6 g) underwent the same experimental procedure but were injected with an equal volume of saline instead of pilocarpine.

Behaviour was monitored visually and classified into six stages according to Racine.[118] After one hour of SE, animals were sedated with diazepam (4 mg/kg i.p., Abbott Laboratories, North Chicago, IL) to suppress seizures and reduce mortality. Only animals that reached stage six were used for further experiments. These animals (hereafter indicated as +SE) were daily video-monitored for one hour and handled several times a day to detect seizures. No behavioural seizures could be detected during the four to eight weeks time interval after SE, or during continuous monitoring in the 12 hours before MR and *ex vivo* studies. Eighteen Li+/pilo injected animals were not sacrificed for MR or histological experiments, but were video-monitored for 19 weeks to detect SRS.

Magnetic resonance experiments

Four and eight weeks after induction of SE, five +SE and five control animals were anesthetized and scanned. The rats were anesthetized, intubated by tracheotomy and ventilated with 0.5% halothane in a mixture of N_2O and O_2 (30/70%). The femoral

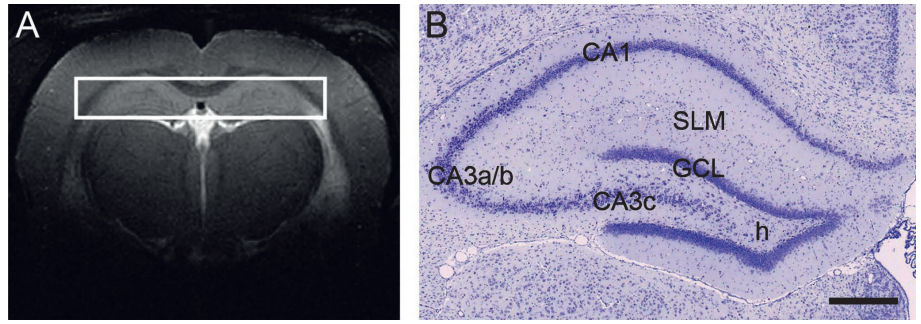

Fig. 5.1 A | Coronal T_2-weighted MR image (TR, 2500 ms; TE, 40 ms) of a healthy control animal at eight weeks (lithium treatment only). The hippocampal volume selected for spectroscopy is indicated by the white box. **B |** Nissl stain of the left hippocampus of a control animal at eight weeks depicting anatomical structure. The granular cell layer (GCL) is a part of the dentate gyrus (DG). SLM = Stratum Lacunosum-Moleculare. Bar = 500 µm.

artery was cannulated for monitoring of blood pressure and blood sampling to determine arterial pCO_2 and pO_2. Throughout the preparation phase and the entire MR protocol, which lasted approximately four hours, physiological variables were maintained within normal limits (pCO_2 = 33–45 mmHg; pO_2 ≥ 120 mmHg; pH = 7.30–7.58; Mean arterial BP = 90–110 mmHg) by small adjustments in tidal volume and ventilation frequency. Animals were placed in the probe, restrained in a head holder and immobilized with d-tubocurarine (0.5 mg/kg/40 min, i.p.). Body core temperature was measured with a rectal thermometer and maintained at 37°C ± 1°C by means of a heated water pad. After the MR experiments, rats were euthanized under anesthesia.

Experiments were performed on a dedicated animal MR system, consisting of a 9.4 T Magnex magnet (Magnex Scientific, Oxford, UK) equipped with a 9 cm diameter gradient coil insert (490 mT/m, 175 µs; Resonance Research Inc., Billerica, MA,). The magnet was interfaced to a Bruker AVANCE console (Bruker, Billerica, MA) operated under Linux running Paravision 3.0.1. A 14 mm diameter surface coil was used for ^1H radiofrequency pulse excitation and signal reception. ^1H MR spectra were obtained from a single voxel (10x2x5 mm) placed over the hippocampus (Fig. 5.1A). Voxel position was determined from multislice EPI images (FOV 2.56x2.56 cm, matrix 128x128, 10 slices of 1 mm slice thickness, TR 2.5 s and echo time TE 10 ms. The rostral-caudal center of the voxel was positioned in the slice showing the most dorsal portion of the medial hippocampus. The voxel position was then slightly adjusted with the help of the adjacent slices so as to minimize contamination from adjacent grey matter structures, corpus callosum and cerebrospinal fluid. ROI analysis of the hippocampus and the voxel, showed that the sampled tissue was for ~73% of hippocampal origin. Magnetic field homogeneity was optimized over the volume of interest with the non-iterative FASTMAP algorithm for all first- and second-order shim coils,[227] resulting in signal line

widths of 14–16 Hz for water and 9–11 Hz for metabolites in the 100 μL volume. 3-D localization of the spectroscopic volume was achieved by a combination of outer volume suppression (OVS), image-selected *in vivo* spectroscopy (ISIS), and slice-selective excitation. Water suppression was achieved with four conventional chemical shift selective pulses (CHESS).[228]

The three methylene resonances of GABA are overlapped by other metabolite resonances in the ^{1}H MR spectrum. Selective GABA detection was achieved by J-based editing of GABA.[229] In this technique, a narrow bandwidth inversion pulse is applied to GABA $^{3}CH_2$ (1.9 ppm) in alternate scans of a spin echo sequence, resulting in refocusing of the outer bands of the J-coupled triplets at 3 ppm and 2.29 ppm. In alternate scans (without inversion), J-modulation occurs and for a TE of $1/J_{GABA}$ (68 ms), the outer triplet bands are inverted in phase relative to the center band. Subtraction of the two subspectra results in the GABA edited spectrum. Partial co-editing of Glu-H2 (3.75 ppm) results from spillover from the inversion pulse exciting the Glu $^{3}CH_2$ multiplet near 2.1 ppm; In practice, total GABA levels are quantified with the GABA $^{4}CH_2$ peak at 3 ppm after correction for editing efficiency. Editing power was calibrated on the water resonance. Editing efficiency was calculated for individual experiments as the percentage of water signal suppressed by the editing pulse. The experiments were performed with a TR of 4 seconds and 64 repetitions with interleaved editing.

MR data analysis

The phase (zero and first order) of MR spectra was adjusted manually. The GABA-edited spectrum was obtained by subtracting the non-edited from the edited spectra. Quantification of metabolite resonances was performed with LCModel[176] with a basis set consisting of the pure chemical compounds measured with the same pulse sequence in phantoms (pH = 7.0, 37°C). The LCModel fits the measured *in vivo* spectrum with this metabolite "library". The fit is constrained by prior knowledge of resonance frequency and line width or T_2. A dedicated version of LCModel, developed in house, was used for analysis. Concentrations were calculated by assuming a total creatine concentration of 10 mM. No correction was made for T_1, because differences in T_1 between tCr and important metabolites are small.[230] Reliability of fits was established by performing Monte Carlo simulations on the obtained results. These were calculated for typical spectra and expressed as a percentage standard deviation (SD) over the average value that indicates the margin of error introduced by the LCModel analysis.[231]

Histology and immunohistochemistry

Four and eight weeks after pilocarpine-induced SE, six +SE and six control animals, that were not previously used for MR experiments, were sacrificed with pentobarbital (300 mg/kg, i.p.) and perfused transcardially with 100 ml of saline containing 500 U of heparin (Leo Pharmaceutical Products, Weesp, The Netherlands), followed by 200-250 ml of 4% (w/v) phosphate buffered paraformaldehyde (pH 7.4). Brains were dissected and postfixed overnight at 4˚C, dehydrated, embedded in paraffin, and sectioned transversally at 7 μm. General histology of brain sections was assessed after cresyl-violet (Nissl) staining. FluoroJade (FJ) staining was performed to analyze neuronal damage.[232] Immunohistochemical staining was performed with specific antibodies against vimentin, to detect reactive glia, against parvalbumin (PV), to detect a subpopulation of GABAergic neurons particularly sensitive to SE in the adult pilocarpine model,[233,234] and against glutamine synthetase (GS), the glial enzyme in the glutamate-glutamine cycle that converts glutamate into glutamine. Per primary antibody, tissue sections from all animals were stained simultaneously to minimize variation in the immunohistochemical reactions. The avidin-biotin detection system (Vectastain Elite ABC Kit; Vector Laboratories, Burlingame, CA) was used with 3,3'-diaminobenzidine tetrahydrochloride (DAB; Sigma Chemical Co., St. Louis, MO) as chromogen.[175] Control experiments without the primary antibodies revealed no detectable staining (data not shown).

Immunohistochemistry was analyzed by visual inspection by two independent observers. Since vimentin staining is either "all or nothing", it was not quantified. The loss of PV-positive neurons in the hippocampus was quantified, counting all PV-positive neuronal cell bodies in the DG and hilus of the right hippocampus of each animal. Quantification of GS-immunoreactivity (IR) was performed by computerized densitometry with the image-processing program ImageJ. Relative optical densities (RODs) for the hilar area of the right hippocampus were measured and normalized to the age-matched control group.

Statistics

Data are expressed as mean±standard error of the mean (SEM). The +SE group was compared with the control group of the same time point and results from the +SE groups were compared between time points. Statistical significance between the time points and between controls and +SE conditions was determined with a one-way ANOVA for multiple groups, after confirmation that all variables had equal variances and a normal distribution, combined with a post-hoc Bonferroni test. $p<0.05$ was considered significant.

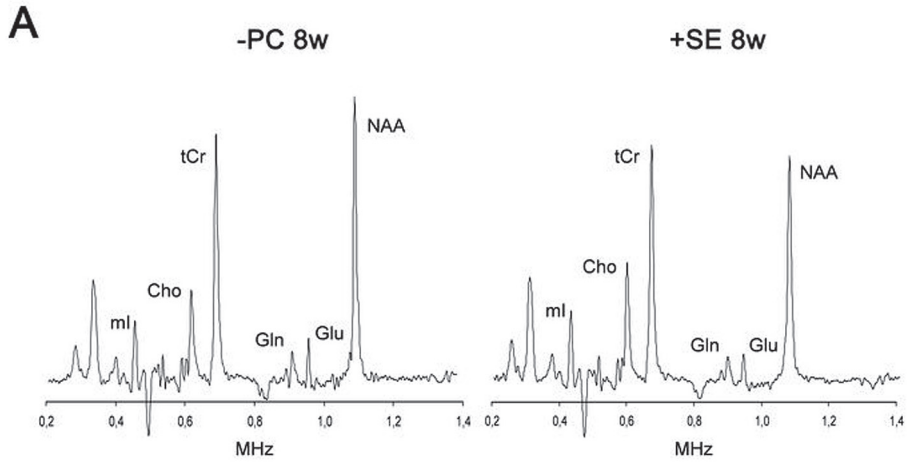

Fig. 5.2. A | Typical unedited spectra of a -PC and +SE animal at eight weeks after injection of pilocarpine: Spectra are normalized to total creatine (tCr). The epileptic animal shows a clear reduction in NAA and glutamate and increased choline compared with control. mI = myo-Inositol, Gln = glutamine. **B |**. A typical LCModel fit of the spectra is shown, where the generally good quality of the fit is shown by the flat residual.

Results

Animal model

Of 85 animals injected with lithium-pilocarpine 56 (66%) progressed to Racine's final stage of SE (stage six), of which 16 (29%) died within the first 24 hours (usually suddenly in the first hour during a tonic seizure). No mortality was observed in the period between SE and MR experiments or histology. Of the 40 surviving animals that developed SE, five each were studied four and eight weeks after SE with terminal MRS experiments, 12 animals from a separate group were sacrificed for immunohistochemistry, and 18 animals were longitudinally followed to determine the time of occurrence of SRS. We detected SRS by video-monitoring in eight out of 18 +SE animals (44%) within a period of 15-18 weeks after induction of SE. At four and eight weeks after SE, none of the animals studied had spontaneous or handling-induced clinical seizures. No significant differences were observed in body weights between control and +SE animals at four weeks (245.5 15.7 g vs. 233.3 10.3 g, mean±SEM, p=0.262); however, body weight was lower in control animals at eight weeks (335.4 6.9 g vs. 355.5 8.4 g, mean±SEM, p=0.040). No mortality or abnormal behaviour was observed in control animals.

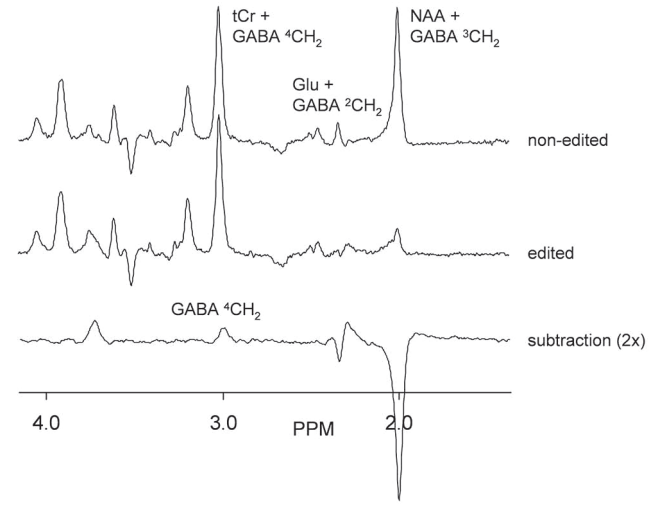

Fig. 5.3 | Typical GABA-edited spectra of a control animal at the four-week time point: The finite bandwidth of the inversion pulse centered at GABA 3-CH_2 (1.9 ppm) also results in partial excitation of NAA and glutamate 3-CH_2, resulting in the inverted NAA peak and coediting of glutamate 4-CH_2 in the difference spectrum. The spectra were quantitated with LCModel as described in Methods.

MR spectroscopy

Figure 5.2A shows a typical non-edited ^1H MR spectrum of a control and +SE animal (eight weeks after injection) with all important metabolites indicated. The LCModel fits and the resulting residual of the control spectrum are presented in figure 5.2B. A typical example of a GABA edited spectrum is shown in figure 5.3. Individual GABA resonances can be distinguished and were quantified. The metabolite concentrations obtained from these spectra are shown in table 5.1 (overleaf).

	-PC (n=5)	+SE (n=5)	-PC (n=5)	+SE (n=5)	MC Simulations
Neuronal dysfunction					
NAA	12.066 ± 0.217	10.695 ± 0.337*	11.585 ± 0.131	10.236 ± 0.760*	0.36%
Gliosis					
Total Choline	5.249 ± 0.187	6.068 ± 0.763*	5.327 ± 0.202	6.037 ± 0.456*	8.66%
Myoinositol	7.703 ± 0.504	7.806 ± 0.442	7.552 ± 0.471	8.461 ± 0.459*	1.00%
Neurotransmission					
GABA	1.041 ± 0.058	0.681 ± 0.114*	0.942 ± 0.082	0.523 ± 0.060*†	7.90%
Glutamate	12.398 ± 0.556	10.539 ± 0.642*	11.461 ± 0.417	9.530 ± 1.29*†	3.28%
Glutamine	4.103 ± 0.182	5.619 ± 0.487*	4.252 ± 0.413	4.734 ± 0.807†	7.09%
Alanine	0.439 ± 0.069	0.414 ± 0.055	0.445 ± 0.105	0.377 ± 0.057	16.92%
Aspartate	1.208 ± 0.076	1.158 ± 0.093	1.129 ± 0.052	1.134 ± 0.100	4.90%
Energy failure					
Lactate	1.351 ± 0.135	1.311 ± 0.225	1.760 ± 0.337	1.309 ± 0.299	12.95%

One Way ANOVA with Pairwise Multiple Comparison Procedures (overall significance level p = 0.05)

Table 5.1 | Metabolite concentrations for control (-PC) and +SE animals, 4 and 8 weeks after SE, quantified with LCModel. Reliability of fits was established by Monte Carlo (MC) simulations, expressed as %SD. * < 0.05 compared with same time point control, † < 0.05 compared with previous time point.

When comparing controls and +SE animals at the respective time points, NAA concentration was decreased by 12% at both time periods ($p<0.0001$) after SE, whereas choline-containing compounds were increased (15% at four weeks, $p<0.05$ and 13% at eight weeks, $p<0.05$). Myo-Inositol was significantly elevated (12%) at eight weeks ($p<0.01$) but not at four weeks. GABA concentration decreased progressively with time after SE, 29% at four weeks ($p<0.001$) and 41% at eight weeks ($p<0.0001$), whereas glutamate concentration was decreased by 15% at four weeks ($p<0.001$) and 17% at eight weeks ($p<0.01$), as compared with their corresponding control groups. Glutamine concentration was increased significantly at four weeks (36%, $p<0.001$) but returned to control levels at eight weeks ($p=0.164$). Levels of alanine and aspartate were unchanged from control values at both time periods. Lactate levels were low and did not differ between time points or experimental groups.

Histology and immunohistochemistry

Cresyl-violet staining revealed no gross morphological alterations or neuron loss comparing +SE and control animals (Fig. 5.4A, B, p. 84). However, FJ staining revealed damaged neurons in +SE animals in the thalamus, part of the cortex and hippocampus in line with the adult pilocarpine model.[117] In the hippocampus FJ-positive neurons and dendrites were only found in the tip of the hilus (Fig. 5.4D, F). This was most pronounced in all six +SE animals four weeks after SE induction. The staining intensity and number of FJ-positive neurons and dendrites decreased eight weeks after SE but was still seen in all six animals. In the control animals FJ-positive neurons were absent (Fig. 5.4C, E), not only in the hippocampus but also in other brain areas (not shown).

All +SE animals showed vimentin-IR (Fig. 5.5, overleaf) in the tip of the hilus and the stratum lacunosum-moleculare. This was most pronounced four weeks after SE (Fig. 5.5B). The number of vimentin-positive cells decreased considerably after eight weeks (Fig. 5.5D). As expected, control animals at both time points only showed vimentin-IR in the wall of blood vessels.

To assess alterations in GABAergic neurons, we focused on PV-containing neurons. PV-IR was observed in neuronal cell bodies and the neuropil of the pyramidal cell layer of all CA areas, the granular cell layer (GCL) of the DG and the hilus (Fig. 5.6A, p. 85). At higher magnification, PV-IR was also seen in dendrites (not shown). Visual inspection revealed a reduction in the number of PV-positive neurons in +SE animals in the hilus and GCL of the DG compared with controls at both time points (Fig. 5.6B, D). Quantification of the total number of PV-positive neurons in these areas indeed showed significant reductions in +SE animals compared with their age-matched controls (44.7% at four weeks, $p=0.001$; 70,2% at eight weeks, $p<0.001$; Fig. 5.6E), as well as between the two time periods (eight weeks vs. four weeks, $p=0.015$).

GS-positive IR was found in the neuropil of all hippocampal areas (Fig. 5.7A, p. 85). Both astroglial cell bodies and processes were stained throughout the hippocampus. Neuronal cell bodies were devoid of GS-IR, consistent with glial specificity. Control animals showed no differences in GS-IR between the two time points. +SE animals showed a decrease in GS-IR in the tip of the hilus. This was visually apparent at four weeks after SE, but even more pronounced at eight weeks after SE (Fig. 5.7B, D). Quantification of the optical density of GS-IR in the hilar area confirmed the significant loss of GS (11.2% at four weeks and 32.4% at eight weeks, the latter reaching significance $p=0.001$; Fig. 5.7E). The reduction in GS-IR with time after SE was significant (eight weeks vs. four weeks, $p=0.037$). No changes were seen in other hippocampal areas when comparing with the control animals.

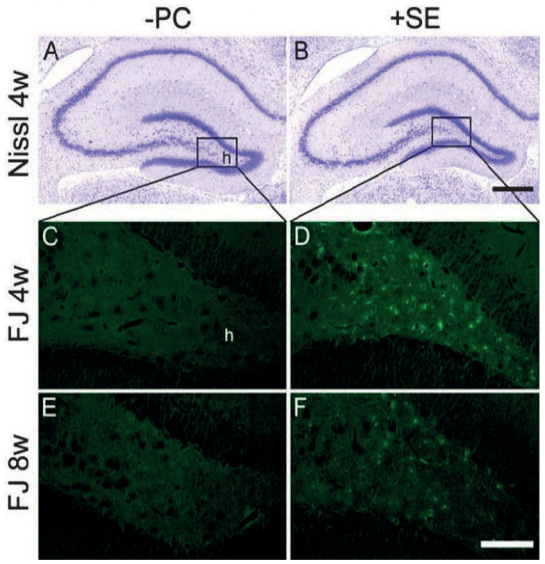

Fig. 5.4 | Histological slices of the hippocampus of -PC and +SE animals: Slices stained with Nissl at four weeks (A, B) and FluoroJade (FJ) at both four (C, D) and eight weeks (E, F) after pilocarpine-induced SE. The boxed regions in A and B indicate the enlargements of the FJ stain. In the hippocampus FJ staining appeared predominantly in the hilus of +SE animals. Bar lengths: 500 µm (B) and 100 µm (F).

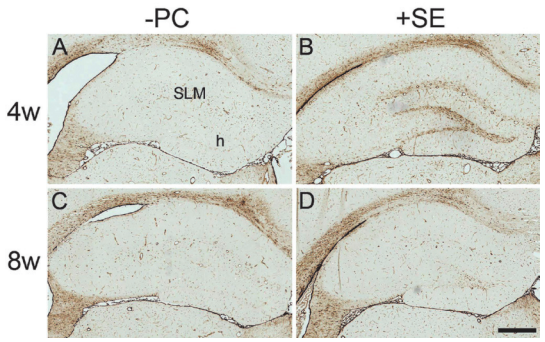

Fig. 5.5 | Vimentin-IR in -PC and +SE animals four and eight weeks after induction of SE: Immunostaining is present in reactive glia in the hilus (h) of the hippocampus and the stratum lacunosum-moleculare (SLM) four weeks after induction of SE. Bar = 500 µm.

Table 5.2 | Summary of findings.
NAA = N-Acetyl Aspartate, Cho = choline,
mI = myoinositol, GABA = γ-aminobutyric acid,
Glu = glutamate, Gln = glutamine,
FJ = Fluoro-Jade, Vim = vimentin,
PV = parvalbumin, GS = glutamine synthetase,
IR = immunoreactivity,
+: increase, -: decrease, =: unchanged.

MRS	metabolite	4w	8w
	NAA	-12%	-12%
	Cho	+15%	+15%
	mI	=	+12%
	GABA	-29%	-41%
	Glu	-15%	-17%
	Gln	+36%	=
Staining	**stain**	**4w**	**8w**
	FJ	+	+
	Vim-IR	++	+
	PV-IR	-46%	-68%
	GS-IR	-11%	-32%

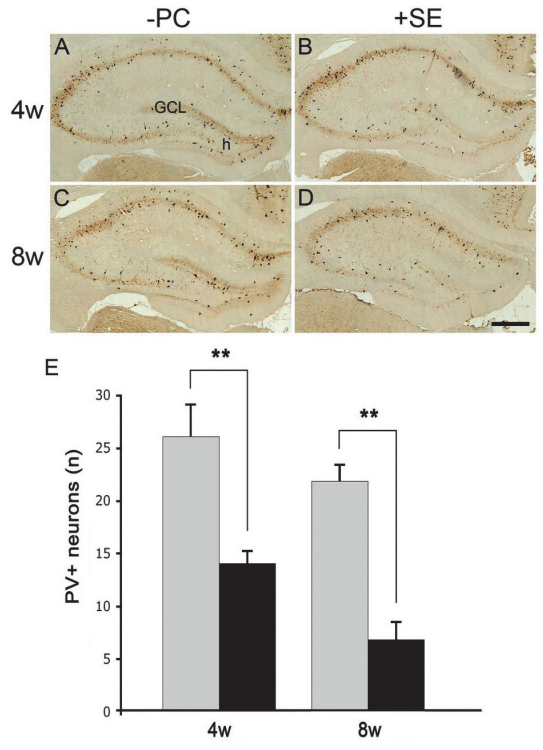

Fig. 5.6 | Parvalbumin (PV)-IR (A-D) in -PC and +SE animals four and eight weeks after induction of SE: Decreased numbers of PV-positive neurons are present in the hilus (h) and the granule cell layer (GCL) of the dentate gyrus of the hippocampus at four and eight weeks after induction of SE. Bar = 500 µm. E. Quantification of PV-positive neurons in the hilus of -PC (grey bars) and +SE (black bars) animals. The number of PV-positive neurons was significantly reduced in +SE animals at both four and eight weeks compared with –PC animals (46.2%; p=0.003 and 68.2%; p=0.0001, respectively). ** p<0.01

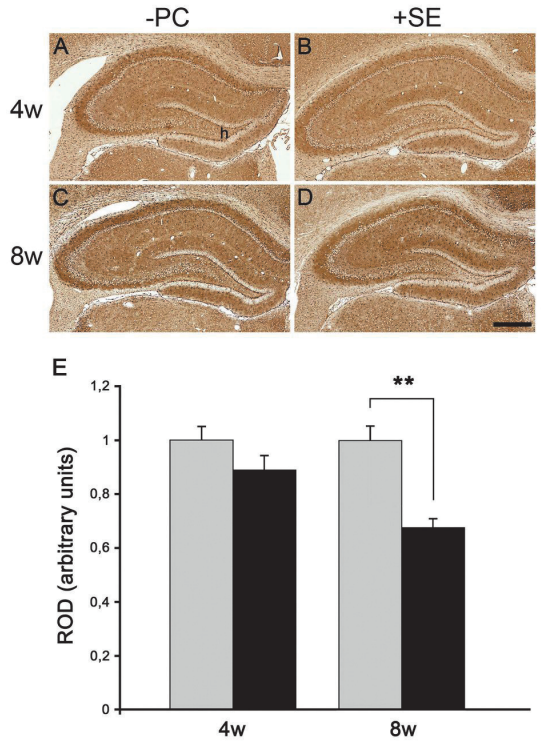

Fig. 5.7 | Glutamine synthetase (GS)-IR (A-D) in -PC and +SE animals four and eight weeks after induction of SE: Decreased immunostaining is apparent in the tip of the hilus (h) of the hippocampus four and eight weeks after induction of SE. Bar = 500 µm. E. Quantification of the relative optical density (OD) of GS-IR in the hilus of the hippocampus of -PC (grey bars) and +SE (black bars) animals, normalized to the age-matched –PC animals. A significant reduction of 32.4% (p=0.001) was found in the eight-week +SE animals compared with their age-matched controls. ** p<0.01

Discussion

In this study we show that pilocarpine induced SE in the juvenile rat causes early but persistent changes in hippocampal structure and neurotransmission. Both *in vivo* and *ex vivo* datasets were consistent with gliosis, neuronal loss (predominantly GABAergic) and involvement of GS. The observed changes are summarized in table 5.2 (overleaf). In general, similar studies in which both *in vivo* and *ex vivo* data has been gathered in the same animal model are scant and we are not aware of such a study performed in a juvenile epilepsy model.

Firstly, *in vivo* NAA and choline measurements provided evidence for structural damage to the hippocampus in terms of neuronal loss and gliosis. NAA was shown to decrease in four- and eight-week +SE animals. Neuronal death was confirmed by an FJ staining showing the presence of damaged neurons in the hilus of the hippocampus, most notably at four weeks.[207] Another key feature of end-stage HS in human TLE, gliosis[235] was also shown to occur in the +SE animals, because increases in choline-containing compounds and myo-Inositol are generally considered an indication of gliosis.[236] The increased IR of vimentin, a marker of reactive glia, confirmed this.

Previous studies performed during or immediately after SE[221] in the adult pilocarpine[117,123,124,214,237,237] or kainate model,[201,203,238,239] show results that are similar but more pronounced. Juvenile epilepsy models are generally milder than adult models and the juvenile lithium pilocarpine model is no exception, with SRS occurring less frequently, being less severe, and the time interval between SE and SRS being considerably longer. Histopathologically, juvenile models show only limited neuronal death and gliosis, compared to the extensive neuronal loss in hilus ánd CA regions that is found in the adult models. The developmental stage the animals are in, the duration of the latent period, and the relatively mild histopathology caused by SE, are more congruent with human pathophysiology. *In vivo*[169,236,240] and *ex vivo*[235] human TLE studies report neuronal damage and gliosis in several hippocampal subregions. However, these end-stage measurements cannot distinguish neuronal injury incurred during the early period of epileptogenesis from later progressive injury due to recurrent seizures. Our study indicates that some part of the neuronal damage and gliosis occurs before the onset of spontaneous seizures.

The neuronal damage described above is proportional to the glutamate, decrease we find with MRS, which is consistent with the fact that the vast majority of neurons are glutamatergic. For this reason, as also found in other studies, a decrease in MRS glutamate concentrations generally correlates well with NAA levels and with the severity of neuronal death.[169,173,236] For GABA a different story applies, because the GABA concentration was severely and disproportionally affected. The significant and progressive loss

of PV-positive interneurons, a significant subpopulation of GABAergic interneurons in the hippocampus, parallels the progressive decrease in hippocampal GABA concentration, implying a relative vulnerability of GABAergic cells for SE.[241] This is consistent with previous studies in human and in animal models of end stage TLE.[100,234,242,243]

Our study shows that a substantial part of the glutamate and GABA reduction found in end-stage TLE is also observable early after SE without spontaneous seizures (yet) being present. Neuronal loss, gliosis and the neurotransmitter imbalance in the hippocampus as such apparently do not immediately cause SRS. However, our study also shows that the GABA decrease is progressive over time, which could ultimately lead to insufficient inhibitory GABA to counteract excitatory neurotransmitters, *i.e.* glutamate.

In addition to the findings described above, we found glutamine concentrations to increase at four weeks and to normalize at eight weeks. Because glutamine is synthesized in astroglia, its resonance may reflect the number of glial cells. However, the increase in glutamine levels (+36%) at four weeks is substantially larger than the effects seen for the other known MRS markers for gliosis, choline (+15%) and myo-Inositol (+12%). Furthermore, the normalization of glutamine argues against gliosis, because gliosis is a permanent condition. Alternatively, metabolic factors may play a role. Glutamine is converted from glutamate by GS and is subsequently transported to the neuron to be converted to glutamate again. This glutamate-glutamine cycle is a finely tuned system that interacts with other metabolic systems (*i.e.* TCA cycle and ammonia homeostasis), which will be compromised by the SE-induced neuronal deathand gliosis. To further investigate this finding, we performed immunohistochemistry for GS, the enzyme responsible for glutamine synthesis, and found a progressive decrease of GS IR in the hilus. The normalized glutamine levels and decreased GS-IR found at eight weeks in our study are concordant with recent human studies that reported normal levels of glutamine in epileptic patients[168] in combination with decreased GS activity in hippocampal tissue specimens from TLE patients.[103,175] We propose the initial glutamine concentration increase to reflect an imbalance in the glutamate-glutamine cycle, with the eight week time point representing a shift towards a new equilibrium. A possible mechanism would be that the glutamatergic and GABAergic cell death decreases the demand for glutamate and GABA, leading to glial accumulation of glutamine, their precursor. This could cause GS down-regulation, explaining the subsequent decrease in glutamine to normal levels. Alternatively, the reduction in GS-IR could be an inherent consequence of gliosis, as has been recently shown.[244]

Interestingly, the abnormalities detected with *ex vivo* immunohistochemistry are restricted to relatively small areas of the hippocampus. Glutamatergic and GABAergic neuronal loss and the decrease of GS staining are most pronounced in the hilus, with

sparing of the CA regions of the hippocampus. Although the hilus is severely affected, the question remains whether these highly localized changes are sufficient to explain the significant alterations in metabolite concentrations detected with MRS in a large voxel that includes the entire hippocampus. It is possible that the chosen histological staining methods lack the sensitivity to reveal more global neuronal cell death. Alternatively, it could be that, while neurons survive, they are functionally impaired. NAA decreases do not only indicate neuronal death, but may also reflect neuronal metabolic failure. Similarly, it can be argued that the neurotransmitter decreases found with MRS not only reflect localized neuronal death in the hilus, but rather point towards more widespread hippocampal metabolic changes of neurotransmitter cycling in surviving neurons. Further studies to unravel the precise nature of mechanisms responsible for the observed neurotransmitter level changes should benefit from the use of dynamic ^{13}C and ^{1}H-[^{13}C]-MRS with ^{13}C-labeled substrates.[245,246]

In summary, the changes observed in this juvenile model occur as a chronic consequence of SE and possibly reflect components of the complex process that eventually leads to spontaneous seizures. The correlation between changes in MRS neurochemical and (immuno)-histochemical markers supports a possible role for the use of MRS in the follow up of children who suffered from SE or prolonged febrile seizures, to study epileptogenesis preceding TLE.

Acknowledgements

We gratefully acknowledge Bei Wang, Sandra Mulder and Arno van der Grijn for their valuable assistance in the experiments. This study was financially supported by the Dutch Epilepsy Fund (NEF 0415).

6

In vivo neurochemical profiling of rat brain by ^{1}H-[^{13}C] NMR spectroscopy: cerebral energetics and glutamatergic/GABAergic neurotransmission

Pieter van Eijsden[1,2]
Kevin L. Behar[3]
Graeme F. Mason[3]
Kees P. J. Braun[1]
Robin A. de Graaf[4]

1. Department of Pediatric Neurology, Rudolf Magnus Institute of Neuroscience, University Medical Center Utrecht, The Netherlands
2. Department of Neurosurgery, Free University Medical Center, Amsterdam, The Netherlands
3. Magnetic Resonance Research Center, Department of Psychiatry, Yale School of Medicine, New Haven, CT, USA
4. Magnetic Resonance Research Center, Department of Diagnostic Radiology, Yale School of Medicine, New Haven, CT, USA

J Neurochem. 2010 Jan;112(1):24-33

The simultaneous detection of excitatory and inhibitory neurotransmission and the associated energy metabolism is crucial for a proper characterization of brain function. While the detection of glutamatergic neurotransmission *in vivo* by ^{13}C NMR spectroscopy is now relatively routine, the detection of GABAergic neurotransmission *in vivo* has remained elusive due to the low GABA concentration and spectral overlap. Using ^{1}H-[^{13}C] NMR spectroscopy at high magnetic field in combination with robust spectral modeling and the use of different substrates, [U-$^{13}C_6$]-glucose and [2-^{13}C]-acetate, it is shown that GABAergic, as well as glutamatergic neurotransmitter fluxes can be detected non-invasively in rat brain *in vivo*.

Introduction

Neurochemistry is concerned with the study of molecular and cellular processes of the nervous system and their relationship to function. Energy metabolism and neurotransmission are two crucial processes affecting almost all aspects of cerebral function. Proper characterization not only involves determination of absolute metabolite concentrations, but also requires knowledge of the dynamic metabolic turnover of the metabolites involved. ^{1}H NMR spectroscopy is currently the only technique that allows the non-invasive detection and quantification of a wide range of neurochemicals.[247] Direct ^{13}C[248] or indirect ^{1}H-observed, ^{13}C-edited (^{1}H-[^{13}C]) NMR spectroscopy[249,250] enables the dynamic detection of ^{13}C labeled product formation, like [4-^{13}C]-glutamate, [4-^{13}C]-glutamine, and [2-^{13}C]-GABA, which are derived from intravenously infused ^{13}C enriched substrates, such as [1-^{13}C]-glucose. ^{1}H-[^{13}C] NMR spectroscopy provides spectral information similar to the more traditional direct ^{13}C NMR spectroscopy approach, but with the higher sensitivity of proton detection.

Previously, ^{13}C and ^{1}H-[^{13}C] NMR spectroscopy have been used to study energy metabolism in the human[250,251-254] and animal[164,166,249,255-257] brain during hibernating[258], resting[164,166,249-257,259,260] and stimulated conditions.[261-263] Glutamatergic neurotransmission has been assessed as a glutamate–glutamine neurotransmitter cycle between neurons and astroglia.[264] In addition, some of the smaller metabolic pathways like anaplerosis[257,265] and astroglial energy metabolism[266,267] have been studied with alternate substrates, such as [2-^{13}C]-acetate (Ace) and [2-^{13}C]-glucose. The results of ^{13}C MR spectroscopy have been validated through the use of FDG PET in the monkey brain.[268] One of the most important findings from these studies was the linear correlation between increments of cerebral energy metabolism and total neurotransmitter cycling.[164] This relation was subsequently refined by separating the contributions of excitatory glutamatergic and inhibitory GABAergic neurotransmission. However, because of the low concentration of GABA and the strong spectral overlap with other metabolites and macromolecules, studies were necessarily performed *ex vivo*.[165] Fortunately, with the availability of higher magnetic fields and the subsequent increase in spectral resolu-

tion and signal-to-noise ratio (SNR), the detection of lower-concentration metabolites, like GABA, became feasible. Several studies have qualitatively observed the formation of [3-^{13}C]-GABA following [1-^{13}C]-glucose or [1,6-$^{13}C_2$]-glucose infusion.[166,260,269] However, because of limited SNR and/or spectral resolution, to date no studies have appeared that *quantitatively* assess the metabolic fluxes associated with GABA turnover in the normal rat brain *in vivo*. Yang *et al.* were able to measure cerebral GABA turnover *in vivo*, but only after administration of a GABA-transaminase inhibitor to elevate GABA levels.[270,271]

The aim of this study is to assess the extent to which ^{1}H-[^{13}C] NMR spectroscopy can provide reliable and quantifiable neurochemical information about brain metabolite concentrations and turnover under physiological conditions in rat brain *in vivo* at 9.4 T. In particular, the ability to *quantitatively* determine metabolic fluxes of GABA, as well as glutamate, *in vivo* will be established. The detection of both excitatory and inhibitory neurotransmission and cerebral energetics should provide a valuable, non-invasive tool in the understanding of brain function.

Methods

Animal preparation

Animal experiments were conducted in accordance with federal guidelines on the care and use of laboratory animals under approved protocols by the Yale Animal Care and Use Committee.

Following an overnight fast (12–16 h), ten Wistar rats (165.6 ± 12.0 g, mean ± SD) were anesthetized with 2–3% halothane in a mixture of N_2O and O_2 (70/27–28%), tracheotomized and ventilated. A femoral artery was cannulated for monitoring of mean arterial blood pressure and blood sampling to determine arterial blood gasses (pCO_2 and pO_2) and pH. Small adjustments in tidal volume and ventilation frequency kept these physiological variables within normal limits (pCO_2 = 33–45 mm Hg; pO_2 ≥ 120 mm Hg; pH = 7.30–7.58; mean arterial blood pressure = 90–110 mmHg). Body core temperature was measured with a rectal thermometer and maintained at 37 ± 1°C by means of a heated water pad. A femoral vein was cannulated for infusion of [U-$^{13}C_6$]-glucose (Glc, n = 5) or [2-^{13}C]-Ace (n = 5; Cambridge Isotope Laboratories Inc, Andover, MA, USA). Briefly, animals received an initial 250 µL intravenous bolus of 0.75 M [U-$^{13}C_6$]-glucose (per 200 g body weight) followed by an intravenous infusion of 0.75 M [U-$^{13}C_6$]-glucose. The infusion rate was decreased manually every 30 s according to a decreasing exponential function during the first 8 min and was constant at 13.7 µL/min for the remainder of the experiment. For acetate, animals received an initial 200 µL intravenous bolus of 2.0 M [2-^{13}C]-Ace over 15 s. The infusion rate was decreased to 50–25 µL/min at 15 s and 240 s, respectively, and remained constant at 12.5 µL/min for the remainder of the experiment (t > 480 s). Following surgery, halothane was reduced to 0.5–1% to maintain a stable blood pressure. Animal heads were shaven to allow for better coil positioning and animals were placed in the probe, restrained in a head holder and were further immobilized with d-tubocurarine (0.5 mg/kg/40 min, i.p.). After the magnetic resonance experiments, the rats were killed while still anaesthetized.

Magnetic resonance spectroscopy

Experiments were performed on a 9.4 T Magnex magnet and Bruker console (Bruker, Billerica, MA, USA) equipped with a 9-cm-diameter gradient coil insert (Resonance Research Inc, Billerica, MA, USA, 490 mT/m in 175 µs). A 14-mm-diameter surface coil was used for ^{1}H RF pulse excitation and signal reception (400.5 MHz). RF pulse transmission on ^{13}C (100.2 MHz) was achieved with two orthogonal 21 mm diameter surface coils driven in quadrature.[272] Multi-slice echo planar images (FOV 2.56 × 2.56 cm, matrix 128 × 128, ten slices of 1 mm thickness, TR/TE = 2500/10 ms) were acquired and used to position the spectroscopic volume of interest (6 × 5 × 6 mm) over the hippocampal area as close to the surface coil as possible, but remaining at least 0.5 mm away from the edges of the brain to improve magnetic field homogeneity. The rostral-caudal center of the voxel was positioned in the slice that showed the most dorsal portion of the medial hippocampus.

The magnetic field homogeneity over the volume of interest was optimized with the non-iterative FASTMAP algorithm for all first- and second-order shim coils.[227] This resulted in signal line widths of 14–16 Hz for water and 9–11 Hz for metabolites in the localized volume of 180 µL. Localized ^{1}H NMR spectra were obtained with the NMR pulse sequence described previously.[166] In short, 3D localization was achieved by a combination of outer volume suppression, image-selected *in vivo* spectroscopy, and slice-selective excitation. Water suppression was performed with SWAMP,[273] an adiabatic analog of the CHESS technique.[228] Discrimination between ^{1}H-[^{13}C] and ^{1}H-[^{12}C] NMR signals was achieved by executing a 4.0 ms AFP pulse (sin40 modulation, 10 kHz bandwidth)[274] on the ^{13}C channel on alternating acquisitions, after which the FIDs obtained with and without the ^{13}C inversion were stored in separate memory blocks. ^{1}H-[^{13}C] NMR signals were obtained by subtraction of the ^{13}C-inverted FIDs from the non-inverted FIDs. Broadband adiabatic ^{13}C decoupling was applied during the total acquisition time of 204.8 ms. The decoupling sequence was executed with a 1.6 ms AFP pulse (HS4 modulation, 6.25 kHz bandwidth)[274] incorporated in a 20-step supercycle[275] to provide adiabatic, frequency-selective decoupling.[276] With the decoupling frequency centered on the [4-^{13}C]-glutamate resonance at 34.2 ppm, the decoupling sequence provides frequency-selective decoupling between circa 3 and 65 ppm, while leaving the [1-^{13}C]-glucose resonances at 92.7 and 96.6 ppm unperturbed. Since the αH1-glucose resonance is resolved in ^{1}H NMR spectra at 9.4 T, frequency-selective decoupling allows

for direct quantification of the ^{13}C fractional enrichment of cerebral glucose from total, unedited ^{1}H NMR spectra.[276]

The total GABA concentration was obtained through homonuclear spectral editing with a double spin-echo sequence using 20 ms Gaussian refocusing pulses selective for the GABA-H3 protons at 1.89 ppm.[277] An echo time of 68 ms (= 1/2J) was chosen to optimize the detection efficiency of the GABA-H4 protons at 3.01 ppm. RF pulse calibration was performed on the water resonance. Editing efficiency on individual animals was calculated from the residual water signal in the presence of spectral editing pulses. The experiments were performed with a TR of 4.0 s and 64 repetitions with interleaved editing. The GABA-edited spectrum was obtained by subtracting the non-edited from the edited spectra.

Data acquisition and processing

All FIDs were acquired with a 32-s time resolution (eight image-selected *in vivo* spectroscopy increments with TR = 4.0 s) to minimize the effects of small frequency shifts between acquisitions and to evaluate motion artifacts. Following a complete experiment of approximately 32 min of continuous signal acquisition, FIDs were zero-filled to 8 K data points, apodized (1.0 Hz Gaussian line broadening), Fourier transformed, and phase corrected (only zero-order phase). The spectra were frequency corrected to account for drift in the main magnetic field, but no amplitude or phase corrections were performed on individual spectra. Next, spectra acquired over 16 min were added to increase the SNR and used for subsequent quantification of metabolite concentrations and fractional enrichments by an in-house frequency-domain fitting program written in Matlab 7.0.4 (The Mathworks, Natick, MA, USA). Similar to LCmodel,[176] the algorithm models the *in vivo* NMR spectrum as a superposition of a basis set of *in vitro* NMR spectra of pure metabolite solutions. ^{1}H NMR spectra were collected *in vitro* under controlled pH and temperature conditions from Ace, Ala, Asp, Cr, GABA, Glc, [U-$^{13}C_6$]-Glc, Glu, Gln, GSH, glycerophosphorylcholine, Lac, myo-inositol, NAA, NAA-glutamate, PCr, phosphocholine, phosphoethanolamine, taurine and valine. A macromolecular baseline was measured separately on a number of animals by "nulling" the metabolite resonances with a double inversion recovery element preceding the ^{1}H-[^{13}C] NMR sequence with 1.0 ms hyperbolic secant modulated AFP pulses (bandwidth 10 kHz), inversion recovery time = 1950 and 550 ms and TR = 6000 ms.[230] Following spectral fitting, the absolute metabolite concentrations were calculated with respect to tCr (= PCr + Cr) under the assumption of a 10 mM tCr concentration. No correction for differential T_2 relaxation was performed. A separate version of the fitting program with additional constraints and a reduced basis set (Ace, Ala, Asp, GABA, Glc, Gln, Glu, Lac, NAA) was used for quantification of the edited ^{1}H-[^{13}C] NMR spectra. Specifically, while the resonance amplitudes of the different isotopically-labeled peaks within one molecule (e.g. [2-^{13}C], [3-^{13}C] and [4-^{13}C]-glutamate) were unconstrained, the line width, phase, and frequency were forced to be identical. The reliability of the spectral fit was evaluated by MCS using 50 iterations. The traditional Cramer-Rao lower bounds were not used, as they are not valid in the presence of an unknown macromolecular baseline. Although the Cramer-Rao lower bounds can be modified to include so-called "nuisance" parameters related to the baseline,[278] we found the use of MCS a more straightforward alternative. The MCS results are expressed as the % (SD MCS/mean MCS) to indicate the percentage of uncertainty in the concentration that is determined from the spectral fitting.

Metabolic modeling

To obtain the rates of the glutamatergic and GABAergic TCA cycles ($V_{TCA,Glu}$ and $V_{TCA,GABA}$) and the rates of glutamatergic and GABAergic neurotransmission ($V_{cycle,GluGln}$ and $V_{cycle,GABAGln}$), the study was designed with two different substrates, [U-$^{13}C_6$]-Glc and [2-^{13}C]-Ace. The dynamic [U-$^{13}C_6$]-Glc study provides information on $V_{TCA,Glu}$, $V_{TCA,GABA}$ and $V_{cycle,total} = V_{cycle,GluGln} + V_{cycle,GABAGln}$. The individual glutamatergic and GABAergic neurotransmitter cycling rates cannot be separated during a [U-$^{13}C_6$]-Glc study since both neurotransmission cycles label the same [4-^{13}C]-Gln position in the astroglial compartment.[165] As detailed below, the steady-state [2-^{13}C]-Ace study is used to obtain the ratio between the neurotransmitter cycle rate and the TCA cycle rate for each neuronal compartment. This ratio is used as a constraint during the metabolic modeling of the dynamic [U-$^{13}C_6$]-Glc study to obtain all four independent rates, $V_{TCA,Glu}$, $V_{TCA,GABA}$, $V_{cycle,GluGln}$, and $V_{cycle,GABAGln}$.

Time-courses for [3-^{13}C]-Glu, [4-^{13}C]-Glu, [3-^{13}C]-Gln, [4-^{13}C]-Gln, [2-^{13}C]-GABA, and [4-^{13}C]-GABA were reconstructed over 16 min intervals during infusion of [U-$^{13}C_6$]-Glc. During the [2-^{13}C]-Ace infusion only the endpoint fractional enrichments were calculated. The glucose time courses were analyzed using a three-compartment metabolic model, comprising glutamatergic neuronal, GABAergic neuronal, and astroglial compartments, similar to the model described by Patel *et al.*[165] Briefly, blood glucose enters the brain via Michaelis-Menten-based transport across the blood–brain barrier. However, since [1-^{12}C]-αH1-glucose and [1-^{13}C]-αH1-glucose levels could be detected and quantified directly in the brain compartment, no assumptions were required regarding glucose transport across the blood–brain barrier. Brain glucose is converted to pyruvate, which enters either the neuronal or astroglial TCA cycles. The ^{13}C label of [U-$^{13}C_6$]-glucose will arrive at the TCA cycle intermediate [4-^{13}C]-α-KG, which is in rapid exchange with [4-^{13}C]-Glu at a rate V_x. Since [3-^{13}C]-Glu and [3-^{13}C]-Gln were both measured and included in the model, no assumptions about V_x were required. After labeling of [4-^{13}C]-Glu, the [4-^{13}C]-Gln position is ultimately labeled by the action of a glutamatergic

neurotransmitter cycle between the glutamatergic neuronal and astroglial compartments. After one additional turn of the TCA cycle also [3-^{13}C]-Glu and [3-^{13}C]-Gln will label. In the GABAergic neuronal compartment, [4-^{13}C]-Glu is quickly converted to [2-^{13}C]-GABA, which ultimately labels [4-^{13}C]-Gln through a neurotransmitter cycle between the GABAergic neuron and the astroglial compartment. In a subsequent turn of the TCA cycle, both [3-^{13}C]-GABA and [4-^{13}C]-GABA are labeled. Infusion of [2-^{13}C]-Ace will first label the small astroglial [4-^{13}C]-Glu pool, after which the label will appear in the larger astroglial [4-^{13}C]-Gln pool. Gln is subsequently shuttled from the astroglia to the neurons where it will label the [4-^{13}C]-Glu pools of both the GABAergic and glutamatergic compartments. Further details on the metabolic model can be found in Patel *et al.*[165]

In this metabolic model, a large set of coupled differential equations (using mass and isotope balance) was used within the CWave software package (Cwave 3.0[279]) to describe the behavior of above mentioned labeled substrates in response to the infusion of [U-$^{13}C_6$]-glucose. This model was restricted by prior knowledge from the steady-state [2-^{13}C]-Ace experiment, from which the ratio between V_{cycle} and V_{TCA} can be determined for the glutamatergic and GABAergic compartments. For this, the differential equations that describe the flow of ^{13}C through the Glu/Gln and GABA/Gln cycles were solved analytically for the steady-state condition, which yielded the following relationships between V_{cycle} and V_{TCA} for glutamatergic and GABAergic neurons

$$V_{cycle\_Glu/Gln}/V_{TCA\_glu} = FE_{Glu4}/ (FE_{Gln4} - FE_{Glu4}) \quad [1]$$

$$V_{cycle\_GABA/Gln}/V_{TCA\_GABA} = FE_{GABA2}/ (FE_{Gln4} - FE_{GABA2}) \quad [2]$$

where FE_{Glu4}, FE_{Gln4}, and FE_{GABA2} represent the steady-state ^{13}C enrichments of these amino acids during the infusion of [2-^{13}C]-Ace.[165]

The model was further constrained by assuming the V_{PC} to be 20% of the rate of total glutamine synthesis.[257] Dilutional fluxes were iterated for the three separate compartments. The cerebral metabolic rates were determined from the best fits of the model to the time-courses of ^{13}C labeling with a Levenberg-Marquardt algorithm hybridized with simulated annealing.[280] $CMR_{Glc(ox)}$ were calculated as $\frac{1}{2}V_{TCA}$. The GABA pool was assigned to the GABAergic neuronal compartment, whereas Glu was divided between glutamatergic neurons (88%), astroglia (10%), and GABAergic neurons (2%).[281,282] Gln was assumed to be synthesized in the astroglial compartment and degraded in the neuronal compartment.

With the described prior knowledge and restrictions, the metabolic model was used to determine the $V_{TCA,Glu}$, the $V_{TCA,GABA}$ and $V_{TCA,A}$, the rate between α-KG and Glu (V_x), the $V_{cycle,GluGln}$, the $V_{GABAshunt}$, the $V_{cycle,GABAGln}$, and the dilutional rates ($V_{dil,Glu}$, $V_{dil,Glial}$, and $V_{dil,GABA}$).

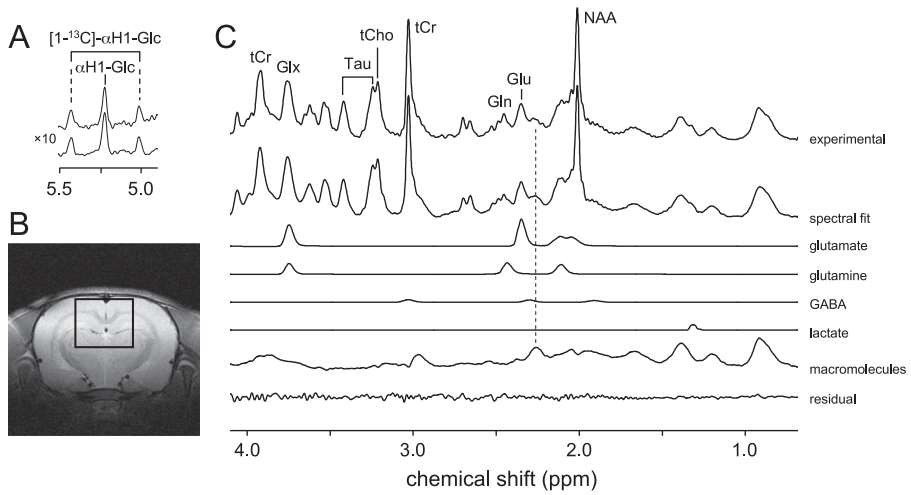

Fig. 6.1 | Localized ^{1}H-[^{13}C] NMR spectroscopy of rat brain in vivo at 9.4 T acquired between 120 and 150 min following the start of intravenous [U-$^{13}C_6$]-glucose infusion. **A** The [1-^{12}C]-αH1-glucose signal appears at 5.22 ppm, whereas the [1-^{13}C]-αH1-glucose signal appears, because of selective decoupling, as a doublet signal with a one-bound ^{1}H-^{13}C scalar coupling of 169 Hz. Because of selective spectral editing, the proton glucose resonances are identical in the absence (upper trace) and presence (lower trace) of the ^{13}C inversion pulse. **B** Location of the 180 µL (= 6 × 5 × 6 mm) voxel. **C** Experimental ^{1}H NMR spectrum averaged over 32 min in the absence of a ^{13}C inversion pulse (top trace), together with the total spectral fit, the spectral contributions of glutamate, glutamine, GABA, lactate and macromolecules to the total spectral fit and the difference between the experimental and fitted ^{1}H NMR spectra (lower trace).

Results

Figure 6.1 shows a typical ^{1}H NMR spectrum from rat brain *in vivo* at 9.4 T acquired between 120 and 150 min following the start of intravenous [U-$^{13}C_6$]-glucose infusion. Figure 6.1(c) shows, besides the experimentally measured spectrum (top trace), the total spectral fit, the spectral contributions of glutamate, glutamine, GABA, and Lac to the total fit, the macromolecular baseline and the difference between the measured and fitted spectra (bottom trace). The absolute metabolite concentrations are listed in Table 6.1 (overleaf).

Since the adiabatic decoupling sequence provides frequency-selective decoupling (from circa 3 ppm to 65 ppm on the ^{13}C channel) all ^{1}H-[^{13}C] NMR resonances upfield from water are perfectly decoupled. Since the ^{13}C resonances from [1-^{13}C]-glucose fall outside the decoupling range, the ^{1}H resonances of [1-^{13}C]-αH1-glucose are not decoupled (Fig. 6.1a). The ^{13}C inversion pulse inverts the ^{1}H-[^{13}C] resonances relative to the ^{1}H-[^{12}C] res-

	Mean (mM)	SD (mM)	MCS (%)
Alanine	0.27	0.09	58.30
Aspartate	2.48	1.00	11.89
Choline	1.71	0.09	9.90
Glycerophosphorylcholine	0.99	0.08	11.59
Phosphocholine	0.72	0.06	24.88
GABA†	1.17	0.31	16.68
Glutamate	10.11	0.93	4.67
Glutamine	4.56	0.53	7.30
Glutathione	1.98	1.28	9.77
Myo-Inositol	3.84	0.48	3.15
N-Acetyl Aspartate	8.95	0.44	1.26
N-Acetyl Aspartate Glutamate	2.90	0.69	13.58
Lactate	0.82	0.15	30.08
Phospho-Ethanolamine	1.58	0.11	10.48
Taurine	3.54	0.11	4.06
Valine	0.39	0.07	20.81

All concentrations are referenced to 10 mM total creatine (n=10). † Obtained from J-difference edited ^{1}H NMR spectra.

Table 6.1 | Metabolite concentrations in rat brain obtained prior to intravenous substrate infusion

onances on subsequent scans. However, since the ^{13}C inversion pulse is also frequency-selective, the [1-^{13}C]-αH1-glucose resonances do not invert and are thus identical in the absence (upper trace) or presence (lower trace) of the ^{13}C editing pulse. Besides the excellent spectral fit, the most noticeable feature of Fig. 6.1(c) is the origin of the signal at 2.2–2.3 ppm as indicated by the dotted line. Even though this signal is commonly referred to as GABA-H2, it is clear from Fig. 6.1(c) that the majority of this signal must be assigned to macromolecules with only a minor, shifted contribution from GABA-H2. When the macromolecular baseline is properly accounted for, it has been shown that GABA can be accurately quantified from short TE ^{1}H NMR spectra.[247] However, in this study, the obtained GABA concentration showed a clear deviation (0.50 ± 0.07 mM) from known GABA levels when calculated directly from the short TE ^{1}H NMR spectrum. As a result, GABA detection was achieved with more conventional homonuclear spectral editing. Figure 6.2 shows two ^{1}H NMR spectra with and without selective refocusing of GABA-H3. The difference between the two NMR spectra reveals the outer two resonances of the GABA-H4 triplet at 3.01 ppm. The finite bandwidth of the selective refocusing pulses leads to partial co-editing of NAA at 2.01 ppm and glutamate/glutamine at 3.75 ppm. However, these resonances are well-separated from GABA-H4 and do not affect

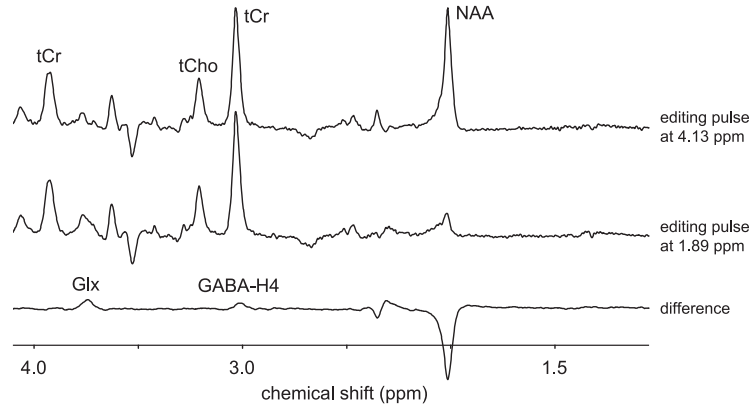

Fig. 6.2 | Spectral editing of GABA in rat brain in vivo at 9.4 T. ^{1}H NMR spectra are acquired in which the 20 ms Gaussian editing pulses selectively refocus the GABA-H3 resonance at 1.89 ppm (middle trace) or at a control position (4.13 ppm, upper trace) mirrored relative to the total creatine resonance at 3.01 ppm. The difference spectrum displays the edited GABA-H4 resonance at 3.01 ppm together with co-edited signals from glutamate/glutamine-H2, GABA-H2, and NAA.

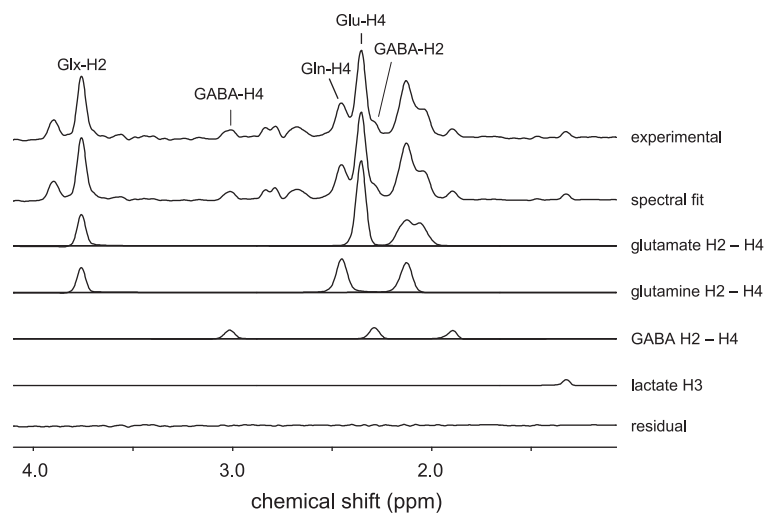

Fig. 6.3 | Localized ^{1}H-[^{13}C] NMR spectroscopy of rat brain in vivo at 9.4 T acquired between 120 and 150 min following the start of intravenous [U-$^{13}C_6$]-glucose infusion. The ^{13}C-edited ^{1}H NMR spectrum is shown (top trace), together with the total spectral fit, as well as the spectral contribution of the glutamate, glutamine, GABA, and lactate resonances to the total fit. The lower trace shows the difference between the experimental and fitted ^{13}C-edited ^{1}H NMR spectra.

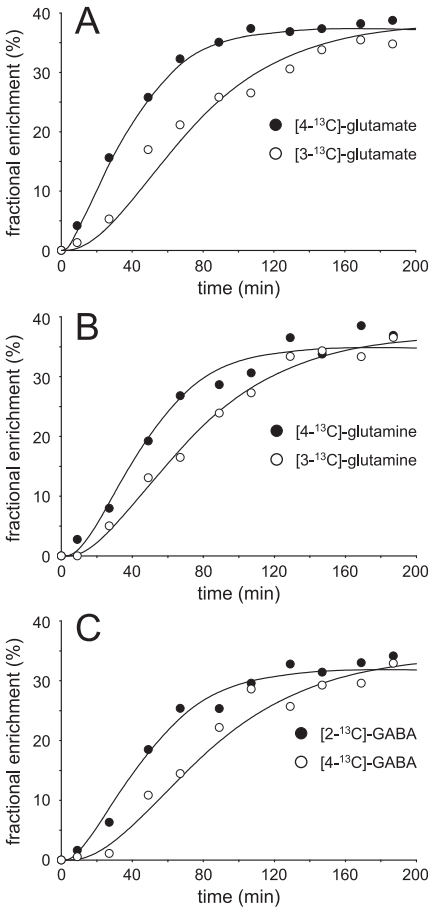

Fig. 6.4 | Metabolic turnover curves for (a) [3-^{13}C] and [4-^{13}C]-glutamate, (b) [3-^{13}C] and [4-^{13}C]-glutamine, and (c) [2-^{13}C] and [4-^{13}C]-GABA during the infusion of [U-^{13}C6]-glucose. The dots represent the experimentally measured fractional enrichment, whereas the solid curves represent the best fit to the metabolic model.

the GABA quantification. As a result of the increased chemical shift dispersion at 9.4 T, co-editing of macromolecules was minimal. The GABA concentration obtained through homonuclear spectral editing was 1.17 ± 0.31 mM.

Figure 6.3 shows the edited ^{1}H-[^{13}C] NMR spectrum obtained from rat brain 120 min following the onset of the [U-$^{13}C_6$]-glucose infusion. The most prominent resonances originated from glutamate, glutamine, and GABA. Note that all spectra were acquired in the presence of selective ^{13}C decoupling, thus eliminating splitting because of heteronuclear scalar coupling. The decoupling and editing pulses did not affect the [1-^{13}C]-α-glucose resonances at 92.7 ppm, such that (i) heteronuclear scalar coupling is still visible on the αH1-glucose resonance at 5.22 ppm; and (ii) [1-^{13}C]-αH1-glucose

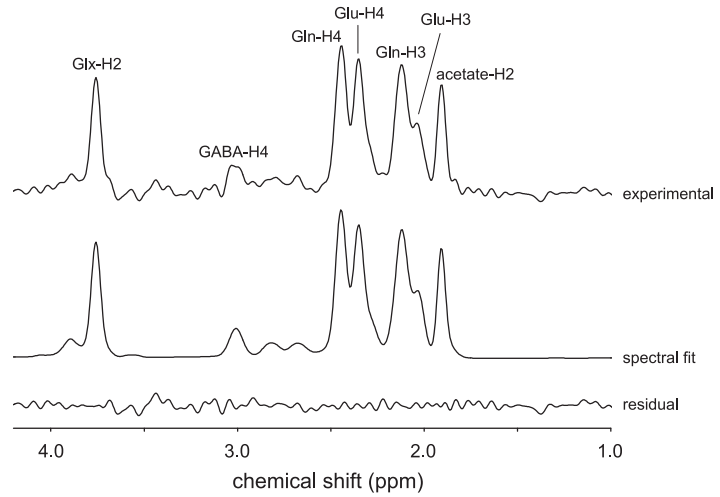

Fig. 6.5 | Localized ^{1}H-[^{13}C] NMR spectroscopy of rat brain in vivo at 9.4 T following intravenous [2-^{13}C]-Ace infusion. The 13C-edited 1H NMR spectrum is shown (top trace), together with the total spectral fit, the spectral contributions of the H2, H3, and H4 label positions of glutamate, glutamine and GABA, the spectral contribution of acetate and the difference between the experimental and fitted ^{13}C-edited ^{1}H NMR spectra (lower trace). The experimental data (top trace) is averaged between 120 and 150 min following the onset of [2-^{13}C]-Ace infusion.

does not appear in the ^{1}H-[^{13}C] difference spectrum (see also Fig. 6.1a). Figure 6.3 also shows the best fit of the measured ^{1}H-[^{13}C] NMR spectrum as well as the spectral contributions of glutamate, glutamine, GABA and Lac. Note that [2-^{13}C]-GABA appears as a clear upfield shoulder of the [4-^{13}C]-glutamate resonance. Repeating the spectral fit without the inclusion of [2-^{13}C]-GABA (data not shown) resulted in a significant residual, indicating that GABA is an essential part of the ^{1}H-[^{13}C] NMR spectrum.

Figure 6.4 shows the turnover curves (n = 5) for (a) [4-^{13}C] and [3-^{13}C]-glutamate, (b) [4-^{13}C] and [3-^{13}C]-glutamine and (c) [2-^{13}C] and [4-^{13}C]-GABA together with the best fit of the metabolic model described in the Methods section. Experimental data was averaged over 16 min in order to increase the signal-to-noise ratio.

Figure 6.5 shows the endpoint ^{1}H-[^{13}C] spectrum acquired 120 min following the start of [2-^{13}C]-Ace infusion. Besides the large [2-^{13}C]-Ace resonance at 1.91 ppm, an increased [4-^{13}C]-glutamine resonance relative to the [4-^{13}C]-glutamate is characteristic, as has been shown previously by direct ^{13}C NMR detection.[266,267] The [3-^{13}C]-GABA resonance was overwhelmed by the much larger [2-^{13}C]-Ace resonance and could not be quantified. The signal upfield from the [4-^{13}C]-Glu resonance can only be explained by the presence of [2-^{13}C]-GABA (dotted line). Omission of GABA leads to a strong degradation of the spectral fit. The MCS uncertainties for GABA-H2 in the glucose and acetate studies were 18.3% and 21.2%, respectively.

From the steady-state [2-^{13}C]-Ace experiment, the ratio between V_{cycle} and V_{TCA} was determined for the glutamatergic ($V_{cycle,GluGln}/V_{TCA,Glu}$ = 0.58 ± 0.076) and GABAergic neurons ($V_{cycle,GABAGln}/V_{TCA,GABA}$ = 0.54 ± 0.063). The endpoint fractional enrichments for Glu-H4, Gln-H4 and GABA-H2 are 11.06 ± 1.50%, 27.11 ± 3.68%, and 9.51 ± 1.49%, respectively. These values were used to constrain the metabolic model during the fitting of the data obtained with [U-$^{13}C_6$]-glucose. The resulting TCA cycle rates were given by $V_{TCA,Glu}$ = 0.472 ± 0.040 µmol/min/g, $V_{TCA,GABA}$ = 0.062 ± 0.009 µmol/min/g, and $V_{TCA,A}$ = 0.144 ± 0.025 µmol/min/g. Using the [2-^{13}C]-Ace data as constraint, the excitatory and inhibitory neurotransmitter cycle rates were given by $V_{cycle,GluGln}$ = 0.274 ± 0.023 µmol/min/g and $V_{cycle,GABAGln}$ = 0.033 ± 0.005 µmol/min/g, representing 89.2% and 10.8% of the total neurotransmitter cycling fluxes, respectively. The GABA shunt, VGABA, was determined as 0.025 ± 0.006 µmol/min/g, whereas the exchange rate between α-KG and Glu, V_x, was 5.5 ± 2.4 µmol/min/g. The dilutional rates were all < 0.065 µmol/min/g.

Discussion

Here, we have shown that the metabolic turnover of the excitatory and inhibitory neurotransmitters, glutamate and GABA, can be detected simultaneously by ^{1}H-[^{13}C]-NMR spectroscopy in rat brain *in vivo*. The infusion of [U-$^{13}C_6$]-glucose gives information about glutamatergic and GABAergic energy metabolism, as well as total neurotransmission. When used in combination with steady-state fractional enrichments following a [2-^{13}C]-Ace infusion, the total neurotransmitter cycle rate can be separated into the glutamatergic and GABAergic contributions.

In this study, we were able to detect the fractional enrichment and concentration of cerebral glucose directly through a combination of selective heteronuclear editing and decoupling and very selective water suppression. The primary benefit of direct cerebral glucose detection is that no assumptions are necessary regarding blood-to-brain glucose transport kinetics. Furthermore, *in vivo* detection allows for a much higher temporal resolution than would be possible with arterial blood sampling.

Although the results demonstrate the feasibility of detecting cerebral GABA turnover by ^{1}H-[^{13}C] NMR spectroscopy, the technique is demanding and optimal experimental conditions must be obtained for successful completion of the study. Foremost, the magnetic field homogeneity must be sufficient to allow the differentiation of glutamate-H4 and GABA-H2. At 9.4 T, this condition required that the line width of water be no more than 16 Hz. Such a line width could only be achieved through the use of all first- and second-order spherical harmonics shims in combination with stabile and optimal animal physiology. To account for temporal magnetic field drifts, it was crucial to store each FID separately and perform a post-acquisition frequency correction prior to any further processing.

Besides optimal magnetic field homogeneity, the spectral SNR was also important for reliable GABA detection. Given a GABA concentration of 1.17 ± 0.31 mmol/L (Table 6.1) and an endpoint fractional enrichment of c. 35% during [U-$^{13}C_6$]-glucose infusion, the spectral sensitivity must be sufficient to detect 0.4 mM GABA in 16 min. The volume size of 180 µL at 9.4 T in this study was sufficient to detect GABA turnover reliably. In future studies, the volume size can potentially be decreased, especially when the magnetic field homogeneity over the smaller volume improves.

The spectral fitting algorithm yielded the total GABA concentration from the total, non-edited ^{1}H NMR spectrum, as was previously reported.[247] However, the non-edited GABA concentration (0.50 ± 0.07 mM) displayed a clear deviation from known GABA concentrations (0.83–2.30 mM) in rat brain *in vivo*.[247] The total GABA concentration (1.17 ± 0.31 mM) obtained by homonuclear spectral editing was in good agreement with literature values. The accuracy of the GABA concentration obtained by spectral editing was lower than that obtained by short TE NMR spectroscopy, likely because of a lower spectral SNR. However, the GABA extracted from short TE ^{1}H NMR spectra was biased toward a lower concentration. This can be attributed to significant spectral overlap of GABA at all spectral positions and a strong correlation between GABA and the macromolecular baseline.[278] In contrast, the edited GABA ^{1}H NMR spectrum has no macromolecular baseline and minimal spectral overlap, such that the accuracy is directly related to the spectral SNR. Given the importance of the absolute GABA concentration, the reliability of homonuclear spectral editing was preferred over the precision of short TE MR spectra.

The value of V_{cycle},GABAGln = 0.033 ± 0.005 µmol/min/g is lower than a previous estimate by Patel *et al.* of 0.135 ± 0.015 µmol/min/g measured for the rat cortex under similar physiological conditions (halothane anesthesia).[165] In contrast, Yang *et al.*, using a selective inhibitor of GABA transaminase (gabaculine) to elevate the GABA pool and enhance ^{13}C label trapping from [1-^{13}C]-glucose, determined a value $V_{cycle,GABAGln}$ = 0.030 ± 0.007 µmol/min/g for the brain of α-chloralose anaesthetized rats.[270] This value is consistent with previous estimates of GABA synthesis and $V_{cycle,GABAGln}$ after acute GABA-transaminase inhibition under similar physiological conditions, but is less than values determined in the absence of such inhibitors.[283] The higher GABA turnover rate in our previous study[165] is likely to result from a higher fraction of pure cortical tissue, whereas the large 180 µL volume of this study contains large amounts (> 60%) of white matter and subcortex, including corpus callosum, hippocampus, and thalamus (Fig. 6.1b). The similarity in the present value of $V_{TCA,n}$ (= $V_{TCA,Glu}$ + $V_{TCA,GABA}$ = 0.53 µmol/g/min)

to the subcortex (0.44 μmol/g/min), but not to the cortex (0.73 μmol/g/min) from a previous study supports this contention.[284]

Yang *et al.* were not able to detect [2-^{13}C]-GABA labeling during [2-^{13}C]-Ace infusion under normal conditions (*i.e.*, without vigabatrin).[270] However, given the low GABA-H2 fractional enrichment and concentration and the 3.5 times smaller volume, the absence of [2-^{13}C]-GABA detection by may simply be explained by an inadequate spectral SNR. Patel *et al.* studied GABAergic neurotransmission in the rat cortex *ex vivo* and found significant GABA turnover from [2-^{13}C]-Ace ($V_{cycle,GABAGln}/V_{TCA,GABA}$ = 0.45),[165] consistent with other studies reporting *ex vivo* measurements of GABA labeling from [1,2-$^{13}C_2$]-Ace in extracts of rat and mouse brain.[285,285]

Conclusions

This work has shown that simultaneous detection of glutamatergic and GABAergic neurotransmission and the associated energy metabolism in rat brain *in vivo* is possible at 9.4 T under optimal experimental conditions. This capacity opens the possibility of studying excitatory and inhibitory neurotransmission during a wide range of conditions, including functional activation and epilepsy.

Acknowledgements

This research was supported by NIH grants R01 DK027121 (K. L. B.) and K02 AA13420 (G. F. M.) and by the Dutch Epilepsy Fund (NEF 0415). The authors thank Bei Wang for expert animal preparation, Peter Brown for construction and maintenance of the ^{1}H-[^{13}C] RF coil and Terence Nixon and Scott McIntyre for system maintenance.

7

Chronic status epilepticus induced changes in hippocampal energy and neurotransmitter metabolism

Pieter van Eijsden[1,3]
Robin A. de Graaf[5]
Puneet Bagga[4]
Kevin L. Behar[6]
Graeme F. Mason[6]
Onno van Nieuwenhuizen[2]
Pierre N.E de Graan[2]
Kees P.J. Braun[2]

1,2. Rudolf Magnus Institute of Neuroscience, Departments of Child Neurology[1] and Neuroscience & Pharmacology[2], University Medical Center Utrecht, The Netherlands
3. Department of Neurosurgery, Free University Medical Center, Amsterdam, The Netherlands
4. Biomedical MR Imaging and Spectroscopy Group, Image Sciences Institute, University Medical Center Utrecht, The Netherlands
5,6. Magnetic Resonance Research Center, Departments of Radiology[5] and Psychiatry[6], Yale University School of Medicine, New Haven, Connecticut, USA

During the development of temporal lobe epilepsy, the hippocampus becomes gliotic, shows neuronal loss of predominantly GABAergic nature and aberrant mossy fiber connections. In addition immunoreactivity of glutamine synthase (GS), an astroglial enzyme essential in the neurotransmitter cycle, has been shown to be decreased in human and experimental TLE. These changes take place before spontaneous seizures (SRS) occur, but may be essential for their development.
This study aims to use ^{1}H-[^{13}C] Magnetic resonance spectroscopy (MRS) to characterize the development of changes in hippocampal neurotransmitter metabolism that could contribute to the development of SRS during the latent phase of a juvenile rat model of TLE.

This study shows that the glutamatergic compartment is relatively intact from a metabolic point of view. However, the GABAergic compartment display a decrease in neurotransmitter turnover and glutamic acid decarboxylase (GAD) activity, the enzyme required for GABA synthesis. In addition a decrease in GS activity was present in the glial compartment. We conclude that in addition to disproportionate cell death, the remaining viable GABAergic neurons are also functioning at a lower metabolic level, adding to the hyperexcitable state. GS downregulation may be due to gliosis proper or by downregulation due to glutamine accumulation. The fact that GS decrease in healthy animals provokes seizures, warrants the assumption that this may represent a crucial step in epileptogenesis.

Introduction

Temporal lobe epilepsy (TLE) is oftentimes preceded by childhood status epilepticus (SE) or febrile seizures. After several years of healthy life following this initial precipitating event (latent phase), spontaneous seizures develop. Apparently, a still largely unknown cascade of pathophysiological events has been triggered, eventually leading to chronic TLE. During this process called epileptogenesis the hippocampus plays a central role. It becomes gliotic, shows neuronal loss and new aberrant mossy fiber connections, and when spontaneous recurrent seizures (SRS) develop, the hippocampus is the seizure onset focus. In patients suffering from TLE, the hippocampus is characterized by an imbalance between the excitatory and inhibitory neurotransmitters glutamate and γ-aminobutyric acid (GABA).[167]

In the hippocampus the majority of neurons is either glutamatergic or GABAergic. Both neurotransmitters serve multiple functions in the mammalian brain, requiring a complex homeostatic system that involves several cell specific elements in both neurons and astrocytes. The predominantly glial uptake of glutamate[157,159] and the fact that neurons need TCA cycle intermediates to synthesize glutamate and GABA from glucose,[160] creates a complex metabolic relationship between neurons and glia and between TCA cycling and neurotransmitter cycling.[64,161,162] In the glutamatergic synapse, glutamate is released and taken up into surrounding astrocytes, where it is transformed into glutamine by the astrocyte-specific enzyme glutamine synthase (GS)[163] and which is then released into the extracellular space and taken up into neurons, where it is converted back to glutamate.[160] In the GABAergic synapse, GABA is taken up into astrocytes and catabolized to the TCA cycle intermediate succinate, which is used for synthesis of glutamate. Glutamate formed in the GABAergic neurons is converted to GABA by the glial enzyme glutamic acid decarboxylase (GAD).

In addition to the aforementioned neurotransmitter imbalance in the epileptogenic hippocampus, various studies have shown a decrease in GS immunoreactivity in human and experimental TLE.[103,175] An inherent limitation of the human brain studies is that patients are operated in the end-stage of TLE, in which the contribution of the initial epileptogenic injury is obscured by the pathological consequences of suffering

from seizures for years. Therefore, to better understand the role of neurotransmitter metabolism in the process of epileptogenesis, we need dynamic metabolic information during the latent phase, following SE and before SRS occur.

This type of research can only be performed in animal models. We chose the juvenile lithium-pilocarpine rat model.[226] In this model SE is induced in 21-day-old rats by pilocarpine, the effect of which is potentiated by lithium. Animals that recover from SE develop normally compared to litter mates, but start to experience SRS with a hippocampal electrophysiological origin and semiology after a latent phase of 10-16 weeks. This model is ideally suited for this study, because of the similarities with human TLE, both in terms of the developmental stage of the subjects and in terms of electrophysiological characteristics and histopathology.[123]

The dynamics of the glutamate-glutamine cycle were studied by ^{1}H-[^{13}C] Magnetic resonance spectroscopy (MRS). This non-invasive approach enables quantification of a wide range of neurochemicals and their turnover. It relies on the dynamic detection of ^{13}C-labeled products, like [4-^{13}C]-glutamate, [4-^{13}C]-glutamine and, as recently shown, [2-^{13}C]-GABA, formed from intravenously infused ^{13}C-enriched substrates.[246] Therefore, ^{1}H-[^{13}C] MR is an ideal tool to study post-SE pathology *in vivo*. An added benefit is that this technique is safe and can easily be adapted for application in a clinical setting. The aim of this study is to characterize with MRS the development of early, persistent changes in hippocampal neurotransmitter metabolism that could contribute to the development of SRS during the latent phase of the pilocarpine-induced SE model of TLE.

Methods

Animal preparation

Animal experiments were conducted in accordance with federal guidelines on the care and use of laboratory animals under an approved protocol by the Yale Animal Care and Use Committee (IACUC).

20-day old male Wistar rats (n=20; 45.6±2.6 g) were injected intraperitoneally (i.p.) with 3 mEq/kg lithium chloride (Merck, Darmstadt, Germany) 20 hours before induction of SE. Thirty minutes before the subcutaneous administration of 40 mg/kg pilocarpine hydrochloride (Sigma, St. Louis, MO), 1 mg/kg of scopolamine methyl nitrate (Sigma) was injected i.p. to antagonize the peripheral cholinergic effects of pilocarpine. Age-matched control animals (n=10, 49.9±3.5 g.) underwent the same experimental procedure, but were injected with an equal volume of saline instead of pilocarpine. Animal behavior was classified into six stages according to Racine.[118] After one hour of SE (stage 6), animals were sedated with 4 mg/kg diazepam i.p. (Abbott Laboratories, North Chicago, IL) to suppress seizures and reduce mortality. Only animals that reached stage 6 were used for further experiments. These animals were closely monitored and handled several times a day to detect seizures. No behavioral spontaneous or handling-induced seizures could be detected during the four to eight weeks time interval after SE, or during continuous monitoring in the 12 hours before MR and *ex vivo* studies. Four and eight weeks after induction of SE, five experimental and five control animals were fasted overnight (12-16 hours) and anaesthetized with 2-3% halothane in a mixture of N_2O and O_2 (70/30%), tracheotomized and ventilated. A femoral artery was cannulated for monitoring of mean arterial blood pressure and blood sampling to determine arterial blood gasses (pCO_2 and pO_2) and pH. Small adjustments in tidal volume and ventilation frequency kept these physiological variables within normal limits (pCO_2 = 33–45 mm Hg; pO_2 ≥ 120 mm Hg; pH = 7.30–7.58; MAP = 90–110 mm Hg). Core body temperature was measured with a rectal thermometer and maintained at 37 ± 1°C by means of a heated water pad. A femoral vein was cannulated for infusion of [U-$^{13}C_6$]-glucose (Cambridge Isotope Laboratories Inc, Andover, MA). Following surgery halothane was reduced to 0.5 – 1% to maintain a stable blood pressure. Animal heads were shaven to allow for better coil positioning and animals were placed in the probe, restrained in a head holder and were further immobilized with d-tubocurarine (0.5 mg/kg/40 min, i.p.). Simultaneous with starting the ^{1}H-[^{13}C] MRS experiment, animals received a 250 µl intravenous bolus of 0.75 M Uniformly ^{13}C-labeled glucose (U-$^{13}C_6$) per 200 gram body weight, followed by an intravenous infusion of 0.75 M [U-$^{13}C_6$]-glucose (formatting is very inconsistent here) with a rate according to a decreasing exponential function during the first 8 min and kept constant at 13.7 µl/min for the remainder of the experiment. Long echo-time ^{1}H- and GABA-edited MRS experiments were performed previous to the ^{1}H-[^{13}C] studies on the same animals, results of which have been described previously.[286] After the magnetic resonance (MR) experiments, the rats were euthanized while still anaesthetized.

Magnetic resonance spectroscopy

Experiments were performed on a 9.4 T Magnex magnet and Bruker console (Bruker, Billerica, MA) equipped with a 9 cm diameter gradient coil insert (Resonance Research Inc, Billerica, MA, 490 mT/m in 175 µs). A 14 mm diameter surface coil was used for ^{1}H RF pulse excitation and signal reception (400.5 MHz). RF pulse transmission on carbon-13 (100.2 MHz) was achieved with two orthogonal 21 mm diameter surface coils driven in quadrature. Multi-slice coronal EPI images (FOV 2.56 × 2.56 cm, matrix 128 × 128, 10 slices of 1 mm thickness, TR/TE = 2500/10 ms) were acquired and used to position the spectroscopic volume of interest (VOI) (10 × 2 × 5 mm) over the hippocampus (Fig. 7.1).

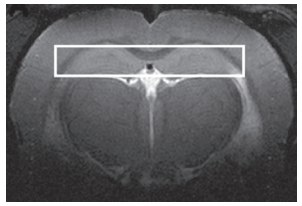

Fig. 7.1 | T_2W image of a healthy rat brain with the hippocampal MRS voxel indicated.

The magnetic field homogeneity over the VOI was optimized with the non-iterative FASTMAP algorithm for all first- and second-order shim coils. This resulted in signal line widths of 14–16 Hz for water and 9–11 Hz for metabolites in the localized volume of 100 µl. Localized ^{1}H NMR spectra were obtained with the NMR pulse sequence described previously (TR 4000 ms, TE 8 ms).[246] In short, 3D localization was achieved by a combination of outer volume suppression (OVS), image-selected *in vivo* spectroscopy (ISIS), and slice-selective excitation. Water suppression was performed with Selective Water suppression with Adiabatic Modulated Pulses, SWAMP, an adiabatic analog of the CHEmical Shift Selective, CHESS, technique. Discrimination between ^{1}H-[^{13}C] and ^{1}H-[^{12}C] NMR signals was achieved by executing a 4.0 ms adiabatic full passage (AFP) pulse (sin40 modulation, 10 kHz bandwidth) on the ^{13}C channel on alternating acquisitions, after which the FIDs obtained with and without the ^{13}C inversion were stored in separate memory blocks. ^{1}H-[^{13}C] NMR signals were obtained by subtraction of the ^{13}C-inverted FIDs from the non-inverted FIDs. Broadband adiabatic ^{13}C decoupling was applied during the total acquisition time of 204.8 ms. The decoupling sequence was executed with a 1.6 ms AFP pulse (HS4 modulation, 6.25 kHz bandwidth) incorporated in a 20-step supercycle to provide adiabatic, frequency-selective decoupling. With the decoupling frequency centered on the [4-^{13}C]-glutamate resonance at 34.2 ppm, the decoupling sequence provided frequency-selective decoupling between circa 3 and 65 ppm, while leaving the [1-^{13}C]-glucose resonances at 92.7 and 96.6 ppm unperturbed. Since the α-[^{1}H]-glucose resonance is resolved in ^{1}H NMR spectra at 9.4 T, frequency-selective decoupling allows for direct quantification of the ^{13}C fractional enrichment of cerebral glucose from total, unedited ^{1}H NMR spectra.

The total GABA concentration was obtained through homonuclear spectral editing with a double spin-echo sequence using 20 ms Gaussian refocusing pulses selective for the GABA-H3 protons at 1.89. An echo time of 68 ms (= 1/(2J)) was chosen to optimize the detection efficiency of the GABA-H4 protons at 3.01 ppm. RF pulse calibration was performed on the water resonance. Editing efficiency on individual animals was calculated from the residual water signal in the presence of spectral editing pulses. The experiments were performed with a repetition time TR of 4.0 s and 64 repetitions with interleaved editing. The GABA-edited spectrum was obtained by subtracting the non-edited from the edited spectra.

Data acquisition and processing

All FIDs were acquired with a 32 s time resolution (eight ISIS increments with TR = 4.0 s) to minimize the effects of small frequency shifts between acquisitions, and to evaluate motion artifacts. Following a complete experiment of approximately 32 minutes of continuous signal acquisition, FIDs were zero-filled to 8 K data points, apodized (1.0 Hz Gaussian line broadening), Fourier transformed, and phase corrected (only zero-order phase). The spectra were frequency corrected to account for drift in the main magnetic field, but no amplitude or phase corrections were performed on individual spectra. Next, spectra acquired over 16 min were added to increase the signal-to-noise ratio (SNR) and used for subsequent quantification of metabolite concentrations and fractional enrichments by an in-house frequency-domain fitting program written in Matlab R2008B (The Mathworks, Natick, MA). Similar to LCmodel, the algorithm models the *in vivo* NMR spectrum as a superposition of a basis set of *in vitro* NMR spectra of pure metabolite solutions. ^{1}H NMR spectra were collected *in vitro* under controlled pH and temperature conditions from acetate (Ace), alanine (Ala), aspartate (Asp), creatine (Cr), GABA, glucose (Glc), [U-$^{13}C_6$]-Glc, glutamate (Glu), glutamine (Gln), glutathione (GSH), glycerophosphorylcholine (GPC), lactate (Lac), myo-inositol (mI), N-acetyl aspartate (NAA), NAA-glutamate, phosphocreatine (PCr), phosphocholine (PC), phosphoethanolamine (PE), taurine (Tau) and valine (Val). A macromolecular baseline was measured separately on a number of animals by "nulling" the metabolite resonances with a double inversion recovery element preceding the ^{1}H-[^{13}C] NMR sequence with 1.0 ms hyperbolic secant modulated AFP pulses (bandwidth 10 kHz), inversion recovery time TI = 1950 and 550 ms and TR = 6000 ms. A separate version of the fitting program with additional constraints was used for quantification of the edited ^{1}H-[^{13}C] NMR spectra. Specifically, while the resonance amplitudes of the different isotopically-labeled peaks within one molecule (e.g. [2-^{13}C], [3-^{13}C] and [4-^{13}C]-glutamate) were unconstrained, the line width, phase and frequency were forced to be identical. The reliability of the spectral fit was evaluated by Monte Carlo simulations (MCS) using 50 iterations. The traditional Cramer-Rao lower bounds were not used, as they are not valid in the presence of an unknown macromolecular baseline. While the CRLBs can be modified to include so-called "nuisance" parameters related to the baseline, we found the use of MCS a more straightforward alternative.[246] The MCS results are expressed as the % (SD MCS/mean MCS), to indicate the percentage of uncertainty in the concentration that is determined from the spectral fitting.

Metabolic modeling

Time courses for [3-^{13}C]-Glu, [4-^{13}C]-Glu, [3-^{13}C]-Gln, [4-^{13}C]-Gln, [2-^{13}C]-GABA and [4-^{13}C]-GABA were reconstructed with 16 min intervals during infusion of [U-$^{13}C_6$]-Glc. The glucose time courses were analyzed using a three-compartment metabolic model, comprising glutamatergic neuronal, GABAergic neuronal and astroglial compartments, similar to the model described by Patel *et al.*[165] Briefly, since brain α-^{1}H-[1-^{12}C]-glucose and α-^{1}H-[1-^{13}C]-glucose levels could be directly detected and quantified, no assumptions were required regarding glucose transport across the blood-brain barrier. Brain

glucose is converted to pyruvate, which enters either the neuronal or astroglial TCA cycles. The ^{13}C-label of [U-$^{13}C_6$]-glucose will arrive at the TCA cycle intermediate [4-^{13}C]-ketoglutarate (KG), which is in rapid exchange with [4-^{13}C]-glutamate at a flux rate V_x. Since [3-^{13}C]-Glu and [3-^{13}C]-Gln were both measured and included in the model, no assumptions about V_x were required. After labeling of [4-^{13}C]-Glu, the [4-^{13}C]-Gln position is ultimately labeled by the action of a glutamatergic neurotransmitter cycle between the glutamatergic neuronal and astroglial compartments. After one additional turn of the TCA cycle also [3-^{13}C]-Glu and [3-^{13}C]-Gln will label. In the GABAergic neuronal compartment, [4-^{13}C]-Glu is quickly converted to [2-^{13}C]-GABA, which ultimately labels [4-^{13}C]-Gln through a neurotransmitter cycle between the GABAergic neuron and the astroglial compartment. In a subsequent turn of the TCA cycle both [3-^{13}C]-GABA and [4-^{13}C]-GABA are labeled. In this metabolic model, a large set of coupled differential equations (using mass and isotope balance) was used within the CWave software package (CWave 3.0) to describe the behavior of above mentioned labeled substrates in response to the infusion of [U-$^{13}C_6$]-glucose.

The model was constrained by assuming the pyruvate carboxylase flow (V_{PC}) to be 20% of the rate of total glutamine synthesis. Dilutional fluxes were iterated for the three separate compartments. The cerebral metabolic fluxes were determined from the best fits of the model to the time-courses of ^{13}C-labeling with a Levenberg-Marquardt algorithm hybridized with simulated annealing. Cerebral metabolic rates of glucose oxidation [$CMR_{Glc(ox)}$] were calculated as $\frac{1}{2}V_{TCA}$. The GABA pool was assigned to the GABAergic neuronal compartment, whereas Glu was divided between glutamatergic neurons (88%), astroglia (10%), and GABAergic neurons (2%).[165] The analysis was performed with fixed compartment volumes (glutamatergic 50%, astroglial 45%, GABAergic 5%), but a separate analysis was performed for the pilocarpine-treated animals in which the compartment volumes were changed relative to the changes in glutamate, choline, GABA (glutamatergic 42%, astroglial 55%, GABAergic 3%). The model was not restricted with a fixed relationship between between V_{cycle} and V_{TCA}. Although this relationship has been characterized under normal physiological conditions, the effect of neuronal death and gliosis on this relationship are unknown.

With the described prior knowledge and restrictions, the metabolic model was used to determine the glutamatergic neuronal TCA cycle flux ($V_{TCA,Glu}$), the GABAergic TCA cycle flux ($V_{TCA,GABA}$) and astroglial TCA cycle flux ($V_{TCA,A}$) and the neurotransmitter flux (V_{cycle},). Assuming that the redistribution of label from the astroglial compartment to either the GABAergic or the glutamatergic compartment is similar in hippocampal tissue as it is in cortex and does not change after SE, additional separate fluxes for the glutamatergic neurotransmitter flux ($V_{cycleGluGln}$) and the GABAergic neurotransmitter flux ($V_{cycle,GABAGln}$) were calculated. GAD activity (V_{GAD}), glutamine synthase activity (V_{GS}) and dilutional fluxes ($V_{dil,Glu}$, $V_{dil,Gln}$ and $V_{dil,GABA}$). Ratios of neurotransmitter cycling over V_{TCA} were determined for both the neuronal compartments to evaluate the coupling between neurotransmitter cycling and TCA cycling.

Statistics

Data are expressed as mean ± standard deviation (SD). The experimental group was compared with the control group of the same time point. Statistically significant differences between the time points and between controls and experimental conditions were determined with a t-test after confirmation that variables had equal variances and a normal distribution. A correction for multiple comparisons was performed with a post-hoc Bonferroni correction, based on the number of independent variables compared. A p-value > 0.05 was considered statistically significant.

Results

Animal model

Of twenty animals injected with pilocarpine, 14 (70%) progressed to Racine's final stage of SE (stage 6), of which 4 (30%) died within the first 24 hours (usually suddenly in the first hour during a tonic seizure). No mortality was observed in the period between SE and MR experiments or histology. Of the ten surviving animals that developed SE, five each were studied four and eight weeks after SE with MRS. No significant differences were observed in body weights between control and experimental animals at four and eight weeks (240 ± 37 g vs. 243 ± 19 g and 346 ± 24 gr. vs. 323 ± 16 g, respectively). No mortality or abnormal behavior was observed in control animals.

^{1}H MRS

Figure 7.2 (overleaf) shows a typical non-edited short echo-time (8 ms) hippocampal ^{1}H MR spectrum, its LC Model fit and the residual of the subtraction of these two (control animal at eight weeks after injection). The absolute concentrations of the measured metabolites are very similar to the concentrations obtained with long echo-time (68 ms) unedited MRS experiments in the same animals, as previously described.[286] To summarize, after SE GABA concentrations decreased progressively with time after SE (29% at four weeks and 41% at eight weeks) as did glutamate by 12% at four weeks and 16% at eight weeks. Glutamine concentration increased significantly at four weeks (19%) but returned to control levels at eight weeks. Levels of alanine and aspartate were unchanged from control values at both time periods. Lactate levels were low and did not differ between time points or experimental groups.

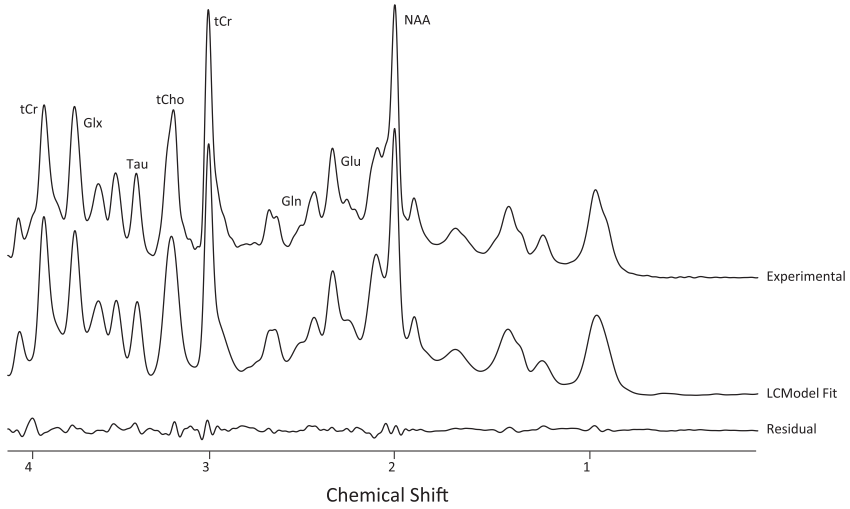

Fig. 7.2 | Top trace: Experimentally acquired spectrum from a healthy rat hippocampus (TE 8 ms). **Middle trace:** LC Model reconstruction of the spectrum for metabolite quantification. **Bottom trace:** result of subtraction of both spectra resulting in virtually no unexplained peaks.

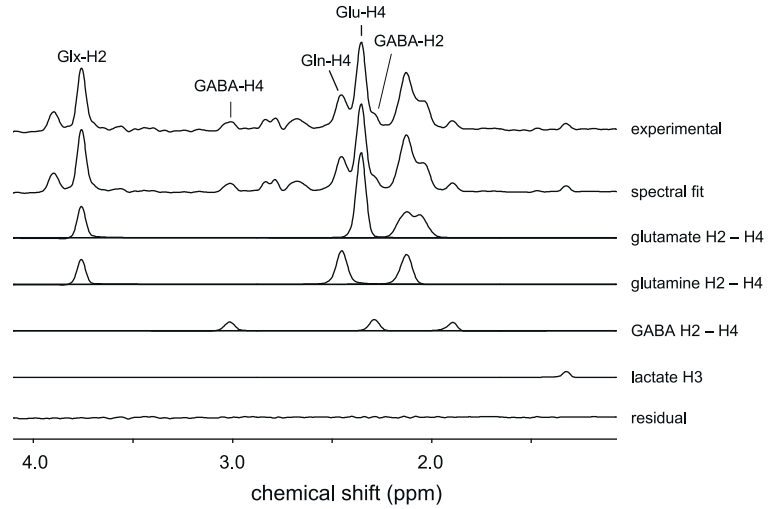

Fig. 7.3 | Top trace: experimentally acquired 13C edited spectrum after two hours of uniformly labeled glucose, with the LC model fit below it. Relevant resonances for this study, glutamate, glutamine and GABA are represented in the following traces. The bottom trace shows the residual after subtraction of the experimental and fitted spectrum. No unexplained peaks are present.

Dynamic MRS

While the ^{1}H NMR resonances from ^{13}C-labeled compounds upfield from water are decoupled, the αH1-glucose resonances downfield from water are not decoupled. As previously shown, this allows for the quantification of brain glucose to use as the input function for further metabolic modeling.[246] Figure 7.3 shows the edited ^{1}H-[^{13}C] NMR spectrum obtained from rat brain 120 min following the onset of the [U-$^{13}C_6$]-glucose infusion. The most prominent resonances originated from glutamate, glutamine and GABA. Note that all spectra were acquired in the presence of selective ^{13}C-decoupling, thus eliminating splitting due to heteronuclear scalar coupling. Figure 7.3 also shows the best fit of the measured ^{1}H-[^{13}C] NMR spectrum.

Figure 7.4 (p. 120) shows the average turnover curves (n = 5) for [4-^{13}C]- and [3-^{13}C]-glutamate, [4-^{13}C]and [3-^{13}C]-glutamine and [2-^{13}C]and [4-^{13}C]-GABA for the 4 week group (upper panel) and 8 week group (bottom panel) together with the best fit of the metabolic model described in the Methods section. Experimental data was averaged over 16 min in order to increase the signal-to-noise ratio. The control group is indicated in black and the +SE group is indicated in grey. Error bars represent the SD of the time points the samples were taken (horizontal) and of the observed fractional enrichments (vertical). Visual inspection reveals differences both in curve shape and endpoint fractional enrichment that are most pronounced in the GS mediated steps. [4-^{13}C]-Glutamate and [2-^{13}C]-GABA remain relatively unaffected in contrast to metabolites that require additional metabolic steps, starting with glutamine synthesis by aid of GS. To avoid facile explanations, the analysis of the significance of the observed differences was performed through metabolic modeling of these turnover curves.

Table 1 (p. 121) summarizes the TCA and neurotransmitter cycle rates and several ratios as calculated by metabolic modeling of the available data. After SE, TCA cycling rates for the glutamatergic compartment significantly decreased at eight weeks compared to control values (0.378 ± 0.081 µmol/min/g vs. 0.559 ± 0.066 µmol/min/g, p=0.024). In the GABAergic compartment, TCA cycling rates significantly decreased at both time points (0.027 ± 0.016 µmol/min/g vs. 0.055 ± 0.009 µmol/min/g, p=0.047 at 4 weeks, and 0.035 ± 0.003 µmol/min/g vs. 0.048 ± 0.007 µmol/min/g, p=0.024, at 8 weeks after SE). The glial compartment showed no change of the TCA cycling rate.

The total neurotransmitter cycle decreased significantly at eight weeks. When assuming a redistribution of label in the glial compartment similar to that of healthy cortex, separate glutamatergic and GABAergic contributions to the cycle can be calculated. The $V_{cycle,GluGln}$ showed only a tendency to decrease at both time points, without reaching statistical significance, but the $V_{cycle,GABAGln}$ was progressively affected, reach-

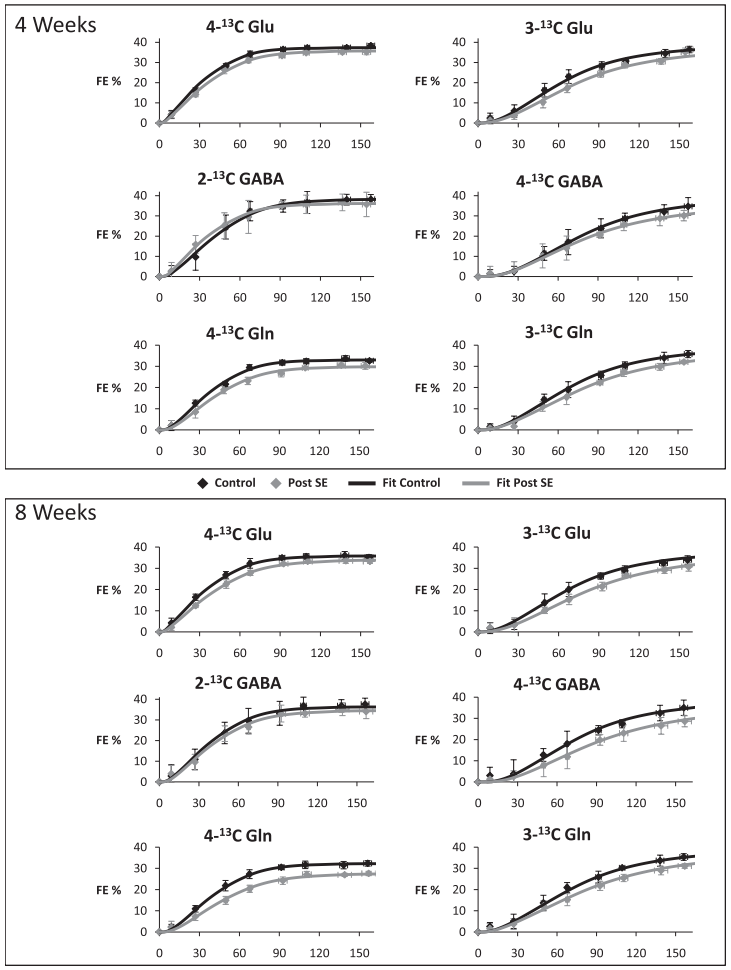

Fig. 7.4 | Turnover curves of 3-^{13}C and 4-^{13}C glutamate and glutamine as well as 2-^{13}C and 4-^{13}C GABA at four and eight weeks after injection of saline (black line) or pilocarpine (grey line). The horizontal axis represents the time in minutes, while the vertical axis represents the fractional enrichment. The time points represent the average of 5 animals with error bars representing the SD. Notice the differences in endpoint FE and curve shape in the 3-^{13}C glutamate, 4-^{13}C GABA and both glutamine traces.

ing significance at eight weeks after SE (0.017 ± 0.006 µmol/min/g vs. 0.045 ± 0.009 µmol/min/g, p=0.002). V_{GAD} was also significantly decreased at eight weeks (0.034 ± 0.005 µmol/min/g vs. 0.058 ± 0.008 µmol/min/g, p=0.003). The V_{GS} decreased at both time points, reaching significance at 8 weeks (0.413 ± 0.105 µmol/min/g vs. 0.635 ± 0.102 µmol/min/g, p=0.047).

	Week 4		Week 8	
TCA cycling	**Control (n=5)**	**Post SE (n=5)**	**Control (n=5)**	**Post SE (n=5)**
V_{TCA} Glu	0.613 ± 0.028	0.542 ± 0.106	0.559 ± 0.066	0.378 ± 0.081*
V_{TCA} GABA	0.055 ± 0.009	0.027 ± 0.016*	0.049 ± 0.007	0.035 ± 0.003*
V_{TCA} Glial	0.203 ± 0.012	0.194 ± 0.028	0.213 ± 0.027	0.177 ± 0.020
Neurotransmitter cycling				
V_{cycle}	0.482 ± 0.071	0.330 ± 0.130	0.508 ± 0.099	0.330 ± 0.094*
$V_{cycle\ Glu}$	0.438 ± 0.064	0.299 ± 0.121	0.463 ± 0.090	0.313 ± 0.088
$V_{cycle\ GABA}$	0.044 ± 0.007	0.031 ± 0.009	0.045 ± 0.009	0.017 ± 0.006**
Enzymes				
V_{GAD}	0.058 ± 0.005	0.061 ± 0.012	0.058 ± 0.008	0.034 ± 0.005**
V_{GS}	0.602 ± 0.074	0.413 ± 0.160	0.635 ± 0.102	0.413 ± 0.105*
V_{PC}	0.120 ± 0.015	0.083 ± 0.032	0.127 ± 0.020	0.082 ± 0.021*
Cycle Coupling				
$V_{cycle}/V_{tca\ GABA}$	0.634 ± 0.108	0.560 ± 0.442	0.736 ± 0.220	0.343 ± 0.120*
$V_{cycle}/V_{tca\ Glu}$	0.714 ± 0.105	0.552 ± 0.308	0.828 ± 0.223	0.828 ± 0.358

Table 7.1 | Turnover rates as calculated by the metabolic modeling. Significant results are indicated with a * for p< 0.05 and ** for p < 0.01.

Apart from simple cycle rates several ratios were also calculated. The relative contribution of each separate compartment to the total TCA cycle rate did not change significantly. To assess the coupling between TCA cycle rate and neurotransmitter cycling rate, the ratio of these two was calculated for the glutamatergic and GABAergic compartment. For the glutamatergic compartment this ratio did not show significant changes, while the GABAergic compartment showed a significant decrease at eight weeks (0.34 ± 0.12 vs. 0.74 ± 0.22 p=0.040). The separate analysis performed for the pilocarpine-treated animals with the compartment volumes adapted according to the observed changes in glutamate, choline and GABA concentrations (glutamatergic 42%, astroglial 55%, GABAergic 3%), revealed only slight differences in the observed cycling rates, that varied between -5.14% (for the $V_{TCA,GABA}$) and 2.97% (for GABA shunting). These changes did not affect statistical significances. The dilutional fluxes did not differ between experimental groups or time points and were all less than 0.115 µmol/min/g, with their sizes reflecting the relative size of their respective compartment. No significant differences were found in any of the rates and ratios between the 4 and 8 week time points in the control groups.

Discussion

Concentrations of several important cerebral metabolites and their turnover rates have changed in the weeks following SE (Table 2). As described previously, neuronal death, gliosis and disproportional loss of GABAergic inhibition occur in the latent phase before the onset of SRS.[286] *In vivo*[169,236,240] and *ex vivo*[235] human TLE studies report neuronal damage and gliosis in several hippocampal subregions. However, these end-stage measurements cannot distinguish neuronal injury incurred after SE during the early period of epileptogenesis, from later progressive injury due to recurrent seizures. Our study indicates that a significant part of the neuronal damage and gliosis occurs before the onset of clinical spontaneous seizures. However, histopathological examination has revealed that in this rather mild model of TLE, neuronal death and reduced GS staining, is limited to the hilus of the hippocampus.[286] The large decrease in neurotransmitter concentration appears not to be congruent with these histochemical observations; therefore we propose that more widespread metabolic mechanisms are at work. The current study examines overall hippocampal metabolism and necessarily reflects pathology in still metabolically active cells, describing a different cell population than the one suffering neuronal death.

Visual inspection reveals an overall reduction in labelling of metabolites in the hippocampus after SE, which is especially pronounced in the metabolites that have passed through the glial compartment at least once. This is in agreement with several studies by Sonnewald *et al.*, who performed direct ^{13}C MRS in both the adult kainate and the adult lithium pilocarpine model in the chronic phase. In these studies, glutamate, GABA and glutamine ^{13}C fractional enrichments showed a general tendency to decrease in the experimental group.[173,239,287-289] However, their studies were performed *ex vivo* and provided only one time point on the turnover curve, usually fifteen minutes after injection of ^{13}C labelled compound. The authors were therefore reluctant in speculating on underlying causes for their observations. Our study provides the entire turnover curve and in combination with a sophisticated metabolic model, inferences can be made about the causes of the observed changes. This model is a necessary abstraction from reality that may not do justice to the complexity of cerebral metabolism. An alternative would have been to discuss the turnover curves without such a model as other authors have done, but this carries the inherent risk that subtle but important interrelationships between metabolic pathways are overlooked.[173,174,288,289] The model, however abstract it may be, provides an overall picture of metabolism. The low dilutional fluxes, proportional to their respective compartment, provide support for the lack of unexplained variability across these compartments.

Concentrations	4 weeks	8 weeks
NAA	-12%	-16%
Cho	23%	27%
MI	=	11%
Glutamate	-14%	-12%
GABA	-29%	-41%
Glutamine	19%	=
Rates		
$V_{TCA\ glu}$	=	-32%
$V_{TCA\ GABA}$	-50%	-28%
V_{cycle}	(-32%)	-35%
$V_{cycle\ GABA}$	(-30%)	-64%
V_{GAD}	=	-41%
V_{GS}	(-31%)	-35%
V_{PC}	(-31%)	-35%
$V_{cycle\ GABA} / V_{TCA\ GABA}$	=	-53%

Table 7.2 | Summary of results. Values between brackets only show a tendency to decrease without reaching statistical significance.

Our results show that the glutamatergic TCA cycling rate decreases at eight weeks. This could be due to a decrease in overall hippocampal activity in the progressively sclerotic state. A similar observation can be made for the GABAergic TCA cycling rate, which already show a significant decline at four weeks. The neurotransmitter cycling has also decreased at eight weeks. Under the assumption of redistribution of label in the glial compartment similar to healthy cortex, it becomes clear that the GABAergic neurotransmitter cycle is severely affected at the eight week time point to a degree that the coupling between the V_{TCA} and $V_{cycleGABAgln}$ even breaks down. This means that, apart from disproportionate cell death amongst GABAergic cells, the remaining cells function at a lower metabolic level and are progressively less capable of metabolizing GABA from glutamine, which is also apparent from a decrease in neuronal GAD activity at the eight week time point. Whether the underlying assumption is accurate, must be determined in future experiments including a 2-^{13}C acetate infusion in these rats. Because this label is exclusively taken up by astrocytes, it will allow us to discriminate the flux from the glial compartment to the GABAergic cells from the flux to the glutamatergic cells.

In the glial compartment the most striking result is the decrease in GS activity. This is in agreement with several studies employing different experimental methods in human and experimental TLE.[103,175] This decrease apparently precedes the onset of SRS. The transient increase in glutamine concentration may indicate accumulation of substrate for the neuronal neurotransmitter synthesis, due to neuronal death or dysfunction. GS down-regulation would be the obvious consequence. An alternative explanation is that the glutamine increase is a mechanism by which the hippocampus attempts to support inhibitory neurotransmission. A recent study has shown that gliosis, independent of its cause, leads to GS down-regulation and a concomitant reduction in inhibitory post-synaptic currents. This reduction in inhibitory capacity can be counteracted by providing exogenous glutamine.[244] The hippocampus may be capable to employ this mechanism transiently to maintain GABAergic inhibition. Interestingly, GS reduction, without underlying pathology, induced by repeated injection of methionine sulfoximine has been shown to be sufficient to induce SRS in the rat.[290] The glial compartment shows the same reduction in V_{PC} as for V_{GS} because these parameters are coupled. This coupling may not hold in the epileptogenic hippocampus as it does in healthy cortex, but future experiment with a 2-^{13}C glucose infusion will allow us to experimentally test this assumption. 2-^{13}C glucose specifically label glutamate in the glial compartment through the V_{PC}, bypassing the TCA cycle.

The histopathological and immunohistochemical changes that were previously described in this model, consisting of neuronal death, gliosis, and decreased GS staining, are mostly limited to the hilus and are known to be much less severe than in similar adult models.[117,123,124,201,203,214,237-239,286] While it is possible that neuronal death is more severe than implied by histopathological staining methods alone, a pervasive metabolic failure with functional neurotransmission alterations in surviving neurons may be present to accentuate the pathology incurred by neuronal death alone.[286] To summarize, this study shows that SE leads to neuronal death or dysfunction of predominantly GABAergic origin in the hippocampus. During the course of several weeks, TCA cycling rates decrease in neurons, again most prominently in the GABAergic system. While the glutamatergic compartment is capable of maintaining its coupling between TCA cycling rate and neurotransmitter turnover, the GABAergic compartment cannot maintain this relationship, contributing to a hypoGABAergic and hyperglutamatergic state, both in terms of absolute concentrations as in terms of neurotransmitter production capacity. Recent studies indicate that gliosis by itself induces this decrease in GS activity, thus contributing to a decrease in inhibitory post synaptic currents which, when severe enough, are sufficient to induce seizures even in the otherwise healthy brain.[290]

These results show that MRS is a powerful tool to investigate transmitter metabolic changes in the early stages of TLE. All of the described MRS techniques are safe and can be used in humans for further elucidation of metabolic failure in neurotransmitter systems in human TLE or epileptogenesis.

Acknowledgements

This research was supported by NIH grants R01 DK027121 (K. L. B.) and K02 AA13420 (G. F. M.) and by the Dutch Epilepsy Fund (NEF 0415). The authors thank Bei Wang for expert animal preparation, Peter Brown for construction and maintenance of the ^{1}H-[^{13}C] RF coil and Terence Nixon and Scott McIntyre for system maintenance.

8 Summary and general discussion

Introduction

Temporal lobe epilepsy (TLE) with hippocampal sclerosis (HS) is a type of epilepsy characterized by recurrent partial complex seizures originating from the mesial temporal structures and a specific pattern of neuronal death, gliosis and mossy fiber sprouting in the hippocampus. Retrospective studies have shown that between 30 and 60% of patients with TLE have histories of prolonged or complex febrile seizures and that children with prolonged febrile seizures have an eightfold increased risk of developing epilepsy.[66-68] This period between the precipitating event in early childhood and development of HS and recurrent temporal lobe seizures in puberty or adolescence, points toward an ongoing process of epileptogenesis in seemingly normal children.[69] In approximately 30-40% of people suffering from TLE, seizures gradually become refractory to antiepileptic medication, suggesting an ongoing or progressive pathological process, that may be identical to, or share similarities with, epileptogenesis.[60]

Studies in human HS-associated TLE have the inherent problem that the pathologic changes observed in these patients could be either the cause or the consequence of recurrent epileptic seizures. For this reason, this thesis focuses on the pre-epileptic hippocampal pathology occurring in response to the initial precipitating event. Research into mechanisms of epileptogenesis, performed before seizures occur, can only be done in animal models. The juvenile lithium-pilocarpine model closely mimics several important characteristics of human TLE; a hippocampal seizure focus, a latent period follow a precipitating event, a high success rate and incidence of HS, and a similar developmental age.

Connectivity

The propagation of aberrant activity in the hippocampus requires signal transduction from one neuron to the next, and from epileptogenic cell clusters to other areas in the vicinity or, in case of generalization, to distant brain structures. Evidence is accumulating that widespread changes occur in the white matter of epilepsy patients. Several

magnetic resonance (MR) studies have been performed in humans and animals, confirming that epilepsy is associated with white matter changes distant from the epileptic focus.[143,150-155] It remains unclear whether these are a cause or consequence of epilepsy. The important question what the underlying pathology of these MR changes is, has received only limited attention and has never been explored in an animal model of TLE.[151] *The first aim of this thesis was to explore the evolution of white matter changes following SE and during epileptogenesis, and to characterize their histopathological correlate.*

Neurotransmission

In the hippocampus virtually all neurons are either glutamatergic or GABAergic. Many studies have indicated that TLE with HS is characterized by an imbalance between glutamatergic and GABAergic neurotransmission. While much is known about the metabolism of the already epileptogenic hippocampus in human or experimental TLE, the preceding latent phase has received limited attention. The lack of GABAergic inhibition probably precedes the onset of spontaneous recurrent seizures (SRS),[119] but more elaborate research on the metabolic background behind this imbalance is lacking. *The second aim of this thesis was to characterize and correlate hippocampal structural changes during epileptogenesis with neurotransmitter levels.*

Whether the aforementioned neurotransmitter imbalance is strictly due to a change in cell populations, related to neuronal death and gliosis, or due to more complex metabolic mechanisms, that affect neurotransmission cycling in intact and surviving neurons and neuroglial contacts, remains a matter of dispute. Detection of turnover rates within the complex neurotransmitter system can be performed by ^{1}H-[^{13}C] magnetic resonance spectroscopy (MRS). Unfortunately, current methods only allow for the characterization of glutamatergic neuroglial interactions, while GABA turnover remains below detection threshold for MRS under normal physiological conditions. *The third aim of this thesis was to optimize currently available techniques and to attempt the detection of GABA turnover under normal physiological conditions.*

When this aim was met, full neurochemical profiling of the hippocampus, for both excitatory and inhibitory neurotransmission became possible. Currently, no studies have been performed that give a comprehensive *in vivo* description of glutamate-glutamine-GABA cycling in a live organism in epilepsy or during epileptogenesis. *The fourth aim of this thesis was to provide a comprehensive description of both excitatory and inhibitory neurotransmission in the course of the process of epileptogenesis.*

Initial exploration

Chapter 3 describes a study we performed during lithium pilocarpine-induced SE in the adult rat. The aim of this study was to show the ability of MR to detect and characterize structural and metabolic abnormalities in the epileptic brain. For the first time, single-voxel ^{1}H MRS, high-resolution quantified T_2- and isotropic DW MRI were combined during pilocarpine-induced SE. A combination of these techniques was chosen because it would allow us to probe several important cerebral morphological and metabolic properties. T_2 relaxation times were globally decreased, most severely in the amygdala and piriformic cortex, in which also a significant decrease in ADC was found. In contrast, ADC values increased transiently in the hippocampus and thalamus. MR spectroscopic results suggested a relative decrease of NAA and choline, and an increase of lactate in a large hippocampal voxel.

The T_2 decrease, attributed to raised deoxyhemoglobin, and the presence of lactate both indicate a mismatch between oxygen demand and delivery. The ADC decrease, indicative of excitotoxicity, confirms that the amygdala and piriformic cortex, both mesiotemporal structures in humans, are particularly vulnerable to pilocarpine induced seizures. The transient ADC increase in the thalamus may reflect the breakdown of the blood–brain barrier, which is shown to occur in this region during SE.[198] Neuronal damage and failure of energy dependent formation of NAA are likely causes of an observed decrease in NAA, while the decrease in choline is possibly due to depletion of the cholinergic system. This study explored the consequences for brain metabolism and structure in the first minutes to hours after SE, and confirmed that relative hypoxia, excitotoxicity and concomitant neuronal damage associated with SE can be probed noninvasively with MR. These pathological phenomena initiate the cascade that follows during the process of epileptogenesis, eventually leading to the occurrence of spontaneous recurrent seizures in a later stage of this animal model.

White matter pathology

After demonstrating that it was possible to detect structural changes in grey matter during pilocarpine induced seizures, we focused our attention on chronic white matter pathology after pilocarpine induced SE. **Chapter 4** further challenges the dogma that epilepsy is a disease of grey matter and explores the background of the white matter pathology that has been observed in a number of recent diffusion tensor imaging (DTI) studies in patients with focal epilepsy.[141,143-146,150-155] In our study, DTI and specific histological staining techniques for myelin and axonal disturbances were performed in juvenile rats, four and eight weeks after pilocarpine induced SE. The results showed that mean diffusivity (MD), the diffusivity along the white matter fibers (λ_1), and a dedicated myelin staining were significantly reduced in the medial corpus callosum four

weeks after SE. Both the myelin stain and the MD recovered after eight weeks, but the λ_1 remained reduced. Similar changes were found in the lateral CC, although statistical significance was not reached with the relatively limited number of animals. In the fornix fimbriae (FF), λ_1 and myelin staining were decreased at both time points, while FA and MD were significantly reduced at eight weeks.

The change in myelin staining unequivocally pointed towards myelin involvement, while we found no significant changes in the axonal staining. The study showed that isolated SE, without SRS, is sufficient to cause long-lasting widespread white matter changes. However, the changes we found differed from those observed in patients with TLE who suffer from spontaneous seizures, many years after SE. While chronic epilepsy is characterized by an MD increase in combination with a prominent FA reduction, we found MD and λ_1 reductions and only modest (FF) or non-significant (CC) FA reductions. We propose that to some extent, these results reflect an early stage of the same pathological process responsible for the DTI changes in chronic epilepsy. Alternatively, at least to some part SE may have interfered with the normal process of myelin deposition, which happens to peak around the day SE is induced.[222]

In the FF, the major efferent pathway of the hippocampus, the progressive changes are not only caused by the preceding SE, but they also parallel the time course of ensuing hippocampal damage that is associated with epileptogenesis in this model (*i.e.* mossy fiber sprouting), indicating a possible important role of the FF in the further development of epilepsy. This FF pathology may reflect downstream degeneration of hippocampal axons after neuronal death. However, severance of the FF itself has been shown to be sufficient to induce epileptiform discharges in the hippocampus and its involvement in epileptogenesis may actually contribute to the development of epilepsy.[156]

Neurotransmission

After having demonstrated that SE induces important changes in the neurochemistry of the hippocampus, the stage was set for a study of hippocampal neurotransmission. In **chapter 5** *in vivo* MRS and GABA-edited MRS of the hippocampus was performed in the juvenile lithium pilocarpine model four and eight weeks after SE, to establish the temporal evolution of hippocampal injury in relation to neurotransmitter imbalance. The MRS results were compared to *ex vivo* immunohistochemistry, performed in a separate group of animals.

MRS showed a decrease in NAA and an increase in choline concentrations, indicating neuronal death and gliosis respectively. These results were confirmed through histological staining for neuronal death by fluorojade (FJ)[207] and for active gliosis by vimentin (Vim-IR).[235] Additionally, a decrease in glutamate, and an even more severe and progressive decrease was found for GABA. The specific severity of GABAergic cell death was confirmed by an impressive decrease in parvalbumin immunoreactivity in the hilus of the hippocampus. Unexpectedly, at four weeks we found an increase of glutamine, the metabolic precursor of both GABA and glutamate. Glutamine concentrations returned to control levels at eight weeks. This subsequent decrease parallels a decrease in GS immunoreactivity in the hilus.

These results led to two new hypotheses. First, we hypothesize the initially increased glutamine concentration to reflect an imbalance in the glutamate-glutamine cycle, with the eight week time point representing a shift towards a new equilibrium. A possible mechanism would be that the glutamatergic and GABAergic cell death decreases the demand for glutamate and GABA, leading to glial accumulation of glutamine, their precursor, and inducing secondary GS down-regulation to normalize glutamine levels.

The second hypothesis is that the neurotransmitter decreases found with MRS not only reflect localized neuronal death in the hilus, but rather point towards more widespread hippocampal metabolic changes of neurotransmitter cycling in surviving neurons. The abnormalities detected with *ex vivo* immunohistochemistry are restricted to the hilus, a relatively small area of the hippocampus. Although the hilus is severely affected, the question remains whether these highly localized changes are sufficient to explain the significant alterations in metabolite concentrations detected with MRS in a large voxel that includes the entire hippocampus.

A comprehensive dynamic *in vivo* MRS study of hippocampal neurotransmitter metabolism, rather than static neurotransmitter concentrations, could be used to test both hypotheses. Until now, however, the quantification of GABAergic metabolism was not possible *in vivo*, since metabolite levels remained below the detection threshold for MRS. **Chapter 6** describes how we optimized available techniques to reliably quantify GABAergic metabolism *in vivo* in the rat. Indirect ^{1}H-observed, ^{13}C-edited (^{1}H-[^{13}C]) MRS is currently the only technique that allows for the *in vivo* and simultaneous detection of a wide array of neurochemicals and their turnover.[249,250] The infusion of uniformly labeled glucose provides information about glutamatergic and GABAergic energy metabolism, as well as total neurotransmission. When used in combination with steady-state fractional enrichments following a [2-^{13}C]-acetate infusion, the total neurotransmitter cycle rate can be separated into the glutamatergic and GABAergic contributions. This, in addition to optimizing the pulse sequence, shimming protocol and analysis tools, allowed us to detect the metabolic turnover of the excitatory and inhibitory neurotransmitters, glutamate and GABA, simultaneously and separately.

Chapter 7 describes the application of this optimized technique in the weeks following lithium pilocarpine-induced SE to test both aforementioned hypotheses. While

the study described in chapter 5 enabled us to probe neuronal death and changes in overall neurotransmitter concentrations, chapter 7 examines hippocampal metabolism, and the results of this study necessarily reflect pathology in still metabolically active cells, inherent to the dynamic MRS ^{13}C labelling studies applied.

The results show a decrease in glutamatergic and GABAergic TCA cycling. Neurotransmitter cycling was decreased at eight weeks after SE. Separate analysis for the glutamatergic and GABAergic compartment shows GABAergic neurotransmitter cycling to be decreased at eight weeks post SE, with the coupling between the TCA cycling rate and the GABAergic neurotransmitter rate breaking down at eight weeks. GAD activity was significantly decreased at eight weeks. In the glial compartment, the most striking result is the decrease in GS activity. This is in agreement with several studies employing different experimental methods in the chronic end stage of human and experimental TLE.[103,175] GS, however, apparently already decreases in the first weeks after SE, preceding the onset of SRS. This supports the hypothesis that the transient increase in glutamine concentrations, at the 4 weeks time point, reflects accumulation of substrate, subsequently inducing GS downregulation.

Synthesis

In this section available knowledge is combined with the research from this thesis into a comprehensive view of what happens to connectivity and neurotransmission during epileptogenesis, and of the relationship between these processes and the development of SRS.

In figure 8.1, I have schematically represented the changes occurring after an epileptogenic event and will run through these changes top to bottom. Most of the epileptogenic events, especially SE or febrile seizures are accompanied by massive Ca^{2+} influx in neurons, leading to excitotoxicity and neuronal death (Chapter 3). The GABAergic death is more progressive and profound than the glutamatergic cell death (Chapter 5). This is the phase which is characterized by damage to the hippocampus.

After several days to weeks there is still ongoing damage as the aftermath of the epileptogenic event, but there are also signs of adaptation and repair. Gliosis starts after several days to weeks and progresses during epileptogenesis and during SRS. There is a transient delay in the energy-consuming process of myelin deposition (Chapter 4) in the corpus callosum, which may not play a role in epileptogenesis. Elsewhere surviving cells adapt and try to find new targets and form new networks. Aberrant mossy fiber projections are formed between the DG and CA region in the hippocampus. These recurrent networks lacking GABAergic inhibition may help in seizure propagation. DTI and

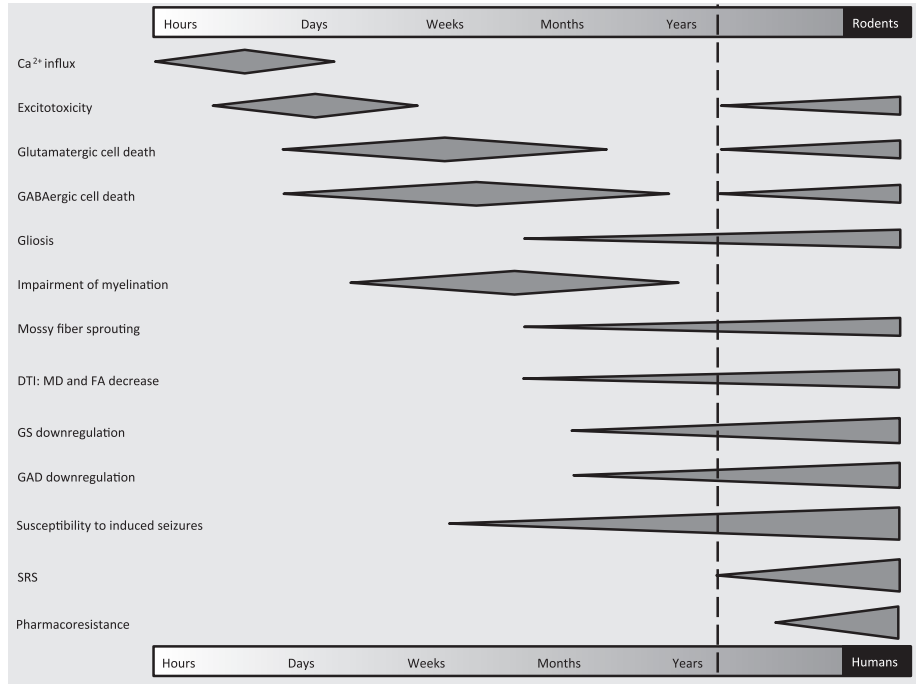

Fig. 8.1 | Time course of SE induced pathological changes with the top time line indicating the time course in rodents and the bottom time line indicating the time course in human TLE. The dotted line indicates the onset of spontaneous seizures.

myelin staining both also show that the fimbriae fornix undergoes additional chronic white matter changes, which are in agreement with changes observed in patients suffering from TLE. These changes appear around the same time as mossy fiber sprouting and may represent Wallerian degeneration and axonal reorganization. This may actually contribute to the development of SRS, because severance of the FF has been shown to lead to epileptiform discharges in the disconnected hippocampus.[244]

Within cell clusters, metabolism also adapts to the new situation. In figure 8.2 (overleaf) the three separate metabolic compartments are shown that were used for modeling the metabolic data. Inside the compartments, various metabolic reactions are shown. The top panel represents the physiological healthy baseline state. The bottom panel represents the state of affairs several weeks after the epileptogenic event. Neuronal death and gliosis have changed the relative size of the compartments, which has had an additional effect on the metabolic fluxes within and between these compartments, indicated by the arrows (Chapter 7). The damaged hippocampus shows

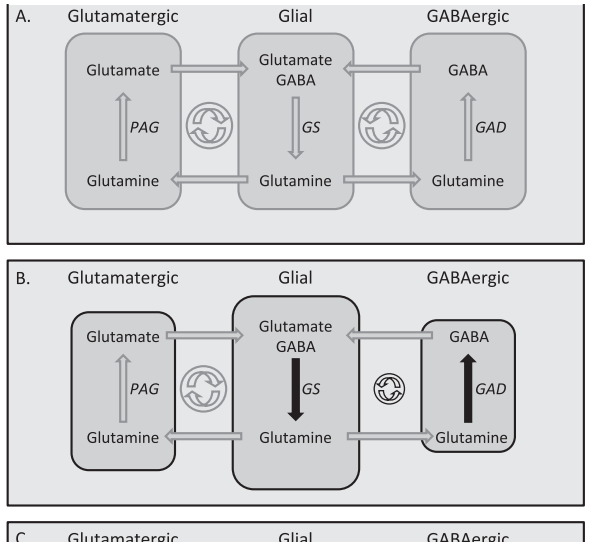

Fig. 8.2 A | Schematic representation of the three compartments with the neurotransmitter cycle indicated. Responsible enzymes are indicated in italics. PAG = Phosphate Activated Glutaminase, GS = Glutamine Synthase, GAD = Glutamic Acid Dehydrogenase. **B |** Changes probed with MRS indicated in black. The relative sizes of the compartment have changed due to neuronal death and gliosis, while activity of GS and GAD has been reduced. The resulting GABAergic neurotransmitter cycle has also been reduced, leading to a relative hyperglutamatergic state.

decreased overall activity and TCA cycling rates in neurons drop. Neuronal damage also leads to a lack in demand of glutamine, which accumulates and causes downregulation of GS. In healthy animals, a decrease in GS activity has been shown to lead to a decrease in inhibitory post synaptic currents which, when severe enough, may contribute to the induction of seizures even in the otherwise healthy brain, let alone the hypoGABAergic brain.[290]

The neurotransmitter cycling in the glutamatergic hippocampal compartment appears to remain relatively spared at the 8 week time point, compared to the GABAergic compartment, which is affected to such a degree that the coupling between the TCA cycling rate and neurotransmitter cycling rate breaks down. This means that, apart from disproportionate cell death amongst GABAergic cells, the remaining cells function at a lower metabolic level and are progressively less capable of metabolizing GABA from glutamine, which is also apparent from the decrease in neuronal GAD activity at the eight week time point. This indicates that the hilar immunohistochemical changes (Chapter 5) are only part of a more widespread neuronal dysfunction of primarily GABAergic nature. Many of these changes contribute to a hypoGABAergic and hyperglutamatergic state, both in terms of absolute concentrations as in terms of neurotransmitter production capacity. However adaptive these processes may be for the individual cell, cell clusters, or the hippocampus as a whole, functionally they contribute to aberrant neuroglial activity that ultimately leads to SRS.

Before SRS occur, it can already be shown that the threshold for induction of seizures drops. Ultimately the threshold has become so low that seizures occur spontaneously. However, as indicated in figure 8.1, the process does not stop there. The fact that many TLE patients can initially be treated by medication, but become refractory to antiepileptic drugs after several months to years, strongly suggest that epileptogenesis progresses.

Future directions

Any future experiment that follows up on these studies should include survival experiments and a chronic time point at which the epileptic fait of the animal is known, and the animals have proven to suffer from TLE with SRS, or not. While we have solid data on the percentage of rats that, on a group level, will become epileptic, only the correlation of several data points in the same animal and confirmed epilepsy in that specific animal would allow for the identification of MR biomarkers for the development of SRS. This approach would also allow for a correlation not only between the occurrence of spontaneous seizures and MR biomarkers, but also between the severity of epilepsy and the severity of MR changes. In a similar vein electrophysiology needs to be included in future experiments. Electrophysiology is the only way to detect short lasting discharges or subclinical electrographical seizures. Electrophysiology offers the most direct tool to measure epileptic activity and attempts should be made to correlate electrophysiological measures with MR parameters.

DTI sequences have been further developed in recent years and one of the future experiments should definitely be an elaboration of the work described in this thesis. Apart from the aforementioned point, longitudinal *in vivo* DTI after SE should be performed with a higher resolution than in our study, allowing for the analysis of changes in intrahippocampal connectivity, specifically mossy fiber sprouting. A separate group can be imaged *ex vivo* and subsequently be used for detailed histological analysis to elucidate the underlying background of observed *in vivo* DTI changes. This would help understanding how these changes contribute to the development of seizures.

With respect to the neurotransmitter studies, additional experiments should be performed to measure several parameters that we have now made assumptions for. The first experiment should be similar to the experiments described in chapter 7, but with

the infusion of [2-^{13}C]-acetate instead of uniformly labeled glucose. This would allow for the unequivocal separation of the glutamatergic from the GABAergic neurotransmitter cycle without relying on assumptions. An additional experiment with [2-^{13}C]-glucose infusion will allow us to measure the anaplerotic flux, for which we have now made an assumption as well. These experiments should also be expanded to include a chronic time point at which the animals are epileptic. Adaptations can be made in the future to make these experiments survival experiments, enabling true longitudinal investigation.

The turnover studies point towards a role for both GAD and GS in the development of seizures. Eid *et al.* have shown that GS inhibition leads to pre-epileptic changes, which can be counteracted by the suppletion of glutamine. It would be interesting to investigate the effects of exogenous glutamine on the metabolic changes and SRS in these rats. GS and GAD themselves could also be interesting targets for future drug development studies.

Because all of the described techniques are FDA approved, attempts should be made to transpose them to the human situation. There are two possible scenarios. The first would entail the identification of children at risk for developing TLE, because they have suffered from prolonged or frequent febrile seizures, or an episode of SE. This scenario has serious feasibility issues. Although these children have an 8-fold risk of developing TLE, this risk still remains low, and a large cohort of children would therefore have to be investigated in order to identify only a few who would later develop TLE. An alternative would be to identify adolescents with newly diagnosed TLE who are at risk of developing refractory epilepsy It is fair to assume that the disease process does not stop the day the patient has had his first seizure. Therefore I propose to identify several interesting biomarkers in animal experiments and compare them in these patients with healthy control subjects. Because usually only one hippocampus is affected by HS, the other hippocampus can also be used as a control. When following these patients over several years, biomarkers for ongoing epileptogenesis could be identified as possible predictors of refractoriness to antiepileptic drug treatment. Early identification of patients who would eventually require surgical treatment could reduce the burden and duration of the epilepsy disorder.

It is clear that MR has a lot to offer in TLE research. The versatility and tolerability of the techniques allows for probing of processes from the molecular level to the organ level in the living and developing human brain. This technique is still young, and higher fields, more sophisticated MR sequences, and analysis methods open new doors every day. Efforts should focus on the translation of animal MR studies into human research, and of scientific applications into true diagnostic tools and ultimately treatments.

References

References

(1) Lüders H.O.: Textbook of Epilepsy Surgery. 2008.

(2) Gorji A, Khaleghi GM: History of epilepsy in Medieval Iranian medicine. Neurosci Biobehav Rev 2001; 25(5):455-461.

(3) Eljamel MS: Robotic application in epilepsy surgery. Int J Med Robot 2006; 2(3):233-237.

(4) Labat R.: Traité akkadien de diagnostics et pronostics médicaux. Paris/Leiden, 1951.

(5) Longrigg J: Epilepsy in ancient Greek medicine–the vital step. Seizure 2000; 9(1):12-21.

(6) Eadie M.J., Bladin B.F.: A disease once called sacred: a history of the medical understanding of epilepsy. Eastleigh, 2001.

(7) Shilleto A.R.: Plutarch's morals. London, 1888.

(8) Adams F.: The Genuine Works of Hippocrates. Baltimore, Williams & Wilins Company, 1939.

(9) Marx F., Spencer W.G.: Aelius Cornelius Celsus: Proemium, liber II: On medicine. Cambridge, University Press, 1935.

(10) Bostock J., Rilly H.T.: The natural history of Pliny. London, 1856.

(11) Beyerstein B.L.: Neuropathology and the legacy of spiritual possession. Skeptical Inquirer 1988; 12(3):248-262.

(12) Altschuler EL: Did Ezekiel have temporal lobe epilepsy? Arch Gen Psychiatry 2002; 59(6):561-562.

(13) Altschuler EL: Temporal lobe epilepsy in the priestly source of the Pentateuch. S Afr Med J 2004; 94(11):870.

(14) Waxman SG, Geschwind N: The interictal behavior syndrome of temporal lobe epilepsy. Arch Gen Psychiatry 1975; 32(12):1580-1586.

(15) Trimble M, Freeman A: An investigation of religiosity and the Gastaut-Geschwind syndrome in patients with temporal lobe epilepsy. Epilepsy Behav 2006; 9(3):407-414.

(16) Freemon FR: A differential diagnosis of the inspirational spells of Muhammad the Prophet of Islam. Epilepsia 1976; 17(4):423-427.

(17) Fyodor Dostoevsky: The Possessed. 1872.

(18) Landsborough D: St Paul and temporal lobe epilepsy. J Neurol Neurosurg Psychiatry 1987; 50(6):659-664.

(19) Cesalpinus A.: Daemonum investigation peripatetica. 1593.

(20) Taxil J.: Traicté de l'êpilepsie, maladie vulgairement appeleé au pays de Provence la gouttete aux petits enfants. 1602.

(21) Le Pois C: de Epilepsia, Consilium. 1733.

(22) Willis T: Dr. Willi's practice of physick, being the whole works of the renowned and famous physician. London, 1684.

(23) Rhodius J.: Observatorium medicinalium centuriae tres. Frankfurt, 1676.

(24) Tissot: Traité de l'épilepsie. Faisant le tome troisième du Traité des nerfs et de leurs maladies. Paris, 1770.

(25) Drelincurtius C: Experimenta anatomica. Leiden, 1682.

(26) Donatus M.: De historia medica mirabili libri sex, opera et studio. Frankfurt am Mainz, 1613.

(27) Portal LB: Observations sur la nature et le traitement de l'épilepsie. 1827.

(28) Bravais LF: Recherches sur les symptômes et le traitement de l'épilepsie hémiplégique. Paris, 1827.

(29) Herpin T: Des Accès incomplets d'épilepsie. Paris, 1867.

(30) Clarke EG: The modern practice of physic. London, Longman, Hurst, Rees & Orme, 1805.

(31) Prichard JC: A treatise on diseases of the nervous System, part the first. London, Octavo, 1828.

(32) Bright R: Reports of medical cases. London, 1831.

(33) Todd RB, Bowman W: On the pathology and treatment of convulsive diseases. Br ForeignMed-Chir Rev 1850;(5):1-36.

(34) Gowers WR: Epilepsy and other chronic convulsive disorders: their causes, symptoms and treatment. London, Churchill, 1881.

(35) Jackson HJ: Selected Writings. London, Hodde & Stoughton, 1931.

(36) Jackson J.H.: On a particular variety of epilepsy ("intellectual aura"), one case with symptoms of organic brain disease. Brain 1880; 11:179-207.

(37) Jackson J.H.: Case of epilepsy with tasting movements and "dreaming state"-very small patch of softening in the left uncinate gyrus. Brain 1898; 21:580-590.

(38) Sommer W: Erkrankung des Ammonschorns als aetiologisches Moment der Epilepsie. Arch Psychiatr Nervenkr 1880; 10:631-675.

(39) Bratz E: Ammonshornbefunde der epileptischen. Arch Psychiatr Nervenkr 1899; 31:820-836.

(40) Haas LF: Hans Berger (1873-1941), Richard Caton (1842-1926), and electroencephalography. J Neurol Neurosurg Psychiatry 2003; 74(1):9.

(41) Stone JL: Frederic A. Gibbs, M.D. Surg Neurol 1994; 41(2):168-171.

(42) Shinnar S: The new ILAE classification. Epilepsia 2010; 51(4):715-717.

(43) Conklin HW: Cause and treatment of epilepsy. J Am Osteopath 1922; 22(1):11-14.

(44) Sneader W: Drug Discovery. John Wiley and Sons, 2005.

(45) Bailey P, Gibbs FA: The surgical treatment of psychomotor epilepsy. JAMA 1951; 145(365):370.

(46) Falconer MA, Pond DA, Meyer A, Woolf AL: Temporal lobe epilepsy with personality and behaviour disorders caused by an unusual calcifying lesion; report of two cases in children relieved by temporal lobectomy. J Neurol Neurosurg Psychiatry 1953; 16(4):234-244.

(47) Falconer MA: Genetic and related aetiological factors in temporal lobe epilepsy. A review. Epilepsia 1971; 12(1):13-31.

(48) Falconer MA: Mesial temporal (Ammon's horn) sclerosis as a common cause of epilepsy. Aetiology, treatment, and prevention. Lancet 1974; 2(7883):767-770.

(49) Wiebe S, Blume WT, Girvin JP, Eliasziw M: A randomized, controlled trial of surgery for temporal-lobe epilepsy. N Engl J Med 2001; 345(5):311-318.

(50) Proposal for revised classification of epilepsies and epileptic syndromes. Commission on Classification and Terminology of the International League Against Epilepsy: Epilepsia 1989; 30(4):389-399.

(51) Babb TL, Brown WJ: Neuronal, dendritic, and vascular profiles of human temporal lobe epilepsy correlated with cellular physiology in vivo. Adv Neurol 1986; 44:949-966.

(52) Engel J, Jr.: Surgery for seizures. N Engl J Med 1996; 334(10):647-652.

(53) Forsgren L, Bucht G, Eriksson S, Bergmark L: Incidence and clinical characterization of unprovoked seizures in adults: a prospective population-based study. Epilepsia 1996; 37(3): 224-229.

(54) Hauser WA, Annegers JF, Kurland LT: Incidence of epilepsy and unprovoked seizures in Rochester, Minnesota: 1935-1984. Epilepsia 1993; 34(3): 453-468.

(55) Juul-Jensen P, Foldspang A: Natural history of epileptic seizures. Epilepsia 1983; 24(3):297-312.

(56) Loiseau J, Loiseau P, Guyot M, Duche B, Dartigues JF, Aublet B: Survey of seizure disorders in the French southwest. I. Incidence of epileptic syndromes. Epilepsia 1990; 31(4):391-396.

(57) Joensen P: Prevalence, incidence, and classification of epilepsy in the Faroes. Acta Neurol Scand 1986; 74(2):150-155.

(58) Hauser WA, Annegers JF, Rocca WA: Descriptive epidemiology of epilepsy: contributions of population-based studies from Rochester, Minnesota. Mayo Clin Proc 1996; 71(6):576-586.

(59) Wiebe S: Epidemiology of temporal lobe epilepsy. Can J Neurol Sci 2000; 27 Suppl 1:S6-10.

(60) Kwan P, Brodie MJ: Clinical trials of antiepileptic medications in newly diagnosed patients with epilepsy. Neurology 2003; 60(11 Suppl 4):S2-12.

(61) Semah F, Picot MC, Adam C, Broglin D, Arzimanoglou A, Bazin B, Cavalcanti D, Baulac M: Is the underlying cause of epilepsy a major prognostic factor for recurrence? Neurology 1998; 51(5):1256-1262.

(62) Stephen LJ, Kwan P, Brodie MJ: Does the cause of localisation-related epilepsy influence the response to antiepileptic drug treatment? Epilepsia 2001; 42(3):357-362.

(63) Cascino GD: When drugs and surgery don't work. Epilepsia 2008; 49 Suppl 9:79-84.

(64) Berg AT, Vickrey BG, Testa FM, Levy SR, Shinnar S, DiMario F, Smith S: How long does it take for epilepsy to become intractable? A prospective investigation. Ann Neurol 2006; 60(1):73-79.

(65) Berg AT, Darefsky AS, Holford TR, Shinnar S: Seizures with fever after unprovoked seizures: an analysis in children followed from the time of a first febrile seizure. Epilepsia 1998; 39(1):77-80.

(66) Aicardi J: Consequences and prognosis of convulsive status epilepticus in infants and children. Jpn J Psychiatry Neurol 1986; 40(3): 283-290.

(67) Sagar HJ, Oxbury JM: Hippocampal neuron loss in temporal lobe epilepsy: correlation with early childhood convulsions. Ann Neurol 1987; 22(3): 334-340.

(68) Nelson KB, Ellenberg JH: Predictors of epilepsy in children who have experienced febrile seizures. N Engl J Med 1976; 295(19):1029-1033.

(69) French JA, Williamson PD, Thadani VM, Darcey TM, Mattson RH, Spencer SS, Spencer DD: Characteristics of medial temporal lobe epilepsy: I. Results of history and physical examination. Ann Neurol 1993; 34(6):774-780.

(70) Ludwig BI, Marsan CA: Clinical ictal patterns in epileptic patients with occipital electroencephalographic foci. Neurology 1975; 25(5):463-471.

(71) Sperling MR, Lieb JP, Engel J, Jr., Crandall PH: Prognostic significance of independent auras in temporal lobe seizures. Epilepsia 1989; 30(3): 322-331.

(72) Sperling MR, O'Connor MJ: Auras and subclinical seizures: characteristics and prognostic significance. Ann Neurol 1990; 28(3):320-328.

(73) Fakhoury T, bou-Khalil B: Association of ipsilateral head turning and dystonia in temporal lobe seizures. Epilepsia 1995; 36(11):1065-1070.

(74) Abou-Khalil B, Welch L, Blumenkopf B, Newman K, Whetsell WO, Jr.: Global aphasia with seizure onset in the dominant basal temporal region. Epilepsia 1994; 35(5):1079-1084.

(75) Fakhoury T, bou-Khalil B, Peguero E: Differentiating clinical features of right and left temporal lobe seizures. Epilepsia 1994; 35(5):1038-1044.

(76) Yen DJ, Su MS, Yiu CH, Shih, Kwan SY, Tsai CP, Lin YY: Ictal speech manifestations in temporal lobe epilepsy: a video-EEG study. Epilepsia 1996; 37(1):45-49.

(77) Geyer JD, Payne TA, Faught E, Drury I: Postictal nose-rubbing in the diagnosis, lateralization, and localization of seizures. Neurology 1999; 52(4): 743-745.

(78) Zijlmans M, van Eijsden P, Ferrier CH, Kho KH, van Rijen PC, Leijten FS: Illusory shadow person causing paradoxical gaze deviations during temporal lobe seizures. J Neurol Neurosurg Psychiatry 2009; 80(6):686-688.

(79) Foerster O, Penfield W: Der Narbenzung am und im Gehirn bei traumatischer Epilepsie in seiner Bedeutung fur das Zurstandekommen der Anfälle und fur die therapeutische Bekämpfung derselben. Gesamte Neurol Psychiatrie 1930;(125):475-572.

(80) Chee MW, Kotagal P, Van Ness PC, Gragg L, Murphy D, Luders HO: Lateralizing signs in intractable partial epilepsy: blinded multiple-observer analysis. Neurology 1993; 43(12):2519-2525.

(81) Kernan JC, Devinsky O, Luciano DJ, Vazquez B, Perrine K: Lateralizing significance of head and eye deviation in secondary generalized tonic-clonic seizures. Neurology 1993; 43(7):1308-1310.

(82) Wyllie E, Luders H, Morris HH, Lesser RP, Dinner DS: The lateralizing significance of versive head and eye movements during epileptic seizures. Neurology 1986; 36(5):606-611.

(83) Bleasel A, Kotagal P, Kankirawatana P, Rybicki L: Lateralizing value and semiology of ictal limb posturing and version in temporal lobe and extratemporal epilepsy. Epilepsia 1997; 38(2): 168-174.

(84) Ferrier CH, Aronica E, Leijten FS, Spliet WG, van Huffelen AC, van Rijen PC, Binnie CD: Electrocorticographic discharge patterns in glioneuronal tumors and focal cortical dysplasia. Epilepsia 2006; 47(9):1477-1486.

(85) Newton MR, Berkovic SF, Austin MC, Reutens DC, McKay WJ, Bladin PF: Dystonia, clinical lateralization, and regional blood flow changes in temporal lobe seizures. Neurology 1992; 42(2): 371-377.

(86) Arzy S, Seeck M, Ortigue S, Spinelli L, Blanke O: Induction of an illusory shadow person. Nature 2006; 443(7109):287.

(87) De RD, Van LK, Dupont P, Menovsky T, Van de HP: Visualizing out-of-body experience in the brain. N Engl J Med 2007; 357(18):1829-1833.

(88) Blanke O, Landis T, Spinelli L, Seeck M: Out-of-body experience and autoscopy of neurological origin. Brain 2004; 127(Pt 2):243-258.

(89) Dierks T, Linden DE, Jandl M, Formisano E, Goebel R, Lanfermann H, Singer W: Activation of Heschl's gyrus during auditory hallucinations. Neuron 1999; 22(3):615-621.

(90) Kerling F, Mueller S, Pauli E, Stefan H: When do patients forget their seizures? An electroclinical study. Epilepsy Behav 2006; 9(2):281-285.

(91) Schulz R, Luders HO, Noachtar S, May T, Sakamoto A, Holthausen H, Wolf P: Amnesia of the epileptic aura. Neurology 1995; 45(2):231-235.

(92) Ebersole JS, Pacia SV: Localization of temporal lobe foci by ictal EEG patterns. Epilepsia 1996; 37(4): 386-399.

(93) Berkovic SF, Andermann F, Olivier A, Ethier R, Melanson D, Robitaille Y, Kuzniecky R, Peters T, Feindel W: Hippocampal sclerosis in temporal lobe epilepsy demonstrated by magnetic resonance imaging. Ann Neurol 1991; 29(2):175-182.

(94) Kuzniecky RI: Neuroimaging of epilepsy: advances and practical applications. Rev Neurol Dis 2004; 1(4):179-189.

(95) Williamson PD, French JA, Thadani VM, Kim JH, Novelly RA, Spencer SS, Spencer DD, Mattson RH: Characteristics of medial temporal lobe epilepsy: II. Interictal and ictal scalp electroencephalography, neuropsychological testing, neuroimaging, surgical results, and pathology. Ann Neurol 1993; 34(6):781-787.

(96) Knowlton RC, Laxer KD, Ende G, Hawkins RA, Wong ST, Matson GB, Rowley HA, Fein G, Weiner MW: Presurgical multimodality neuroimaging in electroencephalographic lateralized temporal lobe epilepsy. Ann Neurol 1997; 42(6):829-837.

(97) Newton MR, Berkovic SF, Austin MC, Rowe CC, McKay WJ, Bladin PF: Postictal switch in blood flow distribution and temporal lobe seizures. J Neurol Neurosurg Psychiatry 1992; 55(10):891-894.

(98) Newton MR, Berkovic SF, Austin MC, Rowe CC, McKay WJ, Bladin PF: SPECT in the localisation of extratemporal and temporal seizure foci. J Neurol Neurosurg Psychiatry 1995; 59(1):26-30.

(99) Ebersole JS, Squires KC, Eliashiv SD, Smith JR: Applications of magnetic source imaging in evaluation of candidates for epilepsy surgery. Neuroimaging Clin N Am 1995; 5(2):267-288.

(100) Mathern GW, Babb TL, Vickrey BG, Melendez M, Pretorius JK: The clinical-pathogenic mechanisms of hippocampal neuron loss and surgical outcomes in temporal lobe epilepsy. Brain 1995; 118 (Pt 1): 105-118.

(101) Mathern GW, Pretorius JK, Babb TL: Influence of the type of initial precipitating injury and at what age it occurs on course and outcome in patients with temporal lobe seizures. J Neurosurg 1995; 82(2):220-227.

(102) Mathern GW, Leiphart JL, De VA, Adelson PD, Seki T, Neder L, Leite JP: Seizures decrease postnatal neurogenesis and granule cell development in the human fascia dentata. Epilepsia 2002; 43 Suppl 5:68-73.

(103) Eid T, Thomas MJ, Spencer DD, Runden-Pran E, Lai JC, Malthankar GV, Kim JH, Danbolt NC, Ottersen OP, de Lanerolle NC: Loss of glutamine synthetase in the human epileptogenic hippocampus: possible mechanism for raised extracellular glutamate in mesial temporal lobe epilepsy. Lancet 2004; 363(9402):28-37.

(104) Sutula T, Pitkanen A: Do Seizures Damage the Brain. Amsterdam, Elsevier, 2002.

(105) Mathern GW, Leite JP, Pretorius JK, Quinn B, Peacock WJ, Babb TL: Severe seizures in young children are associated with hippocampal neuron losses and aberrant mossy fiber sprouting during fascia dentata postnatal development. Epilepsy Res Suppl 1996; 12:33-43.

(106) Bartolomei F, Khalil M, Wendling F, Sontheimer A, Regis J, Ranjeva JP, Guye M, Chauvel P: Entorhinal cortex involvement in human mesial temporal lobe epilepsy: an electrophysiologic and volumetric study. Epilepsia 2005; 46(5):677-687.

(107) Ben-Ari Y, Tremblay E, Riche D, Ghilini G, Naquet R: Electrographic, clinical and pathological alterations following systemic administration of kainic acid, bicuculline or pentetrazole: metabolic mapping using the deoxyglucose method with special reference to the pathology of epilepsy. Neuroscience 1981; 6(7):1361-1391.

(108) Collins RC, McLean M, Olney J: Cerebral metabolic response to systemic kainic acid: 14-C-deoxyglucose studies. Life Sci 1980; 27(10):855-862.

(109) Lothman EW, Bertram EH, Bekenstein JW, Perlin JB: Self-sustaining limbic status epilepticus induced by ‚continuous' hippocampal stimulation: electrographic and behavioral characteristics. Epilepsy Res 1989; 3(2):107-119.

(110) Olney JW, Rhee V, Ho OL: Kainic acid: a powerful neurotoxic analogue of glutamate. Brain Res 1974; 77(3):507-512.

(111) Nevander G, Ingvar M, Auer R, Siesjo BK: Status epilepticus in well-oxygenated rats causes neuronal necrosis. Ann Neurol 1985; 18(3):281-290.

(112) Fisher RS: Animal models of the epilepsies. Brain Res Brain Res Rev 1989; 14(3):245-278.

(113) Benardo LS, Prince DA: Acetylcholine induced modulation of hippocampal pyramidal neurons. Brain Res 1981; 211(1):227-234.

(114) Benardo LS, Prince DA: Cholinergic excitation of mammalian hippocampal pyramidal cells. Brain Res 1982; 249(2):315-331.

(115) Clifford DB, Olney JW, Maniotis A, Collins RC, Zorumski CF: The functional anatomy and pathology of lithium-pilocarpine and high-dose pilocarpine seizures. Neuroscience 1987; 23(3): 953-968.

(116) Mellanby J, George G, Robinson A, Thompson P: Epileptiform syndrome in rats produced by injecting tetanus toxin into the hippocampus. J Neurol Neurosurg Psychiatry 1977; 40(4):404-414.

(117) Turski WA, Cavalheiro EA, Schwarz M, Czuczwar SJ, Kleinrok Z, Turski L: Limbic seizures produced by pilocarpine in rats: behavioural, electroencephalographic and neuropathological study. Behav Brain Res 1983; 9(3):315-335.

(118) Racine RJ: Modification of seizure activity by electrical stimulation. II. Motor seizure. Electroencephalogr Clin Neurophysiol 1972; 32(3):281-294.

(119) Cavalheiro EA: The pilocarpine model of epilepsy. Ital J Neurol Sci 1995; 16(1-2):33-37.

(120) Scorza FA, Arida RM, Naffah-Mazzacoratti MG, Scerni DA, Calderazzo L, Cavalheiro EA: The pilocarpine model of epilepsy: what have we learned? An Acad Bras Cienc 2009; 81(3):345-365.

(121) Turski WA, Cavalheiro EA, Schwarz M, Czuczwar SJ, Kleinrok Z, Turski L: Limbic seizures produced by pilocarpine in rats: behavioural, electroencephalographic and neuropathological study. Behav Brain Res 1983; 9(3):315-335.

(122) Turski L, Ikonomidou C, Turski WA, Bortolotto ZA, Cavalheiro EA: Review: cholinergic mechanisms and epileptogenesis. The seizures induced by pilocarpine: a novel experimental model of intractable epilepsy. Synapse 1989; 3(2):154-171.

(123) Curia G, Longo D, Biagini G, Jones RS, Avoli M: The pilocarpine model of temporal lobe epilepsy. J Neurosci Methods 2008; 172(2):143-157.

(124) Honchar MP, Olney JW, Sherman WR: Systemic cholinergic agents induce seizures and brain damage in lithium-treated rats. Science 1983; 220(4594):323-325.

(125) Goffin K, Nissinen J, Van LK, Pitkanen A: Cyclicity of spontaneous recurrent seizures in pilocarpine model of temporal lobe epilepsy in rat. Exp Neurol 2007; 205(2):501-505.

(126) Cavalheiro EA, Silva DF, Turski WA, Calderazzo-Filho LS, Bortolotto ZA, Turski L: The susceptibility of rats to pilocarpine-induced seizures is age-dependent. Brain Res 1987; 465(1-2):43-58.

(127) Priel MR, Albuquerque EX: Short-term effects of pilocarpine on rat hippocampal neurons in culture. Epilepsia 2002; 43 Suppl 5:40-46.

(128) Liu Z, Nagao T, Desjardins GC, Gloor P, Avoli M: Quantitative evaluation of neuronal loss in the dorsal hippocampus in rats with long-term pilocarpine seizures. Epilepsy Res 1994; 17(3): 237-247.

(129) Dube C, Boyet S, Marescaux C, Nehlig A: Relationship between neuronal loss and interictal glucose metabolism during the chronic phase of the lithium-pilocarpine model of epilepsy in the immature and adult rat. Exp Neurol 2001; 167(2):227-241.

(130) van der Hel WS, Bos IWM, Mulder S, Verlinde S.A.M.W., van Eijsden P, de Graan PN: Decreased hippocampal glutamine synthetase expression in the juvenile rat Li+/pilocarpine model and in human temporal lobe epilepsy. Submitted 2010.

(131) Babb TL, Kupfer WR, Pretorius JK, Crandall PH, Levesque MF: Synaptic reorganization by mossy fibers in human epileptic fascia dentata. Neuroscience 1991; 42(2):351-363.

(132) Sutula T, Cascino G, Cavazos J, Parada I, Ramirez L: Mossy fiber synaptic reorganization in the epileptic human temporal lobe. Ann Neurol 1989; 26(3): 321-330.

(133) Buckmaster PS, Zhang GF, Yamawaki R: Axon sprouting in a model of temporal lobe epilepsy creates a predominantly excitatory feedback circuit. J Neurosci 2002; 22(15):6650-6658.

(134) Isokawa M: Preservation of dendrites with the presence of reorganized mossy fiber collaterals in hippocampal dentate granule cells in patients with temporal lobe epilepsy. Brain Res 1997; 744(2): 339-343.

(135) Isokawa M, Levesque MF, Babb TL, Engel J, Jr.: Single mossy fiber axonal systems of human dentate granule cells studied in hippocampal slices from patients with temporal lobe epilepsy. J Neurosci 1993; 13(4):1511-1522.

(136) Cotman CW, Nadler JV: Reactive synaptogenesis in the hippocampus.; Neuronal Plasticity. New York, Raven Press; 1978, 1978, pp 227-271.

(137) El BB, Lespinet V, Lurton D, Coussemacq M, Le Gal La SG, Rougier A: Correlations between granule cell dispersion, mossy fiber sprouting, and hippocampal cell loss in temporal lobe epilepsy. Epilepsia 1999; 40(10):1393-1401.

(138) Hermann B, Seidenberg M, Bell B, Rutecki P, Sheth RD, Wendt G, O'Leary D, Magnotta V: Extratemporal quantitative MR volumetrics and neuropsychological status in temporal lobe epilepsy. J Int Neuropsychol Soc 2003; 9(3):353-362.

(139) Seidenberg M, Kelly KG, Parrish J, Geary E, Dow C, Rutecki P, Hermann B: Ipsilateral and contralateral MRI volumetric abnormalities in chronic unilateral temporal lobe epilepsy and their clinical correlates. Epilepsia 2005; 46(3):420-430.

(140) Hermann B, Hansen R, Seidenberg M, Magnotta V, O'Leary D: Neurodevelopmental vulnerability of the corpus callosum to childhood onset localization-related epilepsy. Neuroimage 2003; 18(2):284-292.

(141) Kimiwada T, Juhasz C, Makki M, Muzik O, Chugani DC, Asano E, Chugani HT: Hippocampal and thalamic diffusion abnormalities in children with temporal lobe epilepsy. Epilepsia 2006; 47(1): 167-175.

(142) Caplan R, Levitt J, Siddarth P, Taylor J, Daley M, Wu KN, Gurbani S, Shields WD, Sankar R: Thought disorder and frontotemporal volumes in pediatric epilepsy. Epilepsy Behav 2008; 13(4):593-599.

(143) Govindan RM, Makki MI, Sundaram SK, Juhasz C, Chugani HT: Diffusion tensor analysis of temporal and extra-temporal lobe tracts in temporal lobe epilepsy. Epilepsy Res 2008; 80(1):30-41.

(144) Nilsson D, Go C, Rutka JT, Rydenhag B, Mabbott DJ, Snead OC, III, Raybaud CR, Widjaja E: Bilateral diffusion tensor abnormalities of temporal lobe and cingulate gyrus white matter in children with temporal lobe epilepsy. Epilepsy Res 2008; 81(2-3):128-135.

(145) Hutchinson E, Pulsipher D, Dabbs K, Gutierrez A, Sheth R, Jones J, Seidenberg M, Meyerand E, Hermann B: Children with new-onset epilepsy exhibit diffusion abnormalities in cerebral white matter in the absence of volumetric differences. Epilepsy Res 2010; 88(2-3):208-214.

(146) Widjaja E, Yeung R, Geibprasert S, Mahmoodabadi SZ, Snead OC, III, Smith ML: Longitudinal brain volumes in children with intractable partial seizures. Pediatr Neurol 2010; 42(5):315-319.

(147) Le BD: Molecular diffusion, tissue microdynamics and microstructure. NMR Biomed 1995; 8(7-8): 375-386.

(148) Arfanakis K, Hermann BP, Rogers BP, Carew JD, Seidenberg M, Meyerand ME: Diffusion tensor MRI in temporal lobe epilepsy. Magn Reson Imaging 2002; 20(7):511-519.

(149) Rugg-Gunn FJ, Eriksson SH, Symms MR, Barker GJ, Thom M, Harkness W, Duncan JS: Diffusion tensor imaging in refractory epilepsy. Lancet 2002; 359(9319):1748-1751.

(150) Concha L, Beaulieu C, Wheatley BM, Gross DW: Bilateral white matter diffusion changes persist after epilepsy surgery. Epilepsia 2007; 48(5): 931-940.

(151) Concha L, Livy DJ, Beaulieu C, Wheatley BM, Gross DW: In vivo diffusion tensor imaging and histopathology of the fimbria-fornix in temporal lobe epilepsy. J Neurosci 2010; 30(3):996-1002.

(152) Gross DW, Concha L, Beaulieu C: Extratemporal white matter abnormalities in mesial temporal lobe epilepsy demonstrated with diffusion tensor imaging. Epilepsia 2006; 47(8):1360-1363.

(153) Ahmadi ME, Hagler DJ, Jr., McDonald CR, Tecoma ES, Iragui VJ, Dale AM, Halgren E: Side matters: diffusion tensor imaging tractography in left and right temporal lobe epilepsy. AJNR Am J Neuroradiol 2009; 30(9):1740-1747.

(154) Riley JD, Franklin DL, Choi V, Kim RC, Binder DK, Cramer SC, Lin JJ: Altered white matter integrity in temporal lobe epilepsy: association with cognitive and clinical profiles. Epilepsia 2010; 51(4):536-545.

(155) Shon YM, Kim YI, Koo BB, Lee JM, Kim HJ, Kim WJ, Ahn KJ, Yang DW: Group-specific regional white matter abnormality revealed in diffusion tensor imaging of medial temporal lobe epilepsy without hippocampal sclerosis. Epilepsia 2010; 51(4): 529-535.

(156) Buzsaki G, Ponomareff GL, Bayardo F, Ruiz R, Gage FH: Neuronal activity in the subcortically denervated hippocampus: a chronic model for epilepsy. Neuroscience 1989; 28(3):527-538.

(157) Danbolt NC: Glutamate uptake. Prog Neurobiol 2001; 65(1):1-105.

(158) Brooks-Kayal AR, Shumate MD, Jin H, Lin DD, Rikhter TY, Holloway KL, Coulter DA: Human neuronal gamma-aminobutyric acid(A) receptors: coordinated subunit mRNA expression and functional correlates in individual dentate granule cells. J Neurosci 1999; 19(19):8312-8318.

(159) Rothstein JD, Dykes-Hoberg M, Pardo CA, Bristol LA, Jin L, Kuncl RW, Kanai Y, Hediger MA, Wang Y, Schielke JP, Welty DF: Knockout of glutamate transporters reveals a major role for astroglial transport in excitotoxicity and clearance of glutamate. Neuron 1996; 16(3):675-686.

(160) Bak LK, Schousboe A, Waagepetersen HS: The glutamate/GABA-glutamine cycle: aspects of transport, neurotransmitter homeostasis and ammonia transfer. J Neurochem 2006; 98(3): 641-653.

(161) Benjamin AM, Quastel JH: Locations of amino acids in brain slices from the rat. Tetrodotoxin-sensitive release of amino acids. Biochem J 1972; 128(3): 631-646.

(162) Ottersen OP, Zhang N, Walberg F: Metabolic compartmentation of glutamate and glutamine: morphological evidence obtained by quantitative immunocytochemistry in rat cerebellum. Neuroscience 1992; 46(3):519-534.

(163) Norenberg MD, Martinez-Hernandez A: Fine structural localization of glutamine synthetase in astrocytes of rat brain. Brain Res 1979; 161(2): 303-310.

(164) Sibson NR, Dhankhar A, Mason GF, Rothman DL, Behar KL, Shulman RG: Stoichiometric coupling of brain glucose metabolism and glutamatergic neuronal activity. Proc Natl Acad Sci U S A 1998; 95(1):316-321.

(165) Patel AB, de Graaf RA, Mason GF, Rothman DL, Shulman RG, Behar KL: The contribution of GABA to glutamate/glutamine cycling and energy metabolism in the rat cortex in vivo. Proc Natl Acad Sci U S A 2005; 102(15):5588-5593.

(166) de Graaf RA, Brown PB, Mason GF, Rothman DL, Behar KL: Detection of {1,6-13C2}-glucose metabolism in rat brain by in vivo 1H-{13C}-NMR spectroscopy. Magn Reson Med 2003; 49(1):37-46.

(167) During MJ, Spencer DD: Extracellular hippocampal glutamate and spontaneous seizure in the conscious human brain. Lancet 1993; 341(8861):1607-1610.

(168) Cavus I, Kasoff WS, Cassaday MP, Jacob R, Gueorguieva R, Sherwin RS, Krystal JH, Spencer DD, bi-Saab WM: Extracellular metabolites in the cortex and hippocampus of epileptic patients. Ann Neurol 2005; 57(2):226-235.

(169) Petroff OA, Errante LD, Rothman DL, Kim JH, Spencer DD: Glutamate-glutamine cycling in the epileptic human hippocampus. Epilepsia 2002; 43(7):703-710.

(170) Wang L, Liu YH, Huang YG, Chen LW: Time-course of neuronal death in the mouse pilocarpine model of chronic epilepsy using Fluoro-Jade C staining. Brain Res 2008; 1241:157-167.

(171) Boulland JL, Ferhat L, Tallak ST, Ferrand N, Chaudhry FA, Storm-Mathisen J, Esclapez M: Changes in vesicular transporters for gamma-aminobutyric acid and glutamate reveal vulnerability and reorganization of hippocampal neurons following pilocarpine-induced seizures. J Comp Neurol 2007; 503(3):466-485.

(172) Holopainen IE: Seizures in the developing brain: cellular and molecular mechanisms of neuronal damage, neurogenesis and cellular reorganization. Neurochem Int 2008; 52(6):935-947.

(173) Melo TM, Nehlig A, Sonnewald U: Metabolism is normal in astrocytes in chronically epileptic rats: a (13)C NMR study of neuronal-glial interactions in a model of temporal lobe epilepsy. J Cereb Blood Flow Metab 2005; 25(10):1254-1264.

(174) Sonnewald U, Kondziella D: Neuronal glial interaction in different neurological diseases studied by ex vivo 13C NMR spectroscopy. NMR Biomed 2003; 16(6-7):424-429.

(175) van der Hel WS, Notenboom RG, Bos IW, van Rijen PC, van Veelen CW, de Graan PN: Reduced glutamine synthetase in hippocampal areas with neuron loss in temporal lobe epilepsy. Neurology 2005; 64(2):326-333.

(176) Provencher SW: Estimation of metabolite concentrations from localized in vivo proton NMR spectra. Magn Reson Med 1993; 30(6):672-679.

(177) Uematsu S: Surgical management of complex partial seizures. JAMA 1990; 264(6):734-737.

(178) Shorvon S: The course of untreated epilepsy. BMJ 1988; 297(6660):1405.

(179) Trinka E, Unterrainer J, Haberlandt E, Luef G, Unterberger I, Niedermuller U, Haffner B, Bauer G: Childhood febrile convulsions--which factors determine the subsequent epilepsy syndrome? A retrospective study. Epilepsy Res 2002; 50(3): 283-292.

(180) Hirsch E, Baram TZ, Snead OC, III: Ontogenic study of lithium-pilocarpine-induced status epilepticus in rats. Brain Res 1992; 583(1-2):120-126.

(181) Bottomley PA: Spatial localization in NMR spectroscopy in vivo. Ann N Y Acad Sci 1987; 508:333-348.

(182) Woods RP, Cherry SR, Mazziotta JC: Rapid automated algorithm for aligning and reslicing PET images. J Comput Assist Tomogr 1992; 16(4):620-633.

(183) Paxinos G, Watson C: The Ratbrain in Stereotactic Coodinates. North Pride, Academic Press Australia, 1986.

(184) de BR, van den BA, van OD, Pijnappel WW, den Hollander JA, Marien AJ, Luyten PR: Application of time-domain fitting in the quantification of in vivo 1H spectroscopic imaging data sets. NMR Biomed 1992; 5(4):171-178.

(185) Wall CJ, Kendall EJ, Obenaus A: Rapid alterations in diffusion-weighted images with anatomic correlates in a rodent model of status epilepticus. AJNR Am J Neuroradiol 2000; 21(10):1841-1852.

(186) Fabene PF, Marzola P, Sbarbati A, Bentivoglio M: Magnetic resonance imaging of changes elicited by status epilepticus in the rat brain: diffusion-weighted and T2-weighted images, regional blood volume maps, and direct correlation with tissue and cell damage. Neuroimage 2003; 18(2):375-389.

(187) Roch C, Leroy C, Nehlig A, Namer IJ: Magnetic resonance imaging in the study of the lithium-pilocarpine model of temporal lobe epilepsy in adult rats. Epilepsia 2002; 43(4):325-335.

(188) Bhagat YA, Obenaus A, Hamilton MG, Kendall EJ: Magnetic resonance imaging predicts neuropathology from soman-mediated seizures in the rodent. Neuroreport 2001; 12(7):1481-1487.

(189) Payen JF, LeBars E, Wuyam B, Tropini B, Pepin JL, Levy P, Decorps M: Lactate accumulation during moderate hypoxic hypoxia in neocortical rat brain. J Cereb Blood Flow Metab 1996; 16(6):1345-1352.

(190) Fernandes MJ, Dube C, Boyet S, Marescaux C, Nehlig A: Correlation between hypermetabolism and neuronal damage during status epilepticus induced by lithium and pilocarpine in immature and adult rats. J Cereb Blood Flow Metab 1999; 19(2):195-209.

(191) Pereira d, V, Ferrandon A, Nehlig A: Local cerebral blood flow during lithium-pilocarpine seizures in the developing and adult rat: role of coupling between blood flow and metabolism in the genesis of neuronal damage. J Cereb Blood Flow Metab 2002; 22(2):196-205.

(192) Prichard JW, Zhong J, Petroff OA, Gore JC: Diffusion-weighted NMR imaging changes caused by electrical activation of the brain. NMR Biomed 1995; 8(7-8):359-364.

(193) Zhong J, Petroff OA, Prichard JW, Gore JC: Changes in water diffusion and relaxation properties of rat cerebrum during status epilepticus. Magn Reson Med 1993; 30(2):241-246.

(194) Hugg JW, Kuzniecky RI, Gilliam FG, Morawetz RB, Fraught RE, Hetherington HP: Normalization of contralateral metabolic function following temporal lobectomy demonstrated by 1H magnetic resonance spectroscopic imaging. Ann Neurol 1996; 40(2):236-239.

(195) Lansberg MG, O'Brien MW, Norbash AM, Moseley ME, Morrell M, Albers GW: MRI abnormalities associated with partial status epilepticus. Neurology 1999; 52(5):1021-1027.

(196) Handforth A, Treiman DM: Functional mapping of the early stages of status epilepticus: a 14C-2-deoxyglucose study in the lithium-pilocarpine model in rat. Neuroscience 1995; 64(4):1057-1073.

(197) Millan MH, Patel S, Meldrum BS: Olfactory bulbectomy protects against pilocarpine-induced motor limbic seizures in rats. Brain Res 1986; 398(1):204-206.

(198) Leroy C, Roch C, Koning E, Namer IJ, Nehlig A: In the lithium-pilocarpine model of epilepsy, brain lesions are not linked to changes in blood-brain barrier permeability: an autoradiographic study in adult and developing rats. Exp Neurol 2003; 182(2):361-372.

(199) Bertram EH, Zhang DX: Thalamic excitation of hippocampal CA1 neurons: a comparison with the effects of CA3 stimulation. Neuroscience 1999; 92(1):15-26.

(200) Bertram EH, Zhang DX, Mangan P, Fountain N, Rempe D: Functional anatomy of limbic epilepsy: a proposal for central synchronization of a diffusely hyperexcitable network. Epilepsy Res 1998; 32(1-2):194-205.

(201) Ebisu T, Rooney WD, Graham SH, Mancuso A, Weiner MW, Maudsley AA: MR spectroscopic imaging and diffusion-weighted MRI for early detection of kainate-induced status epilepticus in the rat. Magn Reson Med 1996; 36(6):821-828.

(202) Najm IM, Wang Y, Shedid D, Luders HO, Ng TC, Comair YG: MRS metabolic markers of seizures and seizure-induced neuronal damage. Epilepsia 1998; 39(3):244-250.

(203) Tang P, Liachenko S, Melick JA, Xu Y: {31P}/{1H} nuclear magnetic resonance study of mitigating effects of GYKI 52466 on kainate-induced metabolic impairment in perfused rat cerebrocortical slices. Epilepsia 1998; 39(6):577-583.

(204) Lazeyras F, Blanke O, Zimine I, Delavelle J, Perrig SH, Seeck M: MRI, (1)H-MRS, and functional MRI during and after prolonged nonconvulsive seizure activity. Neurology 2000; 55(11):1677-1682.

(205) Mueller SG, Kollias SS, Trabesinger AH, Buck A, Boesiger P, Wieser HG: Proton magnetic resonance spectroscopy characteristics of a focal cortical dysgenesis during status epilepticus and in the interictal state. Seizure 2001; 10(7):518-524.

(206) van der TA, Verheul HB, Berkelbach van der Sprenkel JW, Tulleken CA, Nicolay K: Changes in metabolites and tissue water status after focal ischemia in cat brain assessed with localized proton MR spectroscopy. Magn Reson Med 1994; 32(6):685-691.

(207) Maton BM, Kuzniecky RI: Proton MRS: N-acetyl aspartate, creatine, and choline. Adv Neurol 2000; 83:253-259.

(208) Covolan L, Mello LE: Temporal profile of neuronal injury following pilocarpine or kainic acid-induced status epilepticus. Epilepsy Res 2000; 39(2):133-152.

(209) Fujikawa DG: The temporal evolution of neuronal damage from pilocarpine-induced status epilepticus. Brain Res 1996; 725(1):11-22.

(210) Peredery O, Persinger MA, Parker G, Mastrosov L: Temporal changes in neuronal dropout following inductions of lithium/pilocarpine seizures in the rat. Brain Res 2000; 881(1):9-17.

(211) Hetherington HP, Pan JW, Spencer DD: 1H and 31P spectroscopy and bioenergetics in the lateralization of seizures in temporal lobe epilepsy. J Magn Reson Imaging 2002; 16(4):477-483.

(212) Long RC, Jr., Papas KK, Sambanis A, Constantinidis I: In vitro monitoring of total choline levels in a bioartificial pancreas: (1)H NMR spectroscopic studies of the effects of oxygen level. J Magn Reson 2000; 146(1):49-57.

(213) Satlin A, Bodick N, Offen WW, Renshaw PF: Brain proton magnetic resonance spectroscopy (1H-MRS) in Alzheimer's disease: changes after treatment with xanomeline, an M1 selective cholinergic agonist. Am J Psychiatry 1997; 154(10):1459-1461.

(214) Jope RS, Morrisett RA: Neurochemical consequences of status epilepticus induced in rats by coadministration of lithium and pilocarpine. Exp Neurol 1986; 93(2):404-414.

(215) Jope RS, Simonato M, Lally K: Acetylcholine content in rat brain is elevated by status epilepticus induced by lithium and pilocarpine. J Neurochem 1987; 49(3):944-951.

(216) de Graaf RA: In Vivo NMR Spectroscopy, Principles and Techniques. Chicester, John Wiley & Sons, 1998.

(217) Dube C, da Silva Fernandes MJ, Nehlig A: Age-dependent consequences of seizures and the development of temporal lobe epilepsy in the rat. Dev Neurosci 2001; 23(3):219-223.

(218) Klüver H, Barrera E: A method for the combined staining of cells and fibers in the nervous system. J Neuropathol Exp Neurol 1953; 12(4):400-403.

(219) Cho KO, La HO, Cho YJ, Sung KW, Kim SY: Minocycline attenuates white matter damage in a rat model of chronic cerebral hypoperfusion. J Neurosci Res 2006; 83(2):285-291.

(220) Abramoff MD, Magelhaes PJ, Ram SJ: Image Processing with ImageJ. Biophotonics International 2004; 11(7):36-42.

(221) van Eijsden P, Notenboom RG, Wu O, de Graan PN, van NO, Nicolay K, Braun KP: In vivo 1H magnetic resonance spectroscopy, T2-weighted and diffusion-weighted MRI during lithium-pilocarpine-induced status epilepticus in the rat. Brain Res 2004; 1030(1):11-18.

(222) Norton WT, Poduslo SE: Myelination in rat brain: changes in myelin composition during brain maturation. J Neurochem 1973; 21(4):759-773.

(223) Proper EA, Jansen GH, van Veelen CW, van Rijen PC, Gispen WH, de Graan PN: A grading system for hippocampal sclerosis based on the degree of hippocampal mossy fiber sprouting. Acta Neuropathol 2001; 101(4):405-409.

(224) Blumcke I, Beck H, Lie AA, Wiestler OD: Molecular neuropathology of human mesial temporal lobe epilepsy. Epilepsy Res 1999; 36(2-3):205-223.

(225) Treiman DM: GABAergic mechanisms in epilepsy. Epilepsia 2001; 42 Suppl 3:8-12.

(226) Sankar R, Shin DH, Liu H, Mazarati A, Pereira d, V, Wasterlain CG: Patterns of status epilepticus-induced neuronal injury during development and long-term consequences. J Neurosci 1998; 18(20):8382-8393.

(227) Gruetter R: Automatic, localized in vivo adjustment of all first- and second-order shim coils. Magn Reson Med 1993; 29(6):804-811.

(228) Haase A, Frahm J, Hanicke W, Matthaei D: 1H NMR chemical shift selective (CHESS) imaging. Phys Med Biol 1985; 30(4):341-344.

(229) Rothman DL, Petroff OA, Behar KL, Mattson RH: Localized 1H NMR measurements of gamma-aminobutyric acid in human brain in vivo. Proc Natl Acad Sci U S A 1993; 90(12):5662-5666.

(230) de Graaf RA, Brown PB, McIntyre S, Nixon TW, Behar KL, Rothman DL: High magnetic field water and metabolite proton T1 and T2 relaxation in rat brain in vivo. Magn Reson Med 2006; 56(2):386-394.

(231) Leclerc JH: Quantification of noisy MRS signals with the Pseudo-Wigner Distribution. IEEE Trans Biomed Eng 1994; 41(9):809-819.

(232) Schmued LC, Albertson C, Slikker W, Jr.: Fluoro-Jade: a novel fluorochrome for the sensitive and reliable histochemical localization of neuronal degeneration. Brain Res 1997; 751(1):37-46.

(233) Andre V, Marescaux C, Nehlig A, Fritschy JM: Alterations of hippocampal GAbaergic system contribute to development of spontaneous recurrent seizures in the rat lithium-pilocarpine model of temporal lobe epilepsy. Hippocampus 2001; 11(4):452-468.

(234) Dinocourt C, Petanjek Z, Freund TF, Ben-Ari Y, Esclapez M: Loss of interneurons innervating pyramidal cell dendrites and axon initial segments in the CA1 region of the hippocampus following pilocarpine-induced seizures. J Comp Neurol 2003; 459(4):407-425.

(235) Proper EA, Oestreicher AB, Jansen GH, Veelen CW, van Rijen PC, Gispen WH, de Graan PN: Immunohistochemical characterization of mossy fibre sprouting in the hippocampus of patients with pharmaco-resistant temporal lobe epilepsy. Brain 2000; 123 (Pt 1):19-30.

(236) Peeling J, Sutherland G: 1H magnetic resonance spectroscopy of extracts of human epileptic neocortex and hippocampus. Neurology 1993; 43(3 Pt 1):589-594.

(237) Scantlebury MH, Heida JG, Hasson HJ, Veliskova J, Velisek L, Galanopoulou AS, Moshe SL: Age-dependent consequences of status epilepticus: animal models. Epilepsia 2007; 48 Suppl 2:75-82.

(238) Babb TL, Mathern GW, Leite JP, Pretorius JK, Yeoman KM, Kuhlman PA: Glutamate AMPA receptors in the fascia dentata of human and kainate rat hippocampal epilepsy. Epilepsy Res 1996; 26(1):193-205.

(239) Muller B, Qu H, Garseth M, White LR, Aasly J, Sonnewald U: Amino acid neurotransmitter metabolism in neurones and glia following kainate injection in rats. Neurosci Lett 2000; 279(3):169-172.

(240) Aasly J, Silfvenius H, Aas TC, Sonnewald U, Olivecrona M, Juul R, White LR: Proton magnetic resonance spectroscopy of brain biopsies from patients with intractable epilepsy. Epilepsy Res 1999; 35(3):211-217.

(241) Freund TF, Hajos N, Acsady L, Gorcs TJ, Katona I: Mossy cells of the rat dentate gyrus are immunoreactive for calcitonin gene-related peptide (CGRP). Eur J Neurosci 1997; 9(9):1815-1830.

(242) Gorter JA, Van Vliet EA, Proper EA, de Graan PN, Ghijsen WE, Lopes Da Silva FH, Aronica E: Glutamate transporters alterations in the reorganizing dentate gyrus are associated with progressive seizure activity in chronic epileptic rats. J Comp Neurol 2002; 442(4):365-377.

(243) Zamecnik J, Krsek P, Druga R, Marusic P, Benes V, Tichy M, Komarek V: Densities of parvalbumin-immunoreactive neurons in non-malformed hippocampal sclerosis-temporal neocortex and in cortical dysplasias. Brain Res Bull 2006; 68(6):474-481.

(244) Ortinski PI, Dong J, Mungenast A, Yue C, Takano H, Watson DJ, Haydon PG, Coulter DA: Selective induction of astrocytic gliosis generates deficits in neuronal inhibition. Nat Neurosci 2010; 13(5):584-591.

(245) van der Zijden JP, van Eijsden P, de Graaf RA, Dijkhuizen RM: 1H/13C MR spectroscopic imaging of regionally specific metabolic alterations after experimental stroke. Brain 2008; 131(Pt 8): 2209-2219.

(246) van Eijsden P., Behar KL, Mason GF, Braun KP, de Graaf RA: In vivo neurochemical profiling of rat brain by 1H-{13C} NMR spectroscopy: cerebral energetics and glutamatergic/GABAergic neurotransmission. J Neurochem 2010; 112(1):24-33.

(247) Pfeuffer J, Tkac I, Provencher SW, Gruetter R: Toward an in vivo neurochemical profile: quantification of 18 metabolites in short-echo-time (1)H NMR spectra of the rat brain. J Magn Reson 1999; 141(1):104-120.

(248) Behar KL, Petroff OA, Prichard JW, Alger JR, Shulman RG: Detection of metabolites in rabbit brain by 13C NMR spectroscopy following administration of {1-13C}glucose. Magn Reson Med 1986; 3(6):911-920.

(249) Rothman DL, Behar KL, Hetherington HP, den Hollander JA, Bendall MR, Petroff OA, Shulman RG: 1H-Observe/13C-decouple spectroscopic measurements of lactate and glutamate in the rat brain in vivo. Proc Natl Acad Sci U S A 1985; 82(6):1633-1637.

(250) Rothman DL, Novotny EJ, Shulman GI, Howseman AM, Petroff OA, Mason G, Nixon T, Hanstock CC, Prichard JW, Shulman RG: 1H-{13C} NMR measurements of {4-13C}glutamate turnover in human brain. Proc Natl Acad Sci U S A 1992; 89(20):9603-9606.

(251) Gruetter R, Novotny EJ, Boulware SD, Mason GF, Rothman DL, Shulman GI, Prichard JW, Shulman RG: Localized 13C NMR spectroscopy in the human brain of amino acid labeling from D-{1-13C}glucose. J Neurochem 1994; 63(4):1377-1385.

(252) Gruetter R, Seaquist ER, Ugurbil K: A mathematical model of compartmentalized neurotransmitter metabolism in the human brain. Am J Physiol Endocrinol Metab 2001; 281(1):E100-E112.

(253) Mason GF, Gruetter R, Rothman DL, Behar KL, Shulman RG, Novotny EJ: Simultaneous determination of the rates of the TCA cycle, glucose utilization, alpha-ketoglutarate/glutamate exchange, and glutamine synthesis in human brain by NMR. J Cereb Blood Flow Metab 1995; 15(1):12-25.

(254) Shen J, Petersen KF, Behar KL, Brown P, Nixon TW, Mason GF, Petroff OA, Shulman GI, Shulman RG, Rothman DL: Determination of the rate of the glutamate/glutamine cycle in the human brain by in vivo 13C NMR. Proc Natl Acad Sci U S A 1999; 96(14):8235-8240.

(255) Fitzpatrick SM, Hetherington HP, Behar KL, Shulman RG: The flux from glucose to glutamate in the rat brain in vivo as determined by 1H-observed, 13C-edited NMR spectroscopy. J Cereb Blood Flow Metab 1990; 10(2):170-179.

(256) Mason GF, Behar KL, Rothman DL, Shulman RG: NMR determination of intracerebral glucose concentration and transport kinetics in rat brain. J Cereb Blood Flow Metab 1992; 12(3):448-455.

(257) Sibson NR, Mason GF, Shen J, Cline GW, Herskovits AZ, Wall JE, Behar KL, Rothman DL, Shulman RG: In vivo (13)C NMR measurement of neurotransmitter glutamate cycling, anaplerosis and TCA cycle flux in rat brain during. J Neurochem 2001; 76(4):975-989.

(258) Henry PG, Russeth KP, Tkac I, Drewes LR, Andrews MT, Gruetter R: Brain energy metabolism and neurotransmission at near-freezing temperatures: in vivo (1)H MRS study of a hibernating mammal. J Neurochem 2007; 101(6):1505-1515.

(259) Deelchand DK, Shestov AA, Koski DM, Ugurbil K, Henry PG: Acetate transport and utilization in the rat brain. J Neurochem 2009; 109 Suppl 1:46-54.

(260) Deelchand DK, Nelson C, Shestov AA, Ugurbil K, Henry PG: Simultaneous measurement of neuronal and glial metabolism in rat brain in vivo using co-infusion of {1,6-13C2}glucose and {1,2-13C2}acetate. J Magn Reson 2009; 196(2):157-163.

(261) Chen W, Zhu XH, Gruetter R, Seaquist ER, Adriany G, Ugurbil K: Study of tricarboxylic acid cycle flux changes in human visual cortex during hemifield visual stimulation using (1)H-{(13)C} MRS and fMRI. Magn Reson Med 2001; 45(3):349-355.

(262) Chhina N, Kuestermann E, Halliday J, Simpson LJ, Macdonald IA, Bachelard HS, Morris PG: Measurement of human tricarboxylic acid cycle rates during visual activation by (13)C magnetic resonance spectroscopy. J Neurosci Res 2001; 66(5):737-746.

(263) Patel AB, de Graaf RA, Mason GF, Kanamatsu T, Rothman DL, Shulman RG, Behar KL: Glutamatergic neurotransmission and neuronal glucose oxidation are coupled during intense neuronal activation. J Cereb Blood Flow Metab 2004; 24(9):972-985.

(264) Sibson NR, Dhankhar A, Mason GF, Behar KL, Rothman DL, Shulman RG: In vivo 13C NMR measurements of cerebral glutamine synthesis as evidence for glutamate-glutamine cycling. Proc Natl Acad Sci U S A 1997; 94(6):2699-2704.

(265) Mason GF, Petersen KF, de Graaf RA, Shulman GI, Rothman DL: Measurements of the anaplerotic rate in the human cerebral cortex using 13C magnetic resonance spectroscopy and {1-13C} and {2-13C} glucose. J Neurochem 2007; 100(1):73-86.

(266) Bluml S, Moreno-Torres A, Shic F, Nguy CH, Ross BD: Tricarboxylic acid cycle of glia in the in vivo human brain. NMR Biomed 2002; 15(1):1-5.

(267) Lebon V, Petersen KF, Cline GW, Shen J, Mason GF, Dufour S, Behar KL, Shulman GI, Rothman DL: Astroglial contribution to brain energy metabolism in humans revealed by 13C nuclear magnetic resonance spectroscopy: elucidation of the dominant pathway for neurotransmitter glutamate repletion and measurement of astrocytic oxidative metabolism. J Neurosci 2002; 22(5):1523-1531.

(268) Boumezbeur F, Besret L, Valette J, Gregoire MC, Delzescaux T, Maroy R, Vaufrey F, Gervais P, Hantraye P, Bloch G, Lebon V: Glycolysis versus TCA cycle in the primate brain as measured by combining 18F-FDG PET and 13C-NMR. J Cereb Blood Flow Metab 2005; 25(11):1418-1423.

(269) Pfeuffer J, Tkac I, Choi IY, Merkle H, Ugurbil K, Garwood M, Gruetter R: Localized in vivo 1H NMR detection of neurotransmitter labeling in rat brain during infusion of {1-13C} D-glucose. Magn Reson Med 1999; 41(6):1077-1083.

(270) Yang J, Li SS, Bacher J, Shen J: Quantification of cortical GABA-glutamine cycling rate using in vivo magnetic resonance signal of {2-13C}GABA derived from glia-specific substrate {2-13C}acetate. Neurochem Int 2007; 50(2):371-378.

(271) de Graaf RA, Patel AB, Rothman DL, Behar KL: Acute regulation of steady-state GABA levels following GABA-transaminase inhibition in rat cerebral cortex. Neurochem Int 2006; 48(6-7): 508-514.

(272) Adriany G, Gruetter R: A half-volume coil for efficient proton decoupling in humans at 4 tesla. J Magn Reson 1997; 125(1):178-184.

(273) de Graaf RA, Nicolay K: Adiabatic water suppression using frequency selective excitation. Magn Reson Med 1998; 40(5):690-696.

(274) Tannus A, Garwood M: Improved performance of frequency-swept pulses using offset-independent adiabaticity. J Magn Reson 1996; 120:133-137.

(275) Fujiwara T, Nagayama K: Fujiwara T. and Nagayama K. (1988) Composite inversion pulses with frequency switching and their application to broadband decoupling. J Magn Reson Imaging 1988; 77:53-63.

(276) de Graaf RA: Theoretical and experimental evaluation of broadband decoupling techniques for in vivo nuclear magnetic resonance spectroscopy. Magn Reson Med 2005; 53(6):1297-1306.

(277) Mescher M, Merkle H, Kirsch J, Garwood M, Gruetter R: Simultaneous in vivo spectral editing and water suppression. NMR Biomed 1998; 11(6):266-272.

(278) Ratiney H, Sdika M, Coenradie Y, Cavassila S, van OD, Graveron-Demilly D: Time-domain semi-parametric estimation based on a metabolite basis set. NMR Biomed 2005; 18(1):1-13.

(279) Mason GF, Falk PK, de Graaf RA, Kanamatsu T, Otsuki T, Shulman GI, Rothman DL: A comparison of (13)C NMR measurements of the rates of glutamine synthesis and the tricarboxylic acid cycle during oral and intravenous administration of {1-(13)C}glucose. Brain Res Brain Res Protoc 2003; 10(3):181-190.

(280) Alcolea A, Carrera J, Medina A. A hybrid Marquardt-simulated annealing method for solving the groundwater inverse problem. Proceedings of the ModelCARE 99 Conference , 157-163. 1999. Zürich, Switzerland, IAHS publishing.
Ref Type: Conference Proceeding

(281) Storm-Mathisen J, Leknes AK, Bore AT, Vaaland JL, Edminson P, Haug FM, Ottersen OP: First visualization of glutamate and GABA in neurones by immunocytochemistry. Nature 1983; 301(5900):517-520.

(282) Chaudhry FA, Lehre KP, van Lookeren CM, Ottersen OP, Danbolt NC, Storm-Mathisen J: Glutamate transporters in glial plasma membranes: highly differentiated localizations revealed by quantitative ultrastructural immunocytochemistry. Neuron 1995; 15(3):711-720.

(283) Mason GF, Martin DL, Martin SB, Manor D, Sibson NR, Patel A, Rothman DL, Behar KL: Decrease in GABA synthesis rate in rat cortex following GABA-transaminase inhibition correlates with the decrease in GAD(67) protein. Brain Res 2001; 914(1-2):81-91.

(284) de Graaf RA, Mason GF, Patel AB, Rothman DL, Behar KL: Regional glucose metabolism and glutamatergic neurotransmission in rat brain in vivo. Proc Natl Acad Sci U S A 2004; 101(34): 12700-12705.

(285) Preece NE, Cerdan S: Metabolic precursors and compartmentation of cerebral GABA in vigabatrin-treated rats. J Neurochem 1996; 67(4):1718-1725.

(286) van der Hel WS, van Eijsden P, Bos IWM, de Graaf RA, Behar KL, van NO, de Graan PN, Braun KP. In vivo MR spectroscopy and histochemistry of status epilepticus induced hippocampal pathology in a juvenile model of temporal lobe epilepsy. Submitted. 2011.

(287) Eloqayli H, Dahl CB, Gotestam KG, Unsgard G, Hadidi H, Sonnewald U: Pentylenetetrazole decreases metabolic glutamate turnover in rat brain. J Neurochem 2003; 85(5):1200-1207.

(288) Qu H, Eloqayli H, Muller B, Aasly J, Sonnewald U: Glial-neuronal interactions following kainate injection in rats. Neurochem Int 2003; 42(1):101-106.

(289) Alvestad S, Hammer J, Eyjolfsson E, Qu H, Ottersen OP, Sonnewald U: Limbic structures show altered glial-neuronal metabolism in the chronic phase of kainate induced epilepsy. Neurochem Res 2008; 33(2):257-266.

(290) Eid T, Ghosh A, Wang Y, Beckstrom H, Zaveri HP, Lee TS, Lai JC, Malthankar-Phatak GH, de Lanerolle NC: Recurrent seizures and brain pathology after inhibition of glutamine synthetase in the hippocampus in rats. Brain 2008; 131(Pt 8):2061-2070.

Nederlandse samenvatting

Nederlandse samenvatting

Inleiding

Temporaalkwab epilepsie (TLE) wordt gekenmerkt door epileptische aanvallen die ontstaan in de slaapkwab. Deze aanvallen gaan vaak gepaard met een onprettig opstijgend gevoel vanuit de maagstreek, smakken en automatismen. Ook kan er een stoornis van het bewustzijn en het geheugen optreden. Meestal ontstaan deze aanvallen in de hippocampus, een structuur die diep in de slaapkwab gelegen is. Omdat chirurgie een uitstekende behandeloptie is voor dit type epilepsie is, kunnen we de chirurgisch verwijderde hippocampi bestuderen. Hierdoor weten we dat deze bij patienten verlittekend is. Deze hippocampale sclerose (HS) wordt gekenmerkt door dood van zenuwcellen, woekering van steuncellen (glia) en nieuwe verkeerd aangelegd verbindingen tussen de overlevende zenuwcellen.

Het blijkt dat TLE patienten in 30-60% van de gevallen een episode van langdurige koortsstuipen of een langdurig epileptisch insult hebben doorgemaakt in de vroege jeugd. Ook andere aandoeningen die schade in de hersenen kunnen aanrichten, komen vaker voor bij deze patiënten. De TLE manifesteert zich echter pas jaren later. Dit doet het vermoeden rijzen dat er sprake is van een langzaam ontwikkelende ziekte die start met hersenschade in de vroege jeugd en zich voor het eerst uit met de spontane epileptische aanvallen. Daarna lijkt de ontwikkeling van de ziekte niet te stoppen, want bij 30-40% van de patienten werken medicijnen in eerste instantie goed, maar komen de insulten later toch terug, ondanks het gebruik van deze medicijnen.

Het probleem met het onderzoek dat tot nu toe gedaan is bij epilepsiepatiënten is dat de gevonden afwijkingen in bijvoorbeeld het hippocampusweefsel zowel de oorzaak, als het gevolg van de epilepsie zouden kunnen zijn. Om deze reden ligt de focus van dit proefschrift op de fase voor het eerste insult, ook wel de latente fase genoemd. Dit is uiteraard alleen mogelijk in diermodellen van epilepsie. Er is gekozen voor het juveniele lithium-pilocarpine model, waarbij lithium en pilocarpine worden gebruikt om een insult te induceren in een rat van 21 dagen oud. Na 10-16 weken ontstaan dan spontane insulten. In de tussenliggende periode kan ons onderzoek plaatsvinden. Dit diermodel heeft overeenkomsten met die in de patienten met TLE op het gebied van de ziekte-

ontwikkeling, het ontwikkelingsstadium (leeftijd), als op het gebied van de afwijkingen die gevonden worden in de hippocampus.

Connectiviteit

De afwijkende hersenactiviteit in de hippocampus bij TLE patienten kan alleen leiden tot de waarneembare symptomen als deze wordt voortgeleid naar omliggende en soms zelfs afgelegen delen van de hersenen. Uit geavanceerde MRI scans bij TLE patiënten blijkt dat deze verbindingen, ook wel de witte stof genoemd, zowel dichtbij de epileptische bron, als daar ver vandaan, zijn aangedaan. Opnieuw is onduidelijk of dit een oorzaak of gevolg is van de epilepsie. Bovendien is onduidelijk wat nu het onderliggende probleem op celniveau is dat deze MRI afwijkingen veroorzaakt. *Daarom is het eerste doel van dit proefschrift om de ontwikkeling van witte stofveranderingen na het initiële pilocarpine geïnduceerde insult te vervolgen en deze veranderingen op cellulair niveau te karakteriseren.*

Connectiviteit en neurotransmissie

De zenuwcellen in de hippocampus communiceren met elkaar via de bovengenoemde verbindingen in de witte stof, maar ook via de zogenaamde synaptische signaaloverdracht. Deze signaaloverdracht geschied via neurotransmitters: chemische verbindingen die door de pre-synaptische zenuwcel worden uitgescheiden en een signaal induceren in de postpost-synaptische zenuwcel. In de hippocampus wordt glutamaat als neurotransmitter gebruikt om een positief of exciterend signaal op te wekken en GABA om een negatief of remmend signaal op te wekken. Een logische gevolgtrekking is dat bij epilepsie een onbalans is ontstaan tussen deze twee neurotransmitters en dit is ook aangetoond in TLE patiënten. Opnieuw is onduidelijk of dit probleem al aanwezig is voor de epileptische insulten beginnen, maar er zijn aanwijzingen dat er in die latente fase in ieder geval al een gebrek aan GABA is ontstaan. *Het tweede doel van dit proefschrift is om in de latente fase de neurotransmitterbalans te karakteriseren.*

Een onbalans in het neurotransmitterevenwicht kan worden veroorzaakt doordat de zenuwcellen die de betreffende neurotransmitters afgeven, afgestorven zijn, maar ook doordat de overlevende cellen niet meer in staat zijn de neurotransmitters in voldoende hoeveelheden en met voldoende snelheid te produceren. Deze turnover van neurotransmitters valt te meten met ^{1}H-[^{13}C] magnetic resonance spectroscopy (MRS). Helaas is het met de huidige methoden niet mogelijk de turnover van de relatief lage GABA concentratie te meten. *Daarom is het derde doel van dit proefschrift de beschikbare technieken te optimaliseren in een poging de GABA turnover in het gezonde rattenbrein te meten.*

Indien dit doel is bereikt, wordt het mogelijk de neurotransmitter balans volledig te karakteriseren, zowel wat betreft de concentraties van de glutamaat en GABA als van hun turnover. *Het vierde doel van dit proefschrift is daarom om een volledige beschrijving te geven van de excitatoire en inhibitoire neurotransmissie in de hippocampus tijdens het ontstaan van epilepsie.*

Verkenning

Hoofdstuk 3 beschrijft een studie in volwassen ratten direct na injectie met lithium en pilocarpine. Het doel van deze studie was te laten zien dat we met MRI en MRS verandering in de epileptische rattenhippocampus kunnen vastleggen. We hebben ervoor gekozen een aantal verschillende technieken te combineren die het mogelijk maakten, zowel veranderingen in structuur, als in metabolisme aan te tonen. Er werden inderdaad veranderingen aangetoond en deze duidden op een tekort aan zuurstof in de overactieve hippocampus en op het ontstaan van cellulaire schade in een aantal belangrijke structuren van de temporaalkwab. Deze studie liet zien dat tekort aan zuurstof en cellulaire schade in de eerste minuten tot uren na een insult ontstaan en wij vermoeden dat dit het begin is van het pathologische proces dat uiteindelijk kan leiden tot spontane aanvallen in dit diermodel.

Witte stof pathologie

Na deze initiele verkenning hebben we onze aandacht gericht op de chronische veranderingen in de witte stof. **Hoofdstuk 4** past in een serie recente studies die het idee ondermijnen dat epilepsie een ziekte van de grijze stof is. In deze studie combineren we diffusion tensor imaging (DTI), een MRI techniek die het mogelijk maakt om de richting en dikte van witte stof banen zichtbaar te maken, met histologie om de cellulaire achtergrond van de DTI veranderingen te duiden. Deze studie werd uitgevoerd op vier en acht weken na injectie met pilocarpine, voordat spontane insulten werden gezien. Witte stof bestaat grofweg uit twee onderdelen, het axon en de omhullende myeline. De resultaten wezen er duidelijk op dat er schade optrad aan de myeline, terwijl er geen veranderingen werden gevonden in de axonale component. Hiermee werd aangetoond dat een geïsoleerde status epilepticus, zoals geinduceerd met pilocarpine, voldoende is om langdurig en wijdverspreid veranderingen teweeg te brengen in de myeline. De veranderingen in de DTI parameters, die wij vonden, waren echter anders dan de veranderingen die zijn aangetoond bij TLE patienten. Het is mogelijk dat de veranderingen die wij vinden een vroege fase representeren van hetzelfde proces, maar het is ook mogelijk dat de status epilepticus het normale myelinisatieproces, dat nog niet is voltooid bij ratten op deze leeftijd, heeft verstoord en vertraagd. Deze twee verklaringen kunnen evenwel aanvullend in plaats van conflicterend zijn. In de fornix, de belangrijkste structuur die informatie vanaf de hippocampus naar de rest van het brein vervoerd, werden veranderingen aangetroffen die progressief van aard zijn en een gevolg kunnen zijn van de celdood in de hippocampus zelf, waardoor de afvoerende banen hun nut verliezen. Daarnaast kan dit ook een veroorzakende factor zijn in de epilepsie, omdat is aangetoond dat doorsnijding van de fornix kan leiden tot epileptische ontladingen in de hippocampus.

Neurotransmissie

In **hoofdstuk 5** wordt een poging ondernomen de neurotransmitterbalans in de pre-epileptische hippocampus in kaart te brengen met MRS en histologie. De resultaten wezen op globale dood van zenuwcellen in de hippocampus en gliose, waarmee werd aangetoond dat deze kenmerken van HS al voor het ontstaan van spontane insulten aanwezig zijn in de hippocampus. Verder werd er een daling gevonden van de glutamaat concentratie, maar een veel sterke daling van de GABA concentratie. Aanvullende histologische kleuringen lieten zien dat er sprake was van specifiek uitgesproken celdood van de zenuwcellen die GABA produceren. Een onverwachte bevinding was de tijdelijke stijging van de glutamine concentratie op vier weken na de injectie met pilocarpine. Deze stijging normaliseerde op acht weken. Glutamine wordt in het metabolisme gebruikt als basis voor het maken van zowel GABA als glutamaat, onder invloed van het enzym glutamine synthetase (GS). Verder toonden we aan dat de normalisering van de glutamine concentratie gepaard ging met een daling van de GS activiteit.

Deze resultaten leidden tot de nieuwe hypothese dat de initiele stijging van de glutamine concentratie een onbalans in het neurotransmittermetabolisme weerspiegelde, waarbij de normalisatie vier weken later een verschuiving naar een nieuw evenwicht representeerde. Het onderliggende mechanisme zou kunnen zijn dat de dood van zenuwcellen leidt tot minder vraag naar glutamine voor de synthese van GABA en glutamaat en dus ophoping van glutamine. Door het verminderen van de GS activiteit, lukt het de gliacel, waar de glutamine wordt opgeslagen, om deze concentratie weer naar het normale peil te brengen.

Om deze hypothese verder te onderbouwen wilden wij graag het neurotransmitter metabolisme in de hippocampus volledig in kaart brengen. Het was echter op dat moment niet mogelijk het GABA metabolisme te meten vanwege de relatief lage concentratie van GABA. In **hoofdstuk 6** wordt beschreven dat dit ons uiteindelijk toch gelukt is door optimalisatie van bestaande technieken en de inzet van een geavanceerde 9.4 T MRI scanner, die specifiek geschikt is voor kleine proefdieren. Met de zogenaamde indirecte ^{1}H-observed, ^{13}C-edited (^{1}H-[^{13}C]) MRS en infusie van met het 13C isotoop gelabelde glucose en acetaat werd de inbouw van dit isotoop in GABA zichtbaar gemaakt en gekwantificeerd.

Deze techniek wordt vervolgens in **hoofdstuk 7** toegepast in de pre-epileptische hippocampus van de pilocarpine geinjecteerde rat. Deze studie liet zien dat de energiehuishouding in alle zenuwcellen verlaagd is, maar dat de neurotransmitter productie met name in de cellen die GABA produceren is verlaagd. Ook werd aangetoond dat het enzym dat de productie van GABA verzorgd verlaagd is. Hiermee wordt duidelijk dat de cellen die GABA produceren niet alleen relatief vaker doodgaan na een ernstig epileptisch insult, maar ook op de lange termijn niet meer goed in staat zijn om GABA te produceren. Daarnaast werd aangetoond dat de GS activiteit al daalt voordat de spontane insulten zich voordoen.

Synthese

In deze paragraaf proberen we de gevonden resultaten samen te voegen tot een coherente visie op het ontstaan van epilepsie. De hele cascade wordt in werking gezet met een gebeurtenis waarbij in kwetsbare gebieden celschade optreedt. In de hippocampus lijken de GABA producerende cellen kwetsbaarder te zijn dan de glutamaat producerende cellen, waardoor een onbalans ontstaat. In de periode daarna wordt getracht de schade te herstellen, waarbij de afzetting van nieuwe myeline doorgaat, maar vertraging heeft opgelopen. Bovendien worden er nieuwe verbindingen gevormd. Een deel van deze nieuwe verbindingen wordt gevormd op plaatsen waar dat minder wenselijk is omdat netwerken ontstaan die makkelijk kunnen ontregelen. Bovendien is de remmende werking van GABA op dergelijke netwerken nu deels weggevallen. Dit alles schept de voorwaarden voor het ontstaan van epilepsie, maar is mogelijk nog niet voldoende. Ook op cellulair metabool niveau vinden aanpassingen plaats. Doordat er minder GABA en glutamaat nodig is, hoopt hun metabole voorloper, glutamine, zich op. De hippocampus brengt deze concentratie naar beneden door het enzym dat nodig is voor het maken van glutamine te verlagen. Bij kunstmatige verlaging van de GS activiteit in gezonde dieren is aangetoond dat dit leidt tot verminderde remming in de hippocampus. Deze stap zou een laatste kunnen zijn op weg naar spontane insulten. Deze nieuwe insulten leiden tot een nieuwe cascade, waarmee verklaart wordt dat TLE patienten vaak in eerste instantie wél, maar later niet meer behandeld kunnen worden met medicatie.

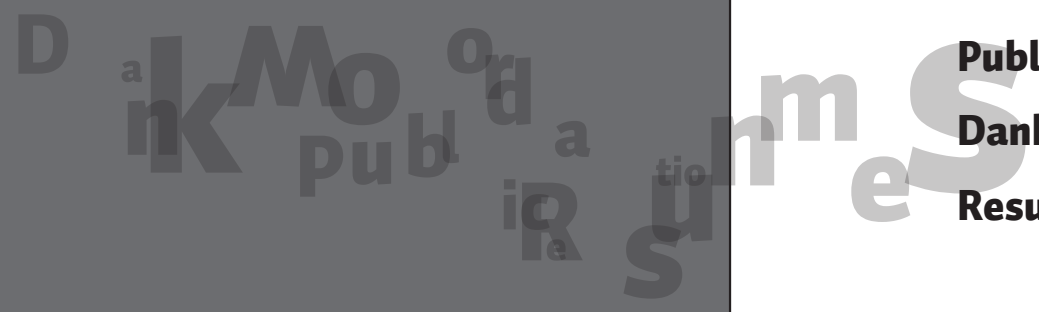

Publications

(1) Braun, K. P.; van, E. P.; Vandertop, W. P.; de Graaf, R. A.; Gooskens, R. H.; Tulleken, K. A.; Nicolay, K. Cerebral Metabolism in Experimental Hydrocephalus: an in Vivo 1H and 31P Magnetic Resonance Spectroscopy Study. J. Neurosurg. 1999, 91, 660-668.

(2) van Eijsden, P.; Braun, K. P.; Vandertop, W. P.; Gooskens, R. H.; Gispen, W. H.; Biessels, G. Visual Evoked Potentials and Brainstem Auditory Evoked Potentials in Experimental Hydrocephalus. Eur. J. Pediatr. Surg. 2000, 10 Suppl 1, 47-48.

(3) Biessels, G. J.; Braun, K. P.; de Graaf, R. A.; van, E. P.; Gispen, W. H.; Nicolay, K. Cerebral Metabolism in Streptozotocin-Diabetic Rats: an in Vivo Magnetic Resonance Spectroscopy Study. Diabetologia 2001, 44, 346-353.

(4) van Eijsden, P.; Notenboom, R. G.; Wu, O.; de Graan, P. N.; van, N. O.; Nicolay, K.; Braun, K. P. In Vivo 1H Magnetic Resonance Spectroscopy, T2-Weighted and Diffusion-Weighted MRI During Lithium-Pilocarpine-Induced Status Epilepticus in the Rat. Brain Res. 2004, 1030, 11-18.

(5) van der Zijden, J. P.; van Eijsden, P.; de Graaf, R. A.; Dijkhuizen, R. M. 1H/13C MR Spectroscopic Imaging of Regionally Specific Metabolic Alterations After Experimental Stroke. Brain 2008, 131, 2209-2219.

(6) van Eijsden P.; Veldink, J. H.; Linn, F. H.; Scheltens, P.; Biessels, G. J. Progressive Dementia and Mesiotemporal Atrophy on Brain MRI: Neurosyphilis Mimicking Pre-Senile Alzheimer's Disease? Eur. J. Neurol. 2008, 15, e14-e15.

(7) Zijlmans, M.; van Eijsden, P.; Ferrier, C. H.; Kho, K. H.; van Rijen, P. C.; Leijten, F. S. Illusory Shadow Person Causing Paradoxical Gaze Deviations During Temporal Lobe Seizures. J. Neurol. Neurosurg. Psychiatry 2009, 80, 686-688.

(8) van Eijsden, P.; Hyder, F.; Rothman, D. L.; Shulman, R. G. Neurophysiology of Functional Imaging. Neuroimage. 2009, 45, 1047-1054.

(9) van Eijsden, P.; Baayen, J. C.; De Witt Hamer, P. C. Commentaar Op "Stand Van Zaken: Epilepsie Van Aanval Tot Zorg". Nederlands Tijdschrift voor Geneeskunde 2009, 153.

(10) van Eijsden P.; Behar, K. L.; Mason, G. F.; Braun, K. P.; de Graaf, R. A. In Vivo Neurochemical Profiling of Rat Brain by 1H-[13C] NMR Spectroscopy: Cerebral Energetics and Glutamatergic/GABAergic Neurotransmission. J. Neurochem. 2010, 112, 24-33.

(11) van Eijsden, P.; Peerdeman, S. M. Het Frontale Meningeoom. Medisch Contact 2010, 64, 129.

(12) van Eijsden, P.; Otte, W. M.; Braun, K. P.; Dijkhuizen, R. M. MR Beeldvorming En Spectroscopie Bij Experimentele Epilepsie. Epilepsie: Periodiek voor professionals 2010, 8, 38-41.

(13) van Eijsden, P.; Otte, W. M.; van der Hel, W. S.; van Nieuwenhuizen, O.; Dijkhuizen, R. M.; de Graaf, R. A.; Braun, K. P. In Vivo Diffusion Tensor Imaging and Ex Vivo Histological Characterization of White Matter Pathology in a Post Status Epilepticus Model of Temporal Lobe Epilepsy. Epilepsia, 2011, 52(3)

(14) van Eijsden, P.; de Graaf, R. A.; Bagga, P.; Behar, K. L.; Mason, G. F.; van Nieuwenhuizen, O.; de Graan, P. N.; Braun, K. P. Chronic Status Epilepticus Induced Changes in Hippocampal Energy and Neurotransmitter Metabolism. Submitted.

(15) van der Hel, W. S.; Bos, I. W. M.; Mulder, S.; Verlinde S.A.M.W.; van Eijsden, P.; de Graan, P. N. Decreased Hippocampal Glutamine Synthetase Expression in the Juvenile Rat Li+/Pilocarpine Model and in Human Temporal Lobe Epilepsy. Submitted.

(16) van der Hel, W. S.; van Eijsden, P.; Bos, I. W. M.; de Graaf, R. A.; Behar, K. L.; van, N. O.; de Graan, P. N.; Braun, K. P. In vivo MR spectroscopy and histochemistry of status epilepticus induced hippocampal pathology in a juvenile model of temporal lobe epilepsy. Submitted.

(17) van Eijsden, P.; Shulman, R. G.; van Gijn, J. Localizing Modules of Mind? An Historical Perspective on Cognitive Neuroimaging. Submitted.

(18) van Eijsden, P.; Buis, D. R.; Vandertop, W. P. Chronic Subdural Hematoma of the Spine Mimicking Meningitis. Submitted.

Dankwoord

Kees Braun – Beste Kees, we kennen elkaar nu ongeveer 14 jaar….. Dat moet even bezinken. Ik ben bij je begonnen als student, waarbij ik een groot deel van jouw promotie-onderzoek heb meegemaakt. Daarna zijn we samen doorgegaan met een NEF aanvraag voor mijn promotie-onderzoek. In al die 14 jaar heb je me nooit teleurgesteld. Correcties kwamen altijd binnen 48 uur, en al was het soms alsof je een bloedneus had gehad, er was altijd grondig naar gekeken en het eindresultaat werd beter. Je gedrevenheid, energie, creativiteit en enthousiasme zijn bepalend geweest voor dit succes en ik benijd je om die eigenschappen. Daarnaast klikt het op persoonlijk vlak erg goed. Daarom hoop ik dat we in de toekomst kunnen blijven samenwerken en in ieder geval goed contact blijven houden.

Robin de Graaf – Beste Robin, wij kennen elkaar ook al uit de tijd dat ik als student met Kees meeliep. Je cum laude proefschrift met daarnaast een standaardwerk over "*in vivo* NMR spectroscopy" was legendarisch. Het was dus niet verwonderlijk dat je naar één van de beste MR centra van de wereld verhuisde en het was voor mij dus een grote eer om daar met je te kunnen samenwerken. Je bent in staat om binnen een mum van tijd een NMR experiment in elkaar te zetten en beheerst alle aspecten van deze experimenten van de hardware tot de duiding van de resultaten. Hierbij weet je bescheiden te blijven. Het moet moeilijk zijn geweest om met een arts te werken, die toch eigenlijk niet altijd begrijpt hoe het zit, maar je hebt dat goed verborgen weten te houden.

Professor van Nieuwenhuizen – Beste Onno, ik ken je misschien nog wel het langst van iedereen, omdat je in mijn eerste studiejaar een practicum "neurologisch onderzoek" hebt gegeven. Zoals altijd wist je er een mooie show van te maken. Later heb ik bij je op de afdeling rondgelopen als co-assistent en AGNIO en heb ik genoten van je prachtige impersonaties. Je bent een begeleider op afstand geweest, maar altijd benaderbaar en ik ben blij dat je mijn promotor bent geweest. Je weet hoe het spel gespeeld wordt en dat is goud waard. Ondanks dat je afscheid aanstaande is, hoop ik dat we nog contact kunnen houden over wederzijdse interesses.

Pierre de Graan – Beste Pierre, vanuit het RMI was je betrokken bij de opzet van dit onderzoek en de NEF aanvraag. We hebben gekozen voor het diermodel waar jij ervaring mee had. Later bleek ons onderzoek perfect aan te sluiten bij het onderzoek van jouw onderzoeker, Saskia van der Hel. Jij verzorgde de histologische en neurowetenschappelijke kennis die de andere betrokkenen misten en wist het geheel zo naar een hoger plan te tillen.

Rick Dijkhuizen – Beste Rick, ik kwam via een mede-student bij jou terecht voor een wetenschappelijke stage. Je had op dat moment echter al een student, de al eerder genoemde Saskia van der Hel, en verwees me door naar je beste vriend Kees Braun (zie zijn dankwoord). Hiermee ben jij de verbindende factor tussen vrijwel alle cruciale betrokkenen bij dit proefschrift. Vanwege onze gezamenlijke interesse in het wielrennen hebben we met name buiten het lab met elkaar te maken gehad en daarom beschouw ik mezelf nu óók als jouw beste vriend. Je hebt een onweerstaanbaar gevoel voor humor en je deur staat altijd open voor een goed gesprek. Ondanks dat jouw wetenschappelijke interesse op een ander terrein ligt (stroke), heb ik toch met je mogen samenwerken bij een aantal projecten, zoals het onderzoek van Jet van der Zijden, Maurits van Meer en Wim Otte. Hierin heb ik je leren kennen als een échte wetenschapper met een hypothesegestuurde aanpak, overzicht en het vermogen te abstraheren tot de essentie. Ik hoop dat we in de toekomst zowel privé als professioneel nog veel met elkaar te maken hebben.

Professor Nicolay – Beste Klaas, als promotor van "de gouden driehoek" Kees-Robin-Rick, en begeleider van mijn eerste stapjes in de wetenschap, sta ook jij aan de basis van dit proefschrift. Dat je in mijn beoordelingscommissie zit, maakt de cirkel rond. Het is tekenend dat ik van jou als eerste en wel binnen anderhalve week een email kreeg dat je mijn proefschrift had gelezen en positief had beoordeeld. Je had er misschien ook al wel een tijd op zitten wachten…..

Saskia van der Hel – Beste Saskia, je bent al twee keer genoemd. Ik kwam je tegen toen jij student was bij Rick en ik bij Kees. Veel lichamelijk ongemak later kwamen we elkaar tegen in het promotie-onderzoek, waarbij jouw studies perfect bleken aan te sluiten op de mijne. Logischerwijze leidde dit tot gezamenlijke papers. Daarnaast was het ook buitengewoon prettig om met je samen te werken. De toevoeging… "the first two authors contributed equally", slaat daarmee dus inderdaad uitsluitend op onze gelijkwaardige bijdrage.

Kevin Behar – Dear Kevin, you are an endless source of knowledge on the intricate workings of the chemistry of the brain. No detail escapes you and you have been invaluable in the interpretation of the POCE data.

Graeme Mason – Dear Graeme, I have spent many hours working with your program CWave, needing your help to get everything to work properly. In the end it always did, because it is a great tool. You were very patient with me, while I am sure you had better things to do.

Professor Shulman – Dear Bob, in the end you could not make it to the thesis defense. This is unfortunate, but understandable. I am happy to have worked with you and have been able to learn from your ideas both scientifically and philosophically. I am proud to have helped you a little bit with two of your books and am looking forward to the publication of the latest of these. I hope we'll be able to keep in touch.

Bei Wang, Xiaoxian Man and all my dear rats - Dear Bei and Xiaoxian, you have prepared many animals for me, both quickly and skillfully. As a future neurosurgeon, I can only admire the dexterity and knowledge you both have.

Gerard van Vliet – Beste Gerard, je bent waarschijnlijk de meest onmisbare persoon op het in vivo NMR lab. Met je droge humor en kijk op de zaken, ben je een prettige collega. Dank voor je hulp bij het opzetten van de experimenten die ik bij jullie heb gedaan.

Jet van der Zijden – Beste Jet, je was een mooie afleiding in New Haven. Je werkte hard en doelgericht, maar er was ook altijd tijd voor een grap…. We hebben samen een mooi paper afgeleverd, met veel input van Rick en Robin uiteraard. Je bent waarschijnlijk één van de weinigen die de frustratie van de LCModel analyses net als ik heb gevoeld.

Maurits van Meer – Beste Maurits, je was een mooie afleiding in New Haven (en Boston). Je werkte hard, maar totaal niet doelgericht…. Ik moet altijd vreselijk met en om je lachen, net als jijzelf. Een fantastische zwartgallige kijk op de wereld, de wetenschap en jezelf, gecombineerd met een oneindige hoeveelheid energie, waardoor je er telkens weer vol tegenaan kan gaan. Je promoveert toch net een klein weekje voor me en hebt dus bewezen het bij het verkeerde eind te hebben ("Dit wordt dus nooit wat, deze bodemloze put van een promotie")…. Veel succes in je baan als radioloog. We komen elkaar vast weer tegen bij hardloopwedstrijden, op de fiets, in de wetenschap of in de kliniek.

Wim Otte – Beste Wim, mijn opvolger. Pieter van Eijsden 2.0… nieuwer, sneller en beter met de computer. Dit wordt een prachtig promotietraject en ik hoop er een beetje bij betrokken te zijn. Onderkoeld cynisme met veel zelfspot, een ideale combinatie met de vrolijke zwartgalligheid van Maurits.

Wouter Veldhuis – Beste Wouter, "Strangely parallel lives", zo heb ik het wel eens omschreven. We zaten in hetzelfde practicumgroepje, zijn zonder het van elkaar te weten met hetzelfde meisje naar een gala geweest, deden onvermoed een wetenschappelijke stage op hetzelfde lab, wat leidde tot een promotie-onderzoek dat veel van elkaar weg heeft. Je hebt me destijds op het lab laten zien wat er voor nodig is om te promoveren. Je was daar een stuk sneller mee dan ik en ik was hevig onder de indruk van jouw prestatie, en nog steeds. Uiteindelijk kwam ik in jouw oude appartement onder je nieuwe appartement te wonen. Je hebt me geïntroduceerd in de wondere wereld van

het toerskiën, waar ik als snowboarder niets te zoeken heb, maar toch word getolereerd. Het is altijd weer een topweek met Mark (H.E.L.D.) en de hilarische WWR. Je bent als radioloog en wetenschapper ongelooflijk getalenteerd en ik vermoed dat we daar nog wel meer van gaan horen.

Ona Wu – Dear Ona, thanks for your help on the "Brain Research" paper and the good times you have showed me in Boston. You were kind enough to offer up your couch years later when I was in Boston again. Sharp as a razor, quick with the computer, a creature of the night and probably involved in some global underground defense against the new world order.

Gustav Strijkers – Beste Gustav, ik heb je leren kennen via Willem en we hebben menig leuk sociaal event meegemaakt. Je hebt bijgedragen aan dit proefschrift door je hulp bij het opzetten en uitwerken van mijn eerste DTI onderzoekje. Je was altijd buitengewoon behulpzaam en snel met het oplossen van een probleem.

Robbert Notenboom – Beste Robbert, jouw hulp bij het opzetten van het pilocarpine model was onontbeerlijk… en wat schetst mijn verbazing dat ik je vorig jaar opeens aantrof bij een neurochirurgische cursus. Veel succes in die baan en wellicht zien we elkaar nog eens.

Dear Michael Sander, Dennis Carr, Chad Rigetti, roommates in New Haven with who I shared many good and some bad moments. It was memorable.

The Yale Cycling Team, supported by Matt and his Devil's gear bike shop represented the highlight of my stay in the US. I had so many beautiful rides, so many races, so much fun. It was a truly great experience. A special thanks to Curtis Eastin and Eric Becker for sharing their interesting view of the world.

Laura Sacolick, Kevin Koch, Anant Patel, Golam Chowdurry, Fahmeed Hyder, Fuyuze Tokoglu, Meko Owens and the other people of the MRRC. You created the social environment of the lab, which was very friendly and thoroughly enjoyable.

Maeike Zijlmans – Beste Maeike, je hebt een groot deel van de totstandkoming van dit proefschrift meegemaakt, inclusief de frustraties die dat met zich meebracht. Je was een uitstekende discussiepartner en hebt mijn denken aangescherpt. Ik wens je alle sterkte toe met je eigen aanstaande promotie en je zwangerschap.

Deze promotie kan niet los worden gezien van mijn opleiding tot neurochirurg alleen al omdat hij er in de tijd mee verweven is. Daarnaast is het een inherent onderdeel van de AGIKO constructie die voor mij gecreëerd werd. Daarom gaat mijn dank ook uit naar Professor Tulleken die mij op de weg van de neurochirurgie heeft gebracht en naar Jan Willem Berkelback van der Sprenkel die mij uiteindelijk heeft aangenomen voor de opleiding. Professor van Gijn wil ik graag speciaal noemen, omdat ik tijdens mijn neurologiestage een uitstekende opleiding heb gekregen, maar ook heb mogen meemaken

hoe iemand op integere wijze kan excelleren in klinische taken, wetenschap en management. Professor Vandertop, mijn dank voor de kans die u mij hebt geboden. Ik geniet ervan om samen te opereren, want ik heb een voorliefde voor vaardigheid met enige schwung.... en die is volop aanwezig. Saskia Peerdeman, mijn dank voor je menselijkheid en de manier waarop je invulling geeft aan het opleiderschap. Het is voor jou niet iets voor erbij, maar een kerntaak die je uitermate serieus neemt. De VU heeft daardoor de beste opleiding van Nederland.....

Casper en Camiel, jullie zijn de laatste tijd weer prominent in mijn leven aanwezig, waar jullie daar ook bij tijd en wijle minder aanwezig in zijn. Misschien een kenmerk van ware vriendschap. Je kan zo weer verder waar je de relatie hebt achtergelaten. Ik voel me bevoorrecht met jullie als vrienden. Camiel, je bent een fantastische, vrijgevige kerel en ik bewonder je om je talent in de sociale wildernis en met name de wereld van markt en strijd. Je beheerst het als geen ander om te geven, maar daarmee uiteindelijk ook je eerlijke deel te nemen. Ik kan goed met je doornemen hoe de zaken werken in het ziekenhuis en het onderzoek, zodat ik er meer vat op krijg. Je bent een goede vriend. Casper, jouw gedachtenwereld is ongelooflijk interessant. Jouw specialiteit is een beschouwing op het leven, maar dan met een onverwachte draai. We delen veel, inclusief een karakterstructuur die slecht samengaat met de stroperigheid van een promotie-onderzoek. Je gaat het redden, echt waar en daarmee doel ik op meer dan alleen een promotie-onderzoek.

Willem, mijn paranimf, zoals ik de jouwe was. Dit is een “bromance”, want als je een vrouw was, was ik met je getrouwd. Je bent de beste vriend van veel mensen, waaaronder ook ik. Dat komt misschien omdat je heel goed bent in het zijn van een vriend. Je bent loyaal, ondersteunend, corrigerend, beschermend en soms totaal onverantwoordelijk.... Qua wetenschap kan ik alleen maar zeggen: ”Wat een talent”. Ik geniet van je vondsten, je snelle begrip, je ideeën om je groep te managen en je verontwaardiging over van alles en nog wat, soms prachtig verwoord in een column.... Daarbij gaan al deze dingen, positief en negatief, gepaard met een grote dosis humor. Niet onvermeld mag blijven jouw talent om op bizarre wijze mensen voor je te winnen.... Op een grote gespierde afro-american in New York afstappen en vragen: “Do you think I’m a skinhead”.... Bij jou leidt dit tot een hele gezellige avond met een nieuwe beste vriend.

Jet, mijn paranimfette, wij delen een bijzondere geschiedenis. Op 28 augustus 1983 droeg ik je de kerk in voor je doop... Ik zag het als een grote verantwoordelijkheid. Ook het paranimf zijn zie jij als een grote verantwoordelijkheid. Je staat hier als de zus waar ik de laatste jaren veel aan heb gehad, maar je staat hier ook als afgevaardigde van de sibs. Hester, Wietske, Gijsbert, Irene, Wiebe, Nelienke, Kars en Jochem. De ruimte is te beperkt om over jullie allemaal iets te zeggen, maar jullie zijn mijn basis en ik geniet er enorm van jullie om me heen te hebben. Negen zeer verwante personen met allemaal een heel eigen persoonlijkheid, die mijn leven verrijken.

Lieve Marlies, we hebben het zo goed samen. Gezelligheid, warmte, mooie trips, samen sporten. Je kan verbazingwekkend goed omgaan met mijn hoekige persoonlijkheid, onder het motto: “zonder gekibbel wordt het gekabbel”. Je bent mijn sociale anker en het is mooi om te zien dat je zo goed met de sibs kan opschieten. Dit werkt, en dat gaat het nog lang doen.

Resume

Pieter van Eijsden was born on February 24th 1976, in Amersfoort, The Netherlands. After obtaining his gymnasium diploma at the Guido de Brès college in Amersfoort in 1993, he started studying medicine and psychology in Utrecht. An internship in ophthalmology was followed in Kuala Lumpur, Malaysia and an elective internship was the basis for the collaboration with Dr. K.P.J. Braun that endures until now. Initially the author worked on Dr. Braun's thesis project concerning experimental hydrocephalus under supervision of Prof. K. Nicolay. Under the wings of Prof. O. van Nieuwenhuizen and the supervision of Dr. K.P.J. Braun, a new research project was started in 2003 leading to the thesis that lies before you. This research project was conceived and performed in close collaboration with Dr. R.A. de Graaf and Dr. K.L. Behar at the Magnetic Resonance Research Center of the Yale Medical School in New Haven, Connecticut, were the author spent a total of two and a half years. In 2001 Pieter received his medical degree and started a residency at the neurosurgery department of the University Medical Center in Utrecht in 2002. His neurosurgical training commenced in 2003 under Prof. C.A.F. Tulleken and Dr. J.W. Berkelbach van der Sprenkel. He was trained in neurology for one year under Prof. J. van Gijn at the University Medical Center in Utrecht, after which he continued his neurosurgical training at the VU Medical Center in Amsterdam under supervision of Prof. Vandertop and Dr. S.M. Peerdeman. He trained for three months in intensive care medicine at the VU Medical Center under Prof. A.R.J. Girbes and for six months in spinal surgery at the St. Lucas Andreas Hospital under Dr. G.J. Bouma. He hopes to complete his neurosurgical training in 2011.

He was a dreamer, a thinker, a speculative philosopher...
or, as his wife would have it, an idiot.

The HitchHiker's Guide to the Galaxy
- Douglas Adams

BINNENZIJDE OMSLAG